

THE ROLE OF PATZ1 TRANSCRIPTION FACTOR  
IN THE DNA DAMAGE RESPONSE

by  
EMRE DENİZ

Submitted to the  
Graduate School of Engineering and Natural Sciences  
in partial fulfillment of  
the requirements for the degree of  
Doctor of Philosophy

Sabanci University

July 2014

THE ROLE OF PATZ1 TRANSCRIPTION FACTOR  
IN THE DNA DAMAGE RESPONSE

APPROVED BY:

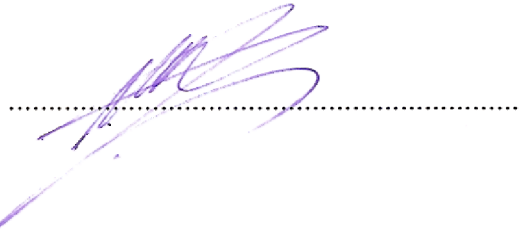
Assoc. Prof. Dr. Batu Erman  
(Thesis Supervisor)



Asst. Prof. Dr. Alpay Taralp



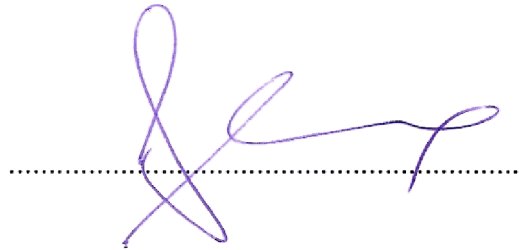
Assoc. Prof. Dr. Murat okol



Prof. Dr. Selim etiner



Asst. Prof. Dr. Stefan H. Fuss



DATE OF APPROVAL: 22.07.2014

© Emre Deniz 2014

All Rights Reserved

## ABSTRACT

### THE ROLE OF PATZ1 TRANSCRIPTION FACTOR IN THE DNA DAMAGE RESPONSE

Emre Deniz

Biological Sciences and Bioengineering, PhD Thesis, 2014

Thesis supervisor: Batu Erman

Keywords: PATZ1, p53, DNA Damage, Tumorigenesis, RNA-Seq

PATZ1 (MAZR) is a transcription factor composed of an N-terminal BTB protein-protein interaction domain and a C-terminal zinc finger and AT-hook DNA binding domain. Recent findings indicate that PATZ1 has a crucial role in the p53 pathway and during tumorigenesis. PATZ1 interacts with p53, is upregulated in various cancers and its absence favors lymphomagenesis. We identified a role for PATZ1 as a regulator of the p53 tumor suppressor protein. We found that upon doxorubicin induced DNA damage, the protein level of PATZ1 decreases, as the p53 protein accumulates. This inverse correlation between PATZ1 and p53 protein levels led us to investigate the biological relevance of these two proteins. We found that PATZ1 loss resulted in decreased proliferation rates in various cell types; while its overexpression accelerated proliferation. We demonstrate that PATZ1 inhibits the transcription activation function of p53 by luciferase reporter assays. While p53 is responsible for inducing the expression of the target genes p21 and Puma, we show that PATZ1 overexpressing cells cannot induce the expression of these genes as effectively as wild type cells. Finally, we performed genome scale RNA-Seq and microarray analysis on doxorubicin treated mouse embryo fibroblasts sufficient or deficient for PATZ1 and found that the absence of PATZ1 results in an alteration of the expression of p53 target genes. These results demonstrate that PATZ1 modulates p53-dependent cellular stress and DNA damage pathways.

## ÖZET

### PATZ1 TRANSKRİPSİYON FAKTÖRÜNÜN DNA HASAR YANITLARINDAKİ ROLÜ

Emre Deniz

Biyoloji Bilimleri ve Biyomühendislik, Doktora Tezi, 2014

Tez Danışmanı: Batu Erman

Anahtar Kelimeler: PATZ1, p53, DNA Hasarı, Tümör Gelişimi, RNA-Sek

PATZ1 (MAZR), N ucunda protein-protein etkileşimlerinde görevli BTB bölgesi, C ucunda ise çinko parmak ve AT-hook motifleri olan bir transkripsiyon faktörüdür. Son zamanlarda bulunan bilgilere göre, PATZ1, p53 yolağında ve tümör gelişimi sırasında kritik rollere sahiptir. PATZ1 proteini p53 proteinine bağlanır, çeşitli kanser tiplerinde yüksek miktarda ifade edilir ve PATZ1'in yokluğunda lenfoma gelişimi kolaylaşır. Biz, PATZ1'i tümör baskılayıcı p53 proteininin düzenleyicisi olarak belirledik. Doksorubisin ilacı ile indüklediğimiz DNA hasarı sonucunda, hücre içerisinde p53 proteini birikirken, PATZ1 proteininin azaldığını bulduk. PATZ1 ve p53 miktarlarının değişimindeki ters ilişki bizi bu iki proteinin biyolojik etkileşimlerini araştırmaya teşvik etti. PATZ1'in aşırı miktarda ifadesinin çeşitli hücre tiplerinde bölünmeyi hızlandırdığını, ifadesinin düşük olmasının ise hücre bölünmesini yavaşlattığını bulduk. Yaptığımız lusiferaz aktivitesi deneyleri sonucunda, PATZ1'in p53'ün transkripsiyon etkinleştirici fonksiyonunu engellediğini kanıtladık. Normalde, p53, p21 ve Puma genlerinin ifadelerini arttırmaya rağmen, PATZ1'i aşırı miktarda ifade eden hücrelerin bu genleri normal durumdaki kadar arttırmadığını gösterdik. Son olarak, PATZ1'in yeterli veya yetersiz ifade edildiği fare embriyo fibroblastlarını doksorubisin ile muamele ederek genom çapında RNA-Seq ve mikroarray analizleri gerçekleştirdik ve PATZ1'in yetersiz olduğu durumlarda p53 hedeflerinin ifadelerinde farklılaşmalar olduğunu bulduk. Bu sonuçlar ile PATZ1'in p53 temelli hücre stresi ve DNA hasar yolaklarını düzenlediğini kanıtladık.

*Sevgili babam ve annem - Faruk & Şükriye Deniz'e...*

## ACKNOWLEDGEMENTS

I am indebted to my advisor Assoc. Prof. Dr. Batu Erman, who gave me the chance to work in his laboratory. During my doctoral study, he helped me to evolve as a young scientist, being patient with me as well as guiding me, encouraging me and expanding my scientific horizons, while giving me the freedom to pursue my research interests. From the first day of my arrival to the laboratory until the end of my degree program, I always felt as a colleague of him but not as a student purely dependent on his supervision. The members of my dissertation committee, Asst. Prof. Dr. Alpay Taralp, Assoc. Prof. Dr. Murat Çokol, Prof. Dr. Selim Çetiner, and Asst. Prof. Dr. Stefan H. Fuss have generously given their time and expertise to better my work. I thank them for their contribution and their good-natured support. I thank Prof. Matthias Dobbstein of the Georg-August-Universität Göttingen for kindly sharing HCT116 and HCT116p53<sup>-/-</sup> cells; Prof. Jean Christophe Bourdon of the University of Dundee for sharing p53a and p53b expression constructs; Dr. Petek Ballar of Ege University for the FLAG-p53 construct, Dr. Meltem Müftüoğlu of Acibadem University for assistance with XCELLigence experiments; Dr. Rengül Çetin Atalay and Tülin Erşahin of Bilkent University for assistance with analyzing the RNA-Seq data; Prof. Wilfried Ellmeier and Dr. Shinya Sakaguchi of Medical University of Vienna for their valuable help and resources that they shared to improve the quality of my study.

I am grateful to my colleagues from Batu Erman's laboratory, who helped me with diverse set of experiments and were great companions for all the hard or happy times. I would like to thank all the students, interns and friends who took part in this project with me. I appreciate all the help and support of Nazlı Keskin, Ceren Tuncer, Jitka Eryılmaz, Manolya Ün, Serra Orey, Bahar Shamloo, Canan Sayitoğlu and other members of the research group. I was privileged for having especially Nazlı as a lab partner with helpful discussions on every single experiment and idea and as a friend with constant support. It would not be possible to go through all the hard times without their presence.

I would like to note the importance of Nazlı in my life. Her friendship is a true gift of Sabanci University to me. Over the years, we have built a very good friendship and we have shared many good and happy times together. We have also overcome many difficulties in our life with the help of each other. I am grateful to have Nazlı as one of my closest friend. She is also a PhD now and I am proud of her as I was for every single achievement in her life and career. I must acknowledge my friends, Mehmet Üskül and Hakan Abak for their presence in my life. I feel really lucky to have them as my close friends. I would like to thank them for their patience, friendship, support, understanding and encouragement. Finally, I owe sincere gratitude to my family for their continuous and unconditional support. I enjoy this life with them.

I would like to acknowledge The European Molecular Biology Organization (EMBO short-term fellowship). I thank to the Scientific and Technological Research Council of Turkey (TÜBİTAK, BİDEB-2211) for supporting my doctoral studies. This project is funded by TUBITAK 1001 “Identification of New Factors Controlling p53 and the DNA Damage Response in T Lymphocytes” Grant Number: 111T401.

## TABLE OF CONTENTS

1. INTRODUCTION.....	1
1.1. Tumor Suppressor Protein p53 .....	1
1.1.1. Paradigm Shift: from an Oncogene to a Tumor Suppressor.....	2
1.1.2. Structure of p53.....	3
1.1.3. Regulation of p53 Stabilization .....	5
1.1.4. Induction of p53 .....	7
1.1.5. p53 Responses in Tumor Suppression .....	9
1.2. POZ-, AT-Hook, and Zinc Finger-Containing Protein PATZ1 .....	11
1.2.1. The BTB-ZF Transcription Factors .....	11
1.2.2. The Role of The BTB-ZF Transcription Factors in Tumorigenesis .....	13
1.2.3. PATZ1 .....	15
2. AIM OF THE STUDY .....	17
3. MATERIALS AND METHODS.....	19
3.1. Materials .....	19
3.1.1. Chemicals .....	19
3.1.2. Equipment.....	19
3.1.3. Buffers and Solutions .....	20
3.1.4. Growth Media .....	21
3.1.5. Commercial Molecular Biology Kits .....	22
3.1.6. Enzymes .....	23
3.1.7. Bacterial Strains .....	23

3.1.8.	Mammalian Cell Lines .....	23
3.1.9.	Plasmids and Primers .....	24
3.1.10.	DNA and Protein Molecular Weight Markers.....	28
3.1.11.	DNA Sequencing .....	28
3.1.12.	Software, Computer-Based Programs, and Websites .....	28
3.2.	Methods .....	29
3.2.1.	Bacterial Cell Culture.....	29
3.2.2.	Plasmid Construction .....	31
3.2.3.	Mammalian Cell Culture .....	33
3.2.4.	RNA-Sequencing and Microarray .....	35
4.	RESULTS.....	36
4.1.	PATZ1 is Expressed in Different Cell Lines.....	36
4.2.	Transcription Repression Activity of PATZ1.....	39
4.3.	Global Effects of PATZ1 on Gene Transcription.....	45
4.4.	Effects of PATZ1 on Cell Proliferation .....	48
4.4.1.	PATZ1 Shortens Cellular Doubling Time.....	48
4.4.2.	Effects of PATZ1 on Cell Cycle Progression.....	51
4.5.	PATZ1 Inhibits the Transcriptional Activity of p53.....	57
4.6.	PATZ1 in DNA Damage .....	63
4.6.1.	PATZ1 is Downregulated upon DNA Damage .....	63
4.6.2.	Endogenous Transcriptional Activity of p53.....	67
4.6.3.	Global Effects of PATZ1 on Gene Transcription in Response to DNA Damage 70	
4.7.	Preliminary Results for Future Directions.....	79
4.7.1.	Knocking out <i>PATZ1</i> in Human Cell Lines.....	79
4.7.2.	Impact of PATZ1 Expression on Tumorigenesis in Murine Xenograph Models 82	
5.	DISCUSSION.....	85
	REFERENCES.....	93
	APPENDIX.....	104
	APPENDIX A: Chemicals Used in the Study.....	104
	APPENDIX B: Equipment Used in the Study .....	106
	APPENDIX C: DNA and Protein Molecular Weight Markers.....	108
	APPENDIX D: Cloning of PATZ1 cDNAs into pmigII-ires-mcherry Plasmid .....	109

APPENDIX E: Cloning of PATZ1 cDNA into pBABE-ires-Puro Plasmid.....	110
APPENDIX F: Cloning of PATZ1 shRNA into LMP Plasmid .....	112

## LIST OF FIGURES

Figure 1.1: The protein structure of the canonical p53 isoform .....	4
Figure 1.2: MDM2 mediated control of p53 stabilization.....	6
Figure 1.3: Induction and response of p53 .....	8
Figure 1.4: Cell-cycle regulation by p53 .....	10
Figure 1.5: Induction of apoptosis by p53 .....	11
Figure 1.6: Epigenetic changes by BTB-ZF proteins.....	12
Figure 1.7: BTB-ZF proteins in p53 regulation .....	14
Figure 4.1: Exon structure of the human PATZ1 gene and the protein products encoded by alternative splice variants.....	37
Figure 4.2: PATZ1 alternative splice variants are expressed in various cell lines .....	38
Figure 4.3: Breeding of PATZ1 deficient or sufficient Thpok reporter mice.....	40
Figure 4.4: Retroviral infection of CD8 SP lymphocytes .....	41
Figure 4.5: Reconstruction of PATZ1 expression in PATZ1 <sup>-/-</sup> CD8 <sup>+</sup> CD4 <sup>-</sup> cells re- represses Thpok.....	42
Figure 4.6: PATZ1 does not require its C-terminus for its transcription repressor activity .....	43
Figure 4.7: Several residues within the zing finger domain of PATZ1 are crucial for transcription repressor activity.....	44
Figure 4.8: Genome wide gene expression analysis of MEFs expressing or deficient in PATZ1 by RNA-Seq .....	47
Figure 4.9: MEFs lacking Patz1 expression proliferate slower .....	48

Figure 4.10: PATZ1 overexpressing HCT116 cells proliferate faster .....	49
Figure 4.11: PATZ1 expression is inversely correlated with doubling time in NIH3T3 cells.....	50
Figure 4.12: The use of Fucci-expressing HeLa cells to investigate cell-cycle progression.....	52
Figure 4.13: Overexpression of PATZ1 in HeLa-Fucci cells does not alter cell-cycle distribution.....	53
Figure 4.14: Cisplatin treatment results in a reversible G2 arrest in HeLa-Fucci cells ..	55
Figure 4.15: Cells that are purified with respect to their cell cycle phase progress through the cell cycle and restore a normal distribution .....	56
Figure 4.16: Schematic representation of the luciferase reporter constructs used in the study .....	58
Figure 4.17: PATZ1 inhibits p53 transcriptional activity in luciferase assays in various cell types.....	59
Figure 4.18: PATZ1 inhibits p53 activity in luciferase assays with different luciferase constructs.....	60
Figure 4.19 : Several residues in PATZ1 are crucial for inhibiting p53 activity.....	62
Figure 4.20: p53 accumulates upon DNA damage induced by doxorubicin in various cell lines.....	64
Figure 4.21: Schematic representation of proteins encoded by PATZ1 alternative splice variants.....	65
Figure 4.22: PATZ1 protein levels decrease upon doxorubicin treatment in MEFs .....	65
Figure 4.23: PATZ1 protein levels, but not mRNA levels, decrease upon doxorubicin treatment of HCT116 cells, independent of the presence or absence of p53 protein.....	66
Figure 4.24: PATZ1 impairs the up-regulation of p53 dependent genes in doxorubicin treated cells .....	68
Figure 4.25: Overexpression of PATZ1 did not have a significant effect on apoptosis related genes.....	69
Figure 4.26: Genome wide gene expression analysis of MEFs expressing or deficient in PATZ1 upon DNA damage induction, by RNA-Seq.....	71
Figure 4.28: Genome wide gene expression analysis of MEFs expressing or deficient in PATZ1 by microarray.....	75
Figure 4.29: P53 pathway is affected in doxorubicin treated PATZ1 deficient MEFs ...	77

Figure 4.30: Doxorubicin treatment in the absence of PATZ1 results in an alteration of the expression of p53 target genes .....	78
Figure 4.31: TALENs against PATZ1 genomic locus .....	79
Figure 4.33: RFLP analysis to the single-cell-derived-colonies of HCT16 cells after TALEN transfection .....	81
Figure 4.34: Creating stably PATZ1 overexpressing or knocked-down EL4-Ova cells.	83
Figure 5.1: Our model of PATZ1 depicting its roles in the absence or presence of DNA damage.....	90
Figure C.1: DNA and Protein Molecular Weight Markers .....	108
Figure D.1: Cloning of PATZ1 cDNAs into pmigII-ires-mcherry Plasmid.....	109
Figure E.1: Cloning of PATZ1 cDNA into pBABE-ires-Puro Plasmid.....	111
Figure F.1: Cloning of PATZ1 shRNA into LMP Plasmid .....	113

## LIST OF TABLES

Table 3.1: The list of the plasmids used in this thesis.....	26
Table 3.2: The list of the primers used in this thesis.....	27
Table 3.3: The list of the software, programs and websites used in this thesis .....	29
Table 3.4: Optimized PCR conditions.....	31
Table 4.1: Biological process GO terms that are enriched in our DEG set (generated by comparing KO vs. WT MEFs).....	46
Table 4.2: Biological process GO terms that are enriched in our DEG set fromRNA-Seq (generated by comparing WTdox vs. WT and KOdox vs. KO MEFs).....	72
Table 4.3: Biological process GO terms that are enriched in our DEG set from RNA-Seq that consists of upregulated genes uniquely in KOdox vs. KO and of more upregulated genes in KOdox vs. KO compared to WTdox vs. WT.....	74
Table 4.4: Biological process GO terms that are enriched in our DEG set from RNA-Seq that consists of downregulated genes uniquely in KOdox vs. KO and of more downregulated genes in KOdox vs. KO compared to WTdox vs. WT comparison.....	75
Table 4.5: Biological process GO terms that are enriched in our DEG set from microarray that consists of upregulated genes uniquely in KOdox vs. KO .....	76
Table 4.6: Biological process GO terms that are enriched in our DEG set from microarray that consists of downregulated genes uniquely in KOdox vs. KO.....	76

## LIST OF SYMBOLS AND ABBREVIATIONS

$\alpha$	Alpha
$\beta$	Beta
$\mu$	Micro
Amp	Ampicillin
A	Amper
AP	Alkaline Phosphatase
bp	Base pair
BTB	Broad-complex, Tramtrack, and Bric-à-brac
CIAP	Calf Intestine Alkaline Phosphatase
CMV	Cytomegalovirus
Col	Colony
Da	Dalton
DBD	DNA Binding Domain
DEG	Differentially Expressed Gene
DMEM	Dulbecco's Modified Eagle Medium
DMSO	Dimethylsulfoxide
DN	Double Negative
DNA	Deoxyribonucleic Acid
DP	Double Positive
DSB	Double Strand Break
ds-cDNA	Double Strand Complementary DNA
E. Coli	Escherichia coli
FACS	Flourescence Activated Cell Sorting
FBS	Fetal Bovine Serum
GEO	Gene Expression Omnibus
GFP	Green Flourescent Protein
GO	Gene Ontology

GOF	Gain of Function
GSEA	Gene Set Enrichment Analysis
h	Hour
HBS	HEPES-Buffered Saline
indel	Insertion Deletion
Kan	Kanamycin
KEGG	Kyoto Encyclopedia of Genes and Genomes
KO	Knock Out
LB	Luria Broth
LOH	Loss of Heterozygosity
M	Molar
MEF	Mouse Embryonic Fibroblast
mESC	Mouse Embryonic Stem Cell
min	Minute
mmu	Mus Musculus
MOMP	Mitochondrial Outer Membrane Permeabilization
mRNA	Messenger RNA
NCBI	National Center for Biotechnology
Neo	Neomycin
NES	Nuclear Export Signal
NHEJ	Non-Homologous End Joining
NLS	Nuclear Localization Signal
OD	Optical Density
OSKM	Oct4, Sox2, Klf4, and c-Myc
PBS	Phosphate Buffered Saline
PCR	Polymerase Chain Reaction
PEI	Polyethylenamine
POZ	Poxviruses and Zinc-finger
PRD	proline rich domain
Pu	Purine
Py	Pyrimidine
RE	Response Element
RFLP	Restriction Fragment Length Polymorphism
RNA	Ribonucleic Acid
RNA-Seq	RNA Sequencing
RPKM	Reads Per Kilobase Per Million
rpm	Rotation per minute
RT-PCR	Real Time Polymerase Chain Reaction
SDM	Site-Directed Mutagenesis
SDS-PAGE	Sodium Dodecyl Sulfate Polyacrilamide Gel Electrophoresis
SP	Single Positive
SV40	Simian Virus 40
TALEN	Transcription Activator-Like Effector Nuclease
TBE	Tris Borate EDTA

TD	Tetramerization Domain
UV	Ultraviolet Light
V	Volt
WT	Wild Type
ZF	Zinc Finger

## **1. INTRODUCTION**

### **1.1. Tumor Suppressor Protein p53**

Since the discovery of p53 35 years ago, there have been a substantial number of studies on this tumor suppressor protein. Pubmed alone lists over 72000 scientific publications and this archive is ever-growing. This immense amount of work on a single protein points to the importance of p53 in maintaining a wide variety of processes within eukaryotic cells. p53 is a sequence specific, cellular stress responsive transcription factor that plays key roles in many important cellular responses. Among these responses are cell cycle arrest, senescence, DNA repair and recombination, autophagy, and apoptosis.

### 1.1.1. Paradigm Shift: from an Oncogene to a Tumor Suppressor

In 1979, several different laboratories independently identified a 53-54 kDa protein as an interaction partner of the oncogenic large T antigen protein of the SV40 virus<sup>1-5</sup>. Following this work, other groups found that p53 cooperated with different oncogenic proteins, such as the adenovirus E1b-57K protein, activated Ha-Ras, and the v-myc protein of the myelocytomatosis virus<sup>6-8</sup>. In addition to these, p53 was found to be overexpressed in different human cancer cell lines<sup>9</sup>. All these observations suggested that p53 itself was indeed an oncogene. However, later on, frequent genetic alterations and loss-of-heterozygosity of the p53 gene locus (*TP53*) were found in many human colorectal cancers<sup>10</sup>. Along with this finding, various groups observed that cells transfected with wild type p53 rarely were transformed and the few transformed clones expressed mutant p53 instead of WT protein<sup>11,12</sup>. These findings identified p53 as a tumor suppressor protein rather than an oncogene.

After this paradigm shift, a large amount of work corroborated the latter findings, showing that in various systems, p53 was indeed a tumor suppressor protein<sup>13</sup>. It is widely quoted that *TP53* is mutated in almost 50% of human tumors and that patients with mutant p53 tumors respond poorly to therapy<sup>14,15</sup>. While this number is impressive, it is likely an underestimation of the impact of p53 protein on tumors, because those tumors which have WT p53 often activate p53 suppressor mechanisms<sup>16</sup>. Germline mutations in the *TP53* gene in humans cause Li-Fraumeni syndrome, which is an inherited disease characterized by a high rate of malignant tumors of different tissues<sup>17</sup>. Mouse models of knock-out *Trp53* are highly prone to spontaneous tumor development<sup>18,19</sup>. These mice often develop lymphomas but the types of the tumors observed are widely variable<sup>19</sup>. Acquiring a mutant p53 allele, either through inheriting or from a spontaneous mutation, usually leads to the loss of the remaining WT allele, which is called loss of heterozygosity (LOH)<sup>20</sup>. Most of the p53 mutations that result in tumor development are missense mutations, a single nucleotide change in the protein coding sequence causing a single amino acid change in the protein<sup>21</sup>. Many mutant p53 proteins function as dominant-negative on WT p53, thereby inhibiting the tumor

suppressor activity of WT p53, and/or acquire gain-of-functions (GOF), which retain only a part of the WT p53 activity that may be beneficial for tumor progression, or provoke activation of a new set of target genes <sup>22</sup>. All these accumulated data over 3 decades secured the critical place of p53 in tumorigenesis and firmly implied that p53 is a tumor suppressor protein.

### **1.1.2. Structure of p53**

The human TP53 gene is located on the short arm (p13.1) of chromosome 17. The gene spans 19200bps and consists of 11 exons (Ensembl accession number ENSG00000141510). It is predicted that from this gene 17 mRNAs are transcribed while only 12 of these encode proteins. The most abundant isoform of p53 is the canonical p53 protein, which is formally named TAp53 $\alpha$  (this isoform will be referred to as p53 throughout this thesis, for the sake of simplicity). p53 encodes a 393 amino acid long 53 kDa protein. p53 consists of several conserved and functionally relevant domains <sup>23</sup> (Figure 1.1). Starting from the very first N-terminal amino acid, there are two transactivation domains (TAD1 and TAD2). TAD1 spans residues 1-42, and TAD2 spans residues 43-62. Following the TADs, there is a proline rich domain (PRD) spanning residues 63-97. After the N-terminal part of the protein, a central core part is located from residue 98 to 292, which encodes a DNA binding domain (DBD). The C-terminal part of the protein has a nuclear localization signal (NLS) spanning residues 300-323, a tetramerization domain (TD) spanning residues 324-355, a nuclear export signal (NES) spanning residues 356-362, followed by an unstructured regulatory domain in the very C-terminus of the protein.

The TAD1 has sites for recruiting coactivators needed for transcriptional activation and it also binds to MDM2, which is the most critical E3 ligase for p53 that governs the levels of cellular p53 protein <sup>24</sup>. The TAD2, on the other hand, is not as

important as TAD1, but it also interacts with coactivators and dictates p53 to induce specific target genes<sup>25</sup>. The PRD interacts with SH3-domain proteins. MDM2 and p300 also bind to this region and this interaction functions to fine-tune p53 stabilization and transactivation<sup>26,27</sup>.



Figure 1.1: The protein structure of the canonical p53 isoform. The full length protein consists of 393 amino acids and has an estimated size of 53 kDa. The conserved and functional domains from the N-terminus of the protein to the C-terminus are the following; two transactivation domains (TAD1 and TAD2), a proline rich domain (PRD), a DNA binding domain (DBD), a nuclear localization signal (NLS), a tetramerization domain (TD), a nuclear export signal (NES), and an unstructured C-terminal regulatory domain.

The DBD has a high affinity to various p53 response elements (RE) in the genome. The REs are composed of two half-sites, each with a consensus of 5'-PuPuPuC(A/T)(T/A)GPyPyPy-3', separated by 0-13 bases (where Pu is a purine, Py is a pyrimidine)<sup>28</sup>. Most of the mutations in human tumors that alter the function of p53 are located within this DBD, causing mis-targeting of p53 to a new set of target genes or impairing DNA binding of p53 completely<sup>29</sup>.

The TD is necessary to form tetramers of the p53 protein. While p53 can bind to DNA as dimers or tetramers, it is transcriptionally active only when it oligomerizes into tetramers<sup>30</sup>. Tetramerization is also important in masking the nuclear export signal, thereby ensuring nuclear retention of the transcriptionally active form of p53<sup>31</sup>. The C-terminal regulatory domain of p53 is extensively and specifically post-translationally modified in response to cellular stress. The different modifications of this domain determine the interaction partners of the p53 protein, akin to the histone code<sup>32</sup>. The regulatory domain was shown to have two functions. First, it modulates overall p53 protein stability by post-translational modifications of the lysine residues within this domain<sup>33</sup>. Secondly, this domain nonspecifically interacts with DNA and promotes the sequence specificity of the DNA binding domain<sup>34</sup>.

### 1.1.3. Regulation of p53 Stabilization

The mRNA levels of p53 do not change upon stress. Rather, the stabilization or degradation of the protein is what determines the levels of the cellular p53. Under normal conditions, without any cellular stress, the level of p53 protein is low in cells due to degradation. Upon a variety of stresses, p53 protein is rapidly stabilized and activated. There are a number of factors that control the stability and activity of p53 in normal and stressed cells. Ubiquitination of p53 has a marked impact on the stability and localization of this protein. While mono-ubiquitination targets p53 out of the nucleus to the cytoplasm, poly-ubiquitination serves as a signal for degradation by the 26S proteasome<sup>35</sup>. The major mechanism for controlling p53 stability is its interaction with MDM2<sup>36,37</sup>. MDM2 is a RING finger E3 ubiquitin-protein ligase. In the nucleus, it mono-ubiquitinates p53 at the C-terminal K370, K372, K373, K381, K382, and K386 residues, unmasking the NES of p53 within the C-terminus and driving the protein out of the nucleus<sup>38</sup>. While nuclear MDM2 does not travel to the cytoplasm along with the mono-ubiquitinated p53, cytoplasmic MDM2 continues to poly-ubiquitinate cytoplasmic p53 (Figure 1.2). The targeted inactivation (knock out) of the MDM2 protein in mice causes embryonic lethality; however, this phenotype is rescued when MDM2<sup>-/-</sup> mice are bred with p53<sup>-/-</sup> mice<sup>36,37</sup>. These findings imply that MDM2 has the most important role on p53 degradation and is not dispensable.

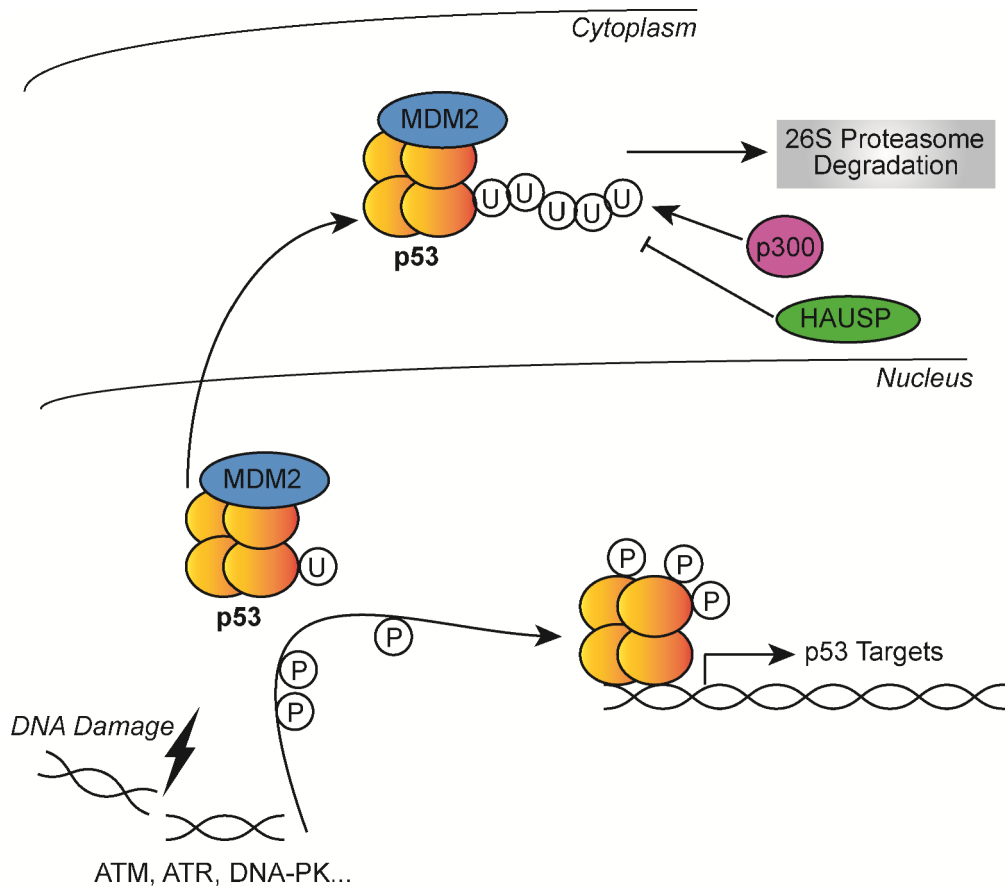


Figure 1.2: MDM2 mediated control of p53 stabilization. MDM2 mono-ubiquitinates p53 by binding to the transactivation domain of p53. This results in the nuclear export of p53 to the cytoplasm for poly-ubiquitination by MDM2 and p300 and subsequently degradation by 26S proteasome. In the case of a cellular stress, such as DNA damage, either various kinases phosphorylate p53 to free it from MDM2 or HAUSP de-ubiquitinates p53. These post-translational modifications stabilize and activate p53.

Another protein that is structurally related to MDM2 is MDMX (alternatively named MDM4). MDMX also has a RING domain however it is incapable of E3 ligase activity towards p53. Instead, it directly inhibits the transcriptional activity of p53 after binding to the transactivation domain of the protein<sup>39</sup>. MDMX also hetero-oligomerizes with MDM2 through their RING domains and stabilizes MDM2 by inhibiting its self-ubiquitination<sup>40</sup>. In turn, MDM2 shuttles MDMX to and from the nucleus because MDMX lacks nuclear localization and export signals. Although not as major as MDM2, there are other ubiquitin ligases that contribute to the stability of p53. Among these, the most famous are Pirh2, Cop1 and p300/CBP<sup>41</sup>. Both Pirh2 and Cop1 E3 ligases are able to ubiquitinate p53 independent of MDM2 function. p300/CBP is a cytoplasmic E4

ligase which polyubiquitinates p53 and as a result directs it to 26S proteosomal degradation<sup>42</sup>.

In response to a wide variety of cellular stresses, p53 is phosphorylated at many different residues, among which the most important are Ser15 and Ser20, by ATM, ATR, DNA-PK and Chk1-2 kinases, rescuing p53 from MDM2 mediated ubiquitination and therefore stabilizing p53<sup>43</sup>. Beside the post-translational modifications on p53, some phosphorylation on MDM2 and MDMX also occur, mostly by ATM and also other kinases, to impair their interaction with p53 and to promote their ubiquitination and nuclear export<sup>44,45</sup>. The acetylation of p53 on the C-terminal lysine residues inhibits the ubiquitination process because these sites compete for acetylation and ubiquitination<sup>46</sup>. p300/CBP plays a dual role in p53 stability and activity; while it polyubiquitinates the mono-ubiquitinated p53 to direct it for proteosomal degradation, it also acetylates the p53 at the C-terminal ubiquitination residues to ensure that MDM2 cannot function on p53, therefore stabilizing p53. One way of stabilizing p53 is rescuing it from the ubiquitination activity of MDM2; however, there are other ways of stabilizing it, which is removing of the ubiquitin modifications, called de-ubiquitination. HAUSP is a p53-interacting protein which specifically targets the ubiquitin moieties on p53 upon induced-cellular stress and removes them by its protease activity<sup>47</sup>. On the other hand, under unstressed conditions, HAUSP de-ubiquitinates MDM2 and MDMX and protects them from degradation, therefore contributes to the establishing of the delicate balance of p53 levels<sup>48</sup>.

#### **1.1.4. Induction of p53**

Cellular stress signals stabilize and activate p53 in a context dependent manner (Figure 1.3). This is because depending on the type and the mechanism of the stress signal, different pathways are utilized and therefore p53 is activated via different post-translational modifications or co-activators. DNA damage is the most effective and

most studied way of inducing p53. Ultraviolet light (UV), ionizing radiation, and genotoxic drugs are also capable of stabilizing p53<sup>49,50</sup>. Upon DNA damage, ATM and ATR along with other kinases effectively phosphorylate p53 to inhibit its interactions with MDM2 and MDMX<sup>45</sup>. On the other hand, these kinases also phosphorylate MDM2 and MDMX, marking them for degradation<sup>48</sup>. p53 is readily induced by activated oncogenes. This is mainly due to the

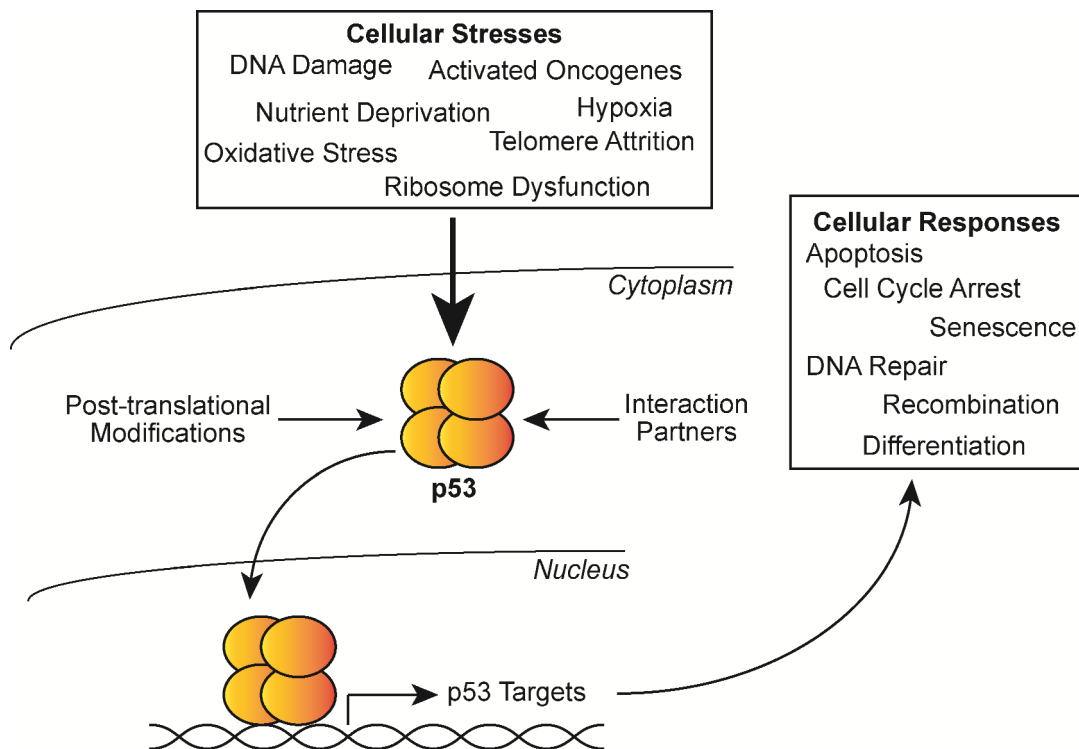


Figure 1.3: Induction and response of p53. Cellular stress induces p53 to be post-translationally modified and to interact with other partners to drive a cellular response.

functions of p14<sup>ARF</sup> (ARF). ARF blocks the interaction between MDM2 and p53 by binding to MDM2, allowing p53 to accumulate<sup>51</sup>. ARF is a perfect example of understanding that every stress signal has its own pathway to induce p53. This is because ARF is incapable of activating p53 in response to DNA damage<sup>52</sup>. Dysfunction of ribosome is also a stress inducer for eukaryotic cells. Proteins (L5, L11, and L23) that are part of the ribosome itself are able to inhibit MDM2 by binding to it<sup>53-55</sup>. Solid tumors experience hypoxic conditions towards the inner parts of the tumor due to insufficient formation of blood vessels, a process called angiogenesis. p53 is stabilized by HIF-1 $\alpha$  by their interaction under hypoxia<sup>56</sup>. HIF-1 $\alpha$  is also noteworthy because

HIF-1 $\alpha$  driven p53 induces a different set of target genes than induced by DNA damage driven p53<sup>57</sup>. Besides these stresses, others such as nutrient deprivation, oxidative stress, and telomere attrition can also stabilize p53<sup>58–60</sup>.

### 1.1.5. p53 Responses in Tumor Suppression

p53 is a very potent tumor suppressor protein that maintains the stability of cellular health and prevents tumorigenesis. Insult to cellular health causes stress for the cell resulting in p53 accumulation. The type and extent of the insult as well as the origin of the cell are the criteria that determines the mechanism of p53 accumulation and the specific outcome of this activation. Therefore, the p53 response is highly context dependent<sup>61</sup>. Specific combinations of various posttranslational modifications and recruited co-factors (either repressors or activators) play roles in context dependent responses. Among the responses of p53 that are important for tumorigenesis are cell-cycle arrest and senescence, DNA repair and recombination, and when the stress is too excessive for the cell, the autophagy and the apoptosis pathways are utilized. It is clear that the roles of p53 on controlling tumorigenesis are through keeping cell growth in control.

Upon cellular stress, such as DNA damage, p53 induces cell-cycle arrest in the G1/S and the G2/M phases of the cell cycle, allowing cells to repair damaged DNA or cellular compartments before progressing into the next phase of the cell cycle<sup>62</sup> (Figure 1.4). It is pivotal for the cells to have such a control mechanism in cell cycle progression because an accumulated damage if not repaired has high risk of inducing tumorigenesis. Upon stabilization, p53 induces G1 arrest by transactivating the expression of p21 protein, a cyclin-dependent kinase (CDK) inhibitor, from the *CDKN1A* gene locus<sup>63</sup>. p21, in turn, inhibits the kinase activity of CDK2, which normally initiates S-phase

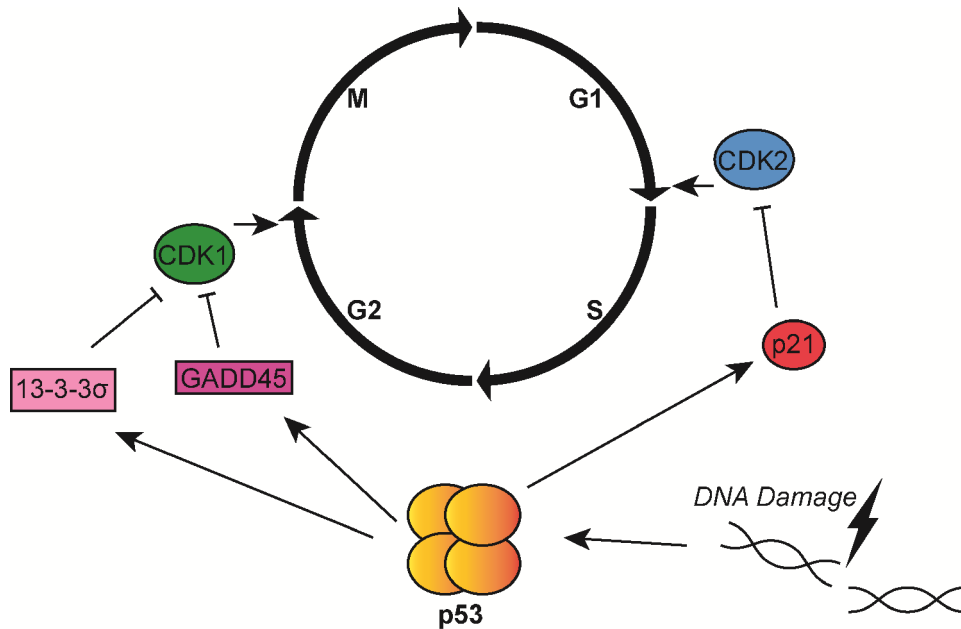


Figure 1.4: Cell-cycle regulation by p53. Cellular stress, such as DNA damage, induces p53 dependent-cell cycle arrest. P53 transactivates p21 and p21 inhibits CDK2 to arrest cells at G1/S phase transition. P53 also transactivates GADD45 and 13-3-3 $\sigma$ , which are inhibitors of CDK1. They arrest cells at G2/M transition.

entry by phosphorylating Rb<sup>64</sup>. p53 also transactivates *GADD45* and *13-3-3 $\sigma$*  in order to induce G2 arrest<sup>65,66</sup>. *GADD45* and *13-3-3 $\sigma$*  work in synchrony in inhibiting mitosis inducing kinase CDK1, either by preventing complex formation of CDK1 with its targets or by exporting CDK1 out of the nucleus<sup>65,66</sup>. The mechanism of the cellular stress determines in which cell cycle check point the cells will arrest. Instead of a reversible cell-cycle arrest, p53 can also induce senescence, which is characterized by permanent cell cycle-arrest<sup>67</sup>.

When the degree of the insult to cellular health is too severe and irreversible, p53 initiates apoptotic pathways (Figure 1.5). While nuclear p53 induces apoptosis using its transcription-dependent activities; cytosolic p53 also contributes to apoptosis through a transcription-independent fashion<sup>68</sup>. p53 transactivates or transrepresses a wide variety of genes for induction of apoptosis, such as *BAX*, *BAD*, *BAK*, *BID*, *NOXA*, *PUMA*, *BCL-2*, *BCL-XL*, and *SURVIVIN*. PUMA is one of the key mediators of apoptosis. It is rapidly upregulated upon DNA damage and initiates apoptosis by localizing to the mitochondria<sup>69</sup>. Cytosolic p53 also localizes to the

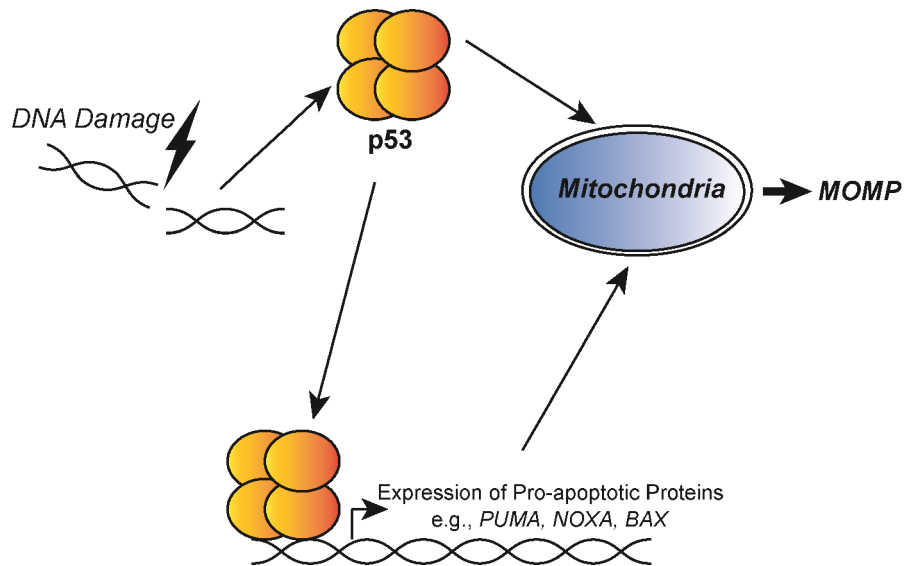


Figure 1.5: Induction of apoptosis by p53. p53 is able to induce apoptosis through transcription-dependent and –independent functions. Stabilized and activated p53 transactivates pro-apoptotic genes, as well as it goes directly to the mitochondria to initiate MOMP.

mitochondria in order to trigger mitochondrial outer membrane permeabilization (MOMP) <sup>68</sup>. MOMP is followed by a series of downstream cascade of events that finally lead to the apoptotic death of the cell.

## 1.2. POZ-, AT-Hook, and Zinc Finger-Containing Protein PATZ1

### 1.2.1. The BTB-ZF Transcription Factors

PATZ1 (POZ (BTB) and AT hook containing zinc finger 1, also known as ZSG, MAZR, PATZ, RIAZ, ZBTB19, ZNF278, dJ400N23) belongs to a class of transcription

factors that have an N-terminal BTB/POK domain for protein-protein interaction and a C-terminal zinc finger motif containing DNA binding domain. BTB stands for Broad-complex, Tramtrack, and Bric-à-brac that are the genes cloned from *Drosophila melanogaster* mutants<sup>70-72</sup>. Another name for BTB is POZ (Poxviruses and Zinc-finger (POZ) and Krüppel). BTB and ZF (zinc finger) are protein domains that are found in eukaryotes and viruses<sup>73</sup>. The BTB domain is about 120 amino acids long and it is used for protein-protein interactions and oligomerization<sup>74</sup>. The ZF motif binds to specific DNA sequences and generally consists of two cysteines followed by two histidines (C<sub>2</sub>H<sub>2</sub>)<sup>75</sup>. The human genome encodes 156 BTB domain-containing proteins and 49 of them have a variable number of ZF motifs, and a couple of them also have an AT-hook motif, which binds to the minor groove of specific AT-rich sequences<sup>76,77</sup>.

BTB-ZF transcription factors use their BTB domain to homo- or hetero-dimerize and to interact with transcription co-factors. Among such factors are SIN3A, SMRT, NCOR1, and p300<sup>78,79</sup>. These co-factors might be transcriptional activators as well as repressors and they can also recruit other histone modifying enzymes, such as HDAC, causing epigenetic changes. Therefore, the role of the BTB-ZF proteins on the transcription is context dependent and depends on the co-factors that they associate with (Figure 1.6). BTB-ZF proteins function in many distinct biological processes including the development of lymphocytes, stem cell biology, fertility, skeletal morphogenesis, neurological development, and tumorigenesis.

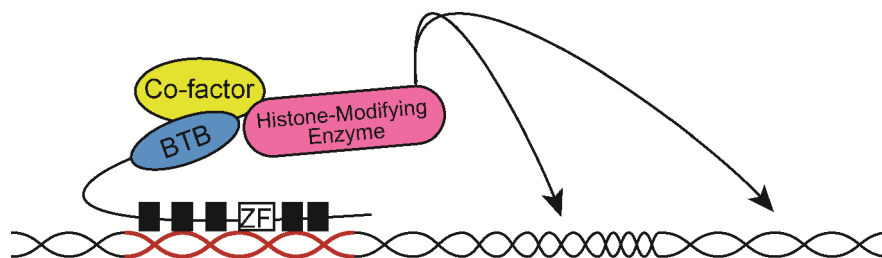


Figure 1.6: Epigenetic changes by BTB-ZF proteins. BTB-ZF proteins recognize their specific response elements on the genome through their ZF motifs and bind to co-factors from their BTB domain. Co-factors recruit histone-modifying enzymes to induce epigenetic changes for heterochromatin (depicted as tight DNA structure) or euchromatin (depicted as relaxed DNA structure) confirmations.

### 1.2.2. The Role of The BTB-ZF Transcription Factors in Tumorigenesis

Apart from their regular functions in a healthy living cell, several BTB-ZF proteins are also associated with DNA damage response and cell cycle regulation during tumorigenesis. These functions were identified as chromosomal translocations in tumors. Some examples to the BTB-ZF proteins that play role in tumorigenesis are PLZF, BCL6, HIC-1, NAC-1, and ZBTB7. PLZF and BCL6 are known to promote tumorigenesis by translocation. The translocation of *PLZF* gene into *RAR- $\alpha$*  gene causes acute promyelocytic leukemia<sup>80</sup>. The resulting PLZF-RAR- $\alpha$  fusion protein gains novel functions by combining the co-factor recruitment capacity of PLZF and the transcriptional activity of RAR- $\alpha$ . Upon translocation, the regular targets of RAR- $\alpha$  involved in DNA repair, cell cycle and apoptosis change their expression patterns. This triggers leukemia transformation by inhibiting the activity of p53<sup>81</sup>. On the other hand, wild type PLZF represses the transcription of the c-myc oncogene. Therefore, by itself, it is also associated with tumor suppression<sup>82</sup>. Another BTB-ZF that is identified through chromosomal translocation is BCL6. BCL6 is found to translocate with many genes, however, these events usually do not create a novel fusion protein because the exons coding for BCL6 protein remain undisturbed after the translocation events and it is rather the promoter that is substituted. This does not affect the production of the wild type protein but it causes a deregulated expression pattern<sup>83</sup>. The translocation of BCL6 results in non-Hodgkin's lymphomas, like diffuse large B cell lymphoma<sup>84</sup>. Actively transcribed BCL6 causes transcriptional repression of the tumor suppressor p53, the DNA damage sensor ATR and the cell cycle mediator CDKN1A (p21)<sup>83,85,86</sup>.

Other BTB-ZF proteins such as HIC-1 and ZBTB7 promote tumorigenesis by upregulating cell cycle regulators. The *HIC-1* gene is located in close proximity to the *TP53* gene and its expression is induced by p53<sup>88</sup>. HIC-1 BTB-ZF protein is in a positive feedback loop for p53 because HIC-1 interacts with SIRT1 and this complex suppresses the transcription of the *SIRT1* gene, whose protein product deacetylates p53 to mark it for degradation<sup>89</sup>. During most types of tumorigenesis, the *HIC-1* locus is either hyper-methylated or lost from the genome completely. This causes upregulation

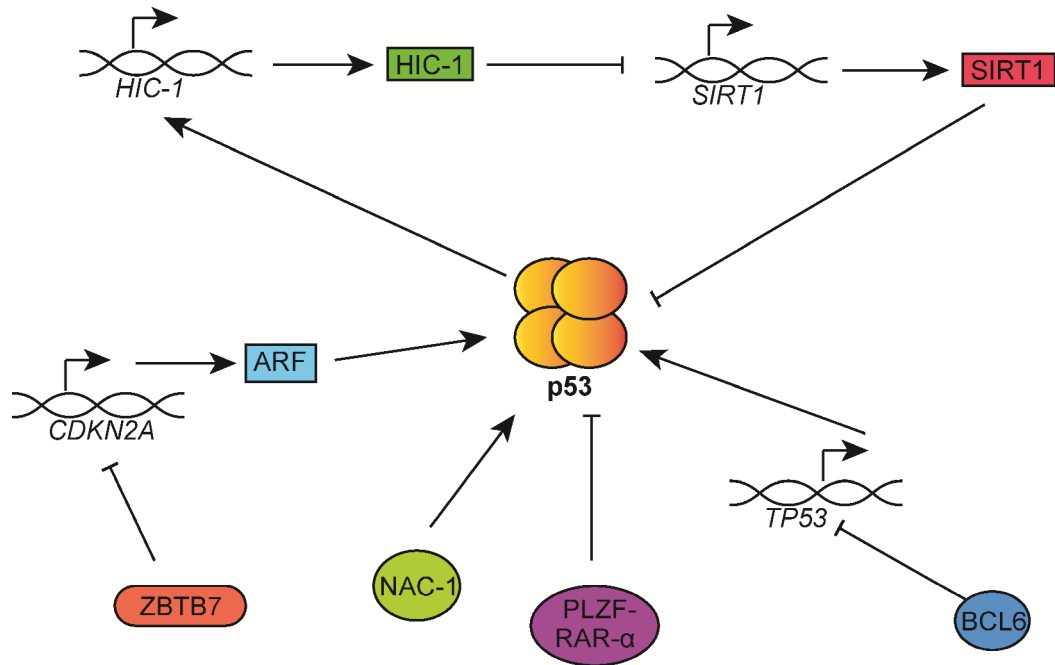


Figure 1.7: BTB-ZF proteins in p53 regulation. Several BTB-ZF proteins are linked to p53 regulation, directly or indirectly. ZBTB7 down regulates *CDKN2A* gene, which expresses ARF, an important protein that regulates the stability of p53. p53 induces HIC-1 expression, which in turn suppresses *SIRT1* gene expression, whose product, SIRT1 protein, deacetylates and inactivates p53. BCL6 represses *TP53* gene. NAC-1 causes increased levels of p53 protein<sup>87</sup>. When PLZF translocates into RAR- $\alpha$  gene, the fusion protein inhibits p53 protein.

of SIRT1 and as a result, degradation of p53. These indications suggest that HIC-1 is a candidate tumor suppressor protein. ZBTB7 is identified as a master regulator of oncogenesis due to its critical role in suppressing ARF expression<sup>90</sup>. In an oncogene transformed cell, ARF is promptly upregulated to activate p53 and apoptosis. However, ZBTB7 is overexpressed in most human cancers and this is a marker for the progression of the disease and outcome of the treatment<sup>91</sup>. Recent studies are directed to target ZBTB7 downregulation in oncogene induced tumorigenesis. These findings indicate that BTB-ZF proteins play important roles during normal biological processes and also during tumorigenesis. Moreover, the functions of BTB-ZF proteins might sometimes coincide with the p53 pathway (Figure 1.7). This is mostly due to their ability to interact with histone modifying enzymes such as histone acetyltransferases (HDAC) and histone deacetylases (HATs) and a wide variety of co-factors.

### 1.2.3. PATZ1

PATZ1 belongs to the BTB-ZF containing transcription factor family. Although there is not a comprehensive study that covers the function of PATZ1 in tumorigenesis, there are a handful of data that indicate that PATZ1 is involved in tumor development. PATZ1 was first discovered as an interaction partner of BACH2, a BTB-ZF family member, through their BTB domains, and it is found to be expressed in brain, thymus, fetal liver, and bone marrow, and especially in B-cell lines in different stages of development<sup>92</sup>. PATZ1 was also found to interact with RNF4, a ring finger protein family member, through its AT-hook domain<sup>93</sup>. RNF4 plays an important role for androgen receptor activation, however, interaction of RNF4 with PATZ1 changes the activation to repression<sup>94</sup>. This shows that PATZ1 has developmental roles since androgen mechanism is critical for the development of the male reproductive system and for normal and tumorigenic prostate<sup>95</sup>. Indeed, PATZ1 knock-out male mice have smaller testes with a very few spermatocytes due to increased spontaneous apoptosis<sup>96</sup>. In the same study, in human testicular cancer tissues, PATZ1 was found to be upregulated; however, it was mislocalized to the cytoplasm. Also the shRNA mediated downregulation of PATZ1 in glioma cells (brain and central nervous system tumors derived from glial cells) makes them vulnerable to apoptotic stimuli<sup>97</sup>.

Early embryonic expression of PATZ1 has a vital importance for mice because PATZ1 knockout mice are born at a non-Mendelian frequency and are smaller in size<sup>98,99</sup>. Recently, it was found that PATZ1 plays a key role for the maintenance of pluripotency of mouse embryonic stem cells (mESCs), in which it positively controls the expression of the *Pou5fl* (Oct4) and *Nanog* genes that are master pluripotency regulators<sup>100</sup>. PATZ1 is also important for controlled and normal development of T lymphocytes, as it negatively regulates the *Cd8* gene expression during the Double Negative (DN) stage of T lymphocyte development by recruiting chromatin modifying co-factors, such as N-CoR, to the enhancer of *Cd8*<sup>101</sup>. However, during the Double Positive (DP) stage, PATZ1 represses the *Thpok* gene by directly binding to its enhancer, directing these cell to the CD8+CD4- lineage<sup>99</sup>. These data suggest that the

PATZ1 transcription factor can control gene expression in more than one way depending on whether it acts alone or in complex with other co-factors. Similarly, PATZ1 was shown to activate or repress the c-myc promoter; these conflicting results likely arise from the activity of the different alternatively spliced isoforms examined in these studies<sup>92,93</sup>. In the later study, the BTB domain of PATZ1 was required for the transcription repressor activity of PATZ1. This suggests that PATZ1 recruits other co-factors to the promoter using its BTB domain.

A link between p53 and PATZ1 was first established in human endothelial cells. Overexpression of PATZ1 in old and senescent fibroblasts resulted in a reversed senescent phenotype, whereas shRNA mediated knock-down of PATZ1 in young and proliferating fibroblasts accelerated premature senescence<sup>102</sup>. However, this premature senescence in cells that do not express PATZ1 is rescued by shRNA mediated knock-down of p53. This study concluded that PATZ1 regulates senescence in fibroblast through a p53 dependent pathway. In a recent study, PATZ1 was shown to interact with p53 and modulate the transcriptional activity of p53<sup>103</sup>. As many other BTB-ZF family members, PATZ1 was also identified in a chromosomal translocation event. Translocation of the BTB domain of PATZ1 into the zinc finger domain of EWS causes Ewing's sarcoma, which is characterized by a highly aggressive bone and soft tissue tumor usually seen in children<sup>104</sup>. PATZ1 and another BTB-ZF protein BCL6 are found to be interacting from their BTB domains<sup>105</sup>. This interaction results in the downregulation of BCL6 expression. In the absence of PATZ1, mice develop BCL6-expressing lymphomas and die earlier compared to their wild type littermates, hence, PATZ1 has a tumor suppressor activity. Moreover, PATZ1 is upregulated in a series of colorectal cancer tissue, human breast cancer cell lines as well as different cancer cell lines<sup>106,107</sup>. It is associated with cell growth, as its overexpression resulted in increased cell proliferation in the colon cancer cell line SW1116, and downregulation resulted in suppressed proliferation<sup>106</sup>. For this reason, PATZ1 is predicted to be a possible proto-oncogene. These findings indicate that PATZ1 is indeed a factor involved in tumor development; however, it is still unclear if PATZ1 is a proto-oncogene or a tumor suppressor. This remains to be elucidated.

## 2. AIM OF THE STUDY

BTB-ZF family transcription factors function in many distinct biological processes including the development of lymphocytes, stem cell biology, fertility, skeletal morphogenesis, neurological development, and tumorigenesis. These proteins can hetero-dimerize with each other to switch on or enhance their transcriptional activities. They also interact with other distinct transcription factors and recruit chromatin remodeling co-factors to the DNA, such as histone acetyltransferases and histone deacetylases. These interactions mediate epigenetic modifications and enable or disable gene transcription. The roles of BTB-ZF transcription factors in many different and important biological processes make them crucial factors during tumorigenesis. Indeed, many BTB-ZF proteins were identified as modulators of the p53 pathway. The p53 tumor suppressor protein is found to play a major role in many cancer types and therefore any factor that controls p53 activity has vital importance for human health.

We identified the BTB-ZF family transcription factor PATZ1 as a regulator of the p53 dependent DNA damage response. PATZ1 is known to be misexpressed in various human cancers and its absence favors lymphomagenesis in mice and the translocation of the *PATZ1* gene is associated with sarcoma development in humans. We aimed to elucidate the molecular mechanisms utilized by PATZ1 in tumorigenesis. We found that PATZ1 was lost upon DNA damage induction. PATZ1 inhibited the transcriptional

activity of p53 in reporter assays. To generalize the finding that PATZ1 regulates p53 activity, we performed genome wide expression analysis in PATZ1 deficient and sufficient cells that were treated with a DNA damage inducing chemical. We identified biological processes in which PATZ1 mediated p53 and DNA damage related functions. In this study, we characterize the transcription factor PATZ1 as a new mediator of the p53 mediated DNA damage response.

### **3. MATERIALS AND METHODS**

#### **3.1. Materials**

##### **3.1.1. Chemicals**

All the chemicals used in this thesis are listed in Appendix A.

##### **3.1.2. Equipment**

All the equipment used in this thesis is listed in Appendix B.

### 3.1.3. Buffers and Solutions

Standard buffers and solutions used in the project were prepared according to the protocols in Sambrook et al., 2001.

Agarose Gel: For 100 ml 1% w/v gel, 1 g of agarose powder was dissolved in 100 ml 0.5X TBE buffer by heating. 0.01% (v/v) ethidium bromide was added to the solution.

Calcium Chloride (CaCl<sub>2</sub>) Solution: 60mM CaCl<sub>2</sub> (diluted from 1M stock), 15% Glycerol, and 10mM PIPES (pH 7.00) were mixed and the solution was filter-sterilized and stored at +4°C.

Blocking Buffer: For 10ml, 0.5 g skim milk powder was dissolved in 10 ml PBS.

FACS Buffer: For 500ml 1X solution, 2.5 g bovine serum albumin (BSA) and 0.5 g sodium azide were mixed in 500 ml 1X PBS and the solution was kept at -20°C.

HEPES-buffered saline (HBS): For 100 ml 2X solution 0.8 g NaCl, 0.027 g Na<sub>2</sub>HPO<sub>4</sub>·2H<sub>2</sub>O and 1.2 g HEPES were dissolved in 90 ml of ddH<sub>2</sub>O. pH was adjusted to 7.05 with 0.5 M NaOH and the solution was completed to 100 ml with distilled water. The buffer was filter-sterilized and stored at -20°C.

PBS-Tween20 (PBST) Solution: For 1 L 1X solution, 0.5 mL Tween20 was added in 1 L 1X PBS.

Phosphate-buffered saline (PBS): For 200 ml 1X solution, 1 tablet of PBS (Sigma P4417) was dissolved in 200 ml ddH<sub>2</sub>O and the solution was filter-sterilized.

Polyethylenamine (PEI) Solution: For 1 mg/ml solution, 100 mg polyethylenamine powder was dissolved in 100 ml ddH<sub>2</sub>O and the pH was adjusted to 7.0 with HCl. The solution was filter sterilized and kept at -20°C.

Protein Loading Buffer: Commercial buffer (Fermentas #R0891) that includes 5X loading dye (0.313 M Tris HCl (pH 6.8 at 25°C), 10% SDS, 0.05% bromophenol blue, 50% glycerol) and 20X reducing agent (2 M DTT) were mixed.

SDS Separation Gel: For 10ml 13% gel, 2.5 ml Tris (1.5M pH 8.8), 3 ml H<sub>2</sub>O, 4.34 ml Acryl: Bisacryl (30%), 100 µl 10% SDS, 100 µl 10% APS, and 10 µl TEMED were mixed.

SDS Running Buffer: For 1 L 10X stock solution, 30.3 g Tris base, 144 g Glycine, and 10 g SDS were dissolved in 1L ddH<sub>2</sub>O.

SDS Stacking Gel: For 5 ml 4% gel, 1.25 ml Tris (0.5 M pH 6.8), 2.70 ml H<sub>2</sub>O, 1 ml Acryl: Bisacryl (30%), 50 µl 10% SDS, 15 µl 10% APS, and 7.5 µl TEMED were mixed.

Transfer Buffer: For 1 L 10X stock solution, 14.5 g Tris and 72 g Glycine were dissolved in 1 L ddH<sub>2</sub>O. Final pH was adjusted to 8.3.

Transfer Buffer: For 800 ml 1X, 80 ml 10X Transfer Buffer, 160 ml methanol, and 560 ml ddH<sub>2</sub>O were mixed.

Tris-Borate-EDTA (TBE) Buffer: For 1 L 10X stock solution, 104 g Tris-base, 55 g boric acid, and 40 ml 0.5M EDTA (pH 8.0) were dissolved in 1 L of ddH<sub>2</sub>O. The solution is kept at room temperature.

#### **3.1.4. Growth Media**

Luria Broth (LB): For 1 L 1X LB media, 20 g LB powder was dissolved in 1 L ddH<sub>2</sub>O and then autoclaved at 121°C for 15 minutes. For selection, kanamycin at a final concentration of 50 µg/ml or ampicillin at a final concentration of 100 µg/ml was added to liquid medium just before use.

LB-Agar: For 1 L 1X agar medium, 20 g LB powder and 15 g bacterial agar powder were dissolved in 1 L ddH<sub>2</sub>O and then autoclaved at 121°C for 15 minutes. Autoclaved medium was poured onto sterile Petri dishes after cooling down to 50°C. For selection, kanamycin at a final concentration of 50 µg/ml or ampicillin at a final concentration of 100 µg/ml was added to the medium before pouring onto petri dishes. Sterile solid agar plates were kept at 4°C.

DMEM: HEK293T, NIH3T3, HeLa, Phoenix, HCT116, HCT116p53<sup>-/-</sup>, U2OS, and H1299 cell lines and primary MEFs were maintained in filter-sterilized DMEM that is supplemented with 10% heat-inactivated fetal bovine serum, 2mM L-Glutamine, 100 unit/ml penicillin and 100 unit/ml streptomycin.

RPMI: 3B4.15, VL3.3M2, EL4, EL4-Ova, AKR1, and RLM11 cell lines and primary CD8<sup>+</sup>CD4<sup>-</sup> thymocyte were maintained in filter-sterilized RPMI1640 that is supplemented with 10% heat-inactivated fetal bovine serum, 2mM L-Glutamine, 100 unit/ml penicillin, 100 unit/ml streptomycin, 1X MEM vitamins, 1X non-essential amino acids and 50µM 2-mercaptoethanol.

Freezing medium: All the cell lines were frozen in heat-inactivated fetal bovine serum containing 10% DMSO (v/v).

### **3.1.5. Commercial Molecular Biology Kits**

- QIAGEN Plasmid Midi Kit, 12145, QIAGEN
- QIAGEN Plasmid Maxi Kit, 12163, QIAGEN
- Qiaprep Spin Miniprep Kit, QIAGEN
- Qiaquick Gel Extraction Kit, 28706, QIAGEN
- Qiaquick PCR Purification Kit, 28106, QIAGEN
- RevertAid First Strand cDNA Synthesis Kit, K1622, FERMENTAS
- SuperScript Double-Stranded cDNA Synthesis Kit, 11917-020, INVITROGEN

- Leukocyte Alkaline Phosphatase Kit, 86R-1kt, SIGMA-ALDRICH

### **3.1.6. Enzymes**

All the restriction enzymes, DNA modifying enzymes and polymerases and their corresponding buffers used in this study were from either Fermentas or NEB.

### **3.1.7. Bacterial Strains**

Escherichia coli DH-5 $\alpha$  (F- endA1 glnV44 thi-1 relA1 gyrA96 deoR nupG lacZdeltaM15 hsdR17) competent cells were used for bacterial transformation of general plasmid DNAs. HB101 strain was used for bacterial transformation of retroviral plasmid DNAs.

### **3.1.8. Mammalian Cell Lines**

HEK293T: Derivative of human embryonic kidney 293 (HEK293) cell line that stably express the large T antigen of SV40 virus (ATCC: CRL-1573™).

NIH3T3: Mouse embryonic fibroblast cell line (ATCC: CRL-1658™).

HeLa: Human epithelial carcinoma cell line (ATCC: CCL-2™).

Phoenix-Eco: Second-generation retrovirus producer cell line based on HEK293T cell line that express gag-pol-env proteins for the generation of helper free ecotropic retroviruses <sup>108</sup>.

HCT116 and HCT116p53-/-: Human colorectal carcinoma cell line and its p53-null derivative (ATCC CCL-247™)

U2OS: Human osteosarcoma cell line (ATCC HTB-96™)

H1299: Human non-small cell lung cancer cell line (ATCC CRL-5803™)

3B4.15: CD4+CD8- murine T cell hybridoma cell line that is specific to pigeon cytochrome C in association with I-E<sup>k</sup> <sup>109</sup>.

VL3.3M2: CD4+CD8+ murine thymic lymphoma cell line <sup>110</sup>.

EL4 and EL4-Ova: CD4+CD8- murine lymphoma cell line and its chicken ovalbumin (OVA) overexpressing derivative (ATCC TIB-39™ and ATCC CRL-2113™, respectively).

AKR1: CD44- murine T-lymphoma cell line <sup>111</sup>.

RLM11: Radiation-induced CD4+CD8- murine thymoma cell line <sup>112</sup>.

### **3.1.9. Plasmids and Primers**

The plasmids and the primers used in this thesis are listed in Table 3.1 and Table 3.2, respectively.

PLASMID NAME	PURPOSE OF USE	SOURCE
PCMV-HA	Cloning	Clontech
pCMV-myc	Cloning	Clontech
pCMV-HA-PATZ1	Mammalian Expression	Lab Construct
pCMV-HA-PATZ1Alt	Mammalian Expression	Lab Construct
pCMV-myc-PATZ1	Mammalian Expression	Lab Construct
pCMV-myc-PATZ1Alt	Mammalian Expression	Lab Construct
pFlag-CMV4	Cloning	Clontech
pFlag-CMV4-p53	Mammalian Expression	Ozoren Lab, Bogazici University
SV40-p53 $\alpha$	Mammalian Expression	Bourdon Lab, Dundee University
SV40-p53 $\beta$	Mammalian Expression	Bourdon Lab, Dundee University
pBABE-Puro	Cloning	Addgene: #1764
pBABE-Puro-PATZ1	Mammalian Expression	Lab Construct
pMIG-GFP/NEO	Cloning	Ellmeier Lab, Medical University of Vienna
pMIG-GFP/NEO-PATZ1	Mammalian Expression	Lab Construct
pMIGII-mCherry	Cloning	Lab Construct
pMIGII-mCherry-PATZ1	Mammalian Expression	Lab Construct
pMIGII-mCherry-PATZ1Alt	Mammalian Expression	Lab Construct
pMIGII-mCherry-PATZ1-R372G	Mammalian Expression	Lab Construct
pMIGII-mCherry-PATZ1-R403G	Mammalian Expression	Lab Construct
pMIGII-mCherry-PATZ1-R424G	Mammalian Expression	Lab Construct
pCMV-HA-PATZ1-R372G	Mammalian Expression	Lab Construct
pCMV-HA-PATZ1-R394G	Mammalian Expression	Lab Construct
pCMV-HA-PATZ1-R403G	Mammalian Expression	Lab Construct
pCMV-HA-PATZ1-R424G	Mammalian Expression	Lab Construct
pCMV-HA-PATZ1-R456G	Mammalian Expression	Lab Construct
pCMV-HA-PATZ1-N495Y	Mammalian Expression	Lab Construct
pCMV-HA-PATZ1-D521Y	Mammalian Expression	Lab Construct
pCMV-HA-PATZ1-D521Y/D527Y	Mammalian Expression	Lab Construct
LMP-sh29 (shPATZ1)	Knocking Down Mouse PATZ1 Expression	Lab Construct
LMP-sh62	Knocking Down Mouse PATZ1 Expression	Lab Construct
pcDNA-GFP	Mammalian Expression	Lab Construct
pG13	Luciferase Reporter	Addgene: #16442
mG15	Luciferase Reporter	Addgene: #16443
p21-LUC	Luciferase Reporter	Addgene: #16451
Puma-LUC	Luciferase Reporter	Addgene: 16591
pRLSV40	Luciferase Normalization	Promega
pCAG-T7	Cloning	Starker Lab, University of

		Minnesota
pCAG-T7-hMAZR-TALENfwd	Disrupting Human <i>PATZI</i> Gene	Lab Construct
pCAG-T7-hMAZR-TALENrev	Disrupting Human <i>PATZI</i> Gene	Lab Construct
MSCV pGK eGFP	Cre-mediated loxP recombination	Ellmeier Lab, Medical University of Vienna
MSCV pGK eGFP-CRE	Cre-mediated loxP recombination	Ellmeier Lab, Medical University of Vienna
pIRES2eGFP	Cloning	Clontech
pIRES2eGFP-mCAT	Mammalian Expression	Lab Construct

Table 3.1: The list of the plasmids used in this thesis. Plasmid names, their purpose of uses and sources are given.

PRIMER NAME	SEQUENCE	PURPOSE OF USE
h_p21rt_fwd	GCAGACCAGCATGACAGATTT	p21 qPCR
h_p21rt_rev	GGATTAGGGCTTCCTCTTGGA	p21 qPCR
puma fwd	ACCAGCCCAGCAGCACTTAG	puma qPCR
puma rev	TCTTCTTGTCTCCGCCGCTC	puma qPCR
gapdh fwd	TCCTGCACCACCAACTG	gapdh fwd
gapdh rev	TCTGGGTGGCAGTGATG	gapdh rev
mouse e2f	GCACACTTCTGAGCGACCTCACAAGTG	semi q rtPCR
mouse e3r	TGCTGGAGTGTGCTGGACTCAGG	semi q rtPCR
mouse e6r	TCAATCAGATCCTGATGTGAGCAT	semi q rtPCR
human e4f	GGCCCAGCAACTTCTGCAGTATC	semi q rtPCR
human e6r	TGAGAGGTCACCATAGGAGTCAGAG	semi q rtPCR
human e2f	TCAAGCAGGTGCACACTTCTGAG	semi q rtPCR
human e3r	TGGGACGACCTCCACAAAGC	semi q rtPCR
human e4f qPCR	CAATGCTTCTTTTGCCACCC	Patz degradation qPCR
human e4-6r qPCR	ATTTCTGGCCTTCTCGGTTACA	Patz degradation qPCR
F2	GGGTCTAGCCCTTTTATTAGAGC	mouse

		Patz1 genotyping
R2	GAAGCTCTCGTCGCCTACTC	mouse Patz1 genotyping
CreR2	GTTATGTTCTATTAAGGTCCAGTGACC	mouse Patz1 genotyping
EBV-rev	GTGGTTTGTCCAAACTCATC	sequencing
CMV-fwd	CGCAAATGGGCGGTAGGCGTG	sequencing
Arg372Gly-Fwd	TATACCATCTCAACGGGCATAAAGCTTTCC	PATZ1 Arg372Gly mutation
Arg372Gly-Rev	CGTCACGAAAGATCTTGCCACAGATC	PATZ1 Arg372Gly mutation
Arg403Gly-Fwd	TCGTACCATGTGGGGTCCCATGATG	PATZ1 Arg403Gly mutation
Arg403Gly-Rev	CATTCGGTCTTTTCTCTTGAACCGCAG	PATZ1 Arg403Gly mutation
Arg424Gly-Fwd	GAAAGGTTTCTCCGGGCCAGATCACTTG	PATZ1 Arg424Gly mutation
Arg424Gly-Rev	CCACAGCTCTGGCAGATGTACGGTTTG	PATZ1 Arg424Gly mutation
hMAZRtALENcontrolFwd	TGGCAGGCGCGTTTGCAG	Human PATZ1 genotyping after TALEN
hMAZRtALENcontrolRev	GAAGCTCTCGTCGCCTACCC	Human PATZ1 genotyping after TALEN

Table 3.2: The list of the primers used in this thesis. Primer names, their sequences, and their purpose of uses are given.

### 3.1.10. DNA and Protein Molecular Weight Markers

DNA ladders and protein molecular weight markers used in this thesis are listed in Appendix C.

### 3.1.11. DNA Sequencing

Sequencing service was commercially provided by McLab, CA, USA. (<http://www.mclab.com/>).

### 3.1.12. Software, Computer-Based Programs, and Websites

The software and computer based programs used in this project are listed in Table 3.3

<b>SOFTWARE, PROGRAM, WEBSITE NAME</b>	<b>COMPANY/WEBSITE ADDRESS</b>	<b>PURPOSE OF USE</b>
NCBI BLAST	<a href="http://blast.ncbi.nlm.nih.gov/Blast.cgi">http://blast.ncbi.nlm.nih.gov/Blast.cgi</a>	Basic local alignment search tool
FlowJo V10	Tree Star Inc.	Viewing and analyzing flow cytometry data
ImageJ	<a href="http://imagej.nih.gov/ij/">http://imagej.nih.gov/ij/</a>	Counting IPSC colonies

CLC Main Workbench	CLC bio	Constructing vector maps, restriction analysis, DNA sequencing analysis, DNA alignments, etc
Ensembl Genome Browser	<a href="http://www.ensembl.org/index.html">http://www.ensembl.org/index.html</a>	Human and mouse genome
LightCycler 480 SW 1.5	ROCHE	Analysing qPCR results
RTCA Software 2.0	ACEA Biosciences	Real-time cell growth analysis
DAVID Bioinformatics Resources 6.7	NIAID, NIH	Bioinformatics analysis of RNAseq data
ANAIS	<a href="http://anais.versailles.inra.fr/">http://anais.versailles.inra.fr/</a>	Bioinformatics analysis of NimbleGen arrays
Cytoscape	<a href="http://www.cytoscape.org/">http://www.cytoscape.org/</a>	Network data integration, analysis, and visualization
GenePattern	<a href="http://genepattern.broadinstitute.org/">http://genepattern.broadinstitute.org/</a>	Creating heatmaps for RNAseq data

Table 3.3: The list of the software, programs and websites used in this thesis. Name of the software, programs, and websites, their producers/websites and purpose of uses are given.

## 3.2. Methods

### 3.2.1. Bacterial Cell Culture

**Bacterial Culture Growth:** Escherichia coli (E. coli) DH5 $\alpha$  strain was grown in Luria Broth (LB) or 2XLB (low salt), overnight at 37°C, shaking at 250 rpm. For long-term storage of bacterial cells, glycerol was added to the overnight grown culture to a

final concentration of 10% in 1 mL in a cryovial. Bacterial glycerol stocks were stored at -80°C. In order to obtain single colonies, bacteria were spread on LB/agar containing petri dishes using glass beads and incubated overnight at 37°C without any shaking. All growth medium were supplemented with or without selective antibiotic prior to any application.

Preparation and Transformation of Competent Bacteria: A single colony of *E.coli* DH5 $\alpha$  was picked from an LB/agar petri dish (incubated overnight without any antibiotic selection). The colony was inoculated in 50 mL LB without any selective antibiotics in a 200 mL flask and incubated at 37°C overnight, shaking at 250 rpm. The next day, 4 mL from this overnight culture was diluted in 400 mL LB medium in a 2 L flask and incubated at 37°C overnight, shaking at 250 rpm until the optical density (at 590 nm) reached 0.375. The culture was then transferred into 50 ml polypropylene tubes (8 tubes in total) and incubated on ice for 10 min, followed by a centrifugation at 1600 g for 10 min at 4°C. After centrifugation, each pellet was resuspended in 10 mL ice-cold CaCl<sub>2</sub> solution and centrifuged at 1100 g for 5 min at 4°C. The pellets were again resuspended in 10mL ice-cold CaCl<sub>2</sub> solution and incubated on ice for 30 min. Following the final centrifugation at 1100 g for 10 min at 4°C, this time the pellets were resuspended in 2mL ice-cold CaCl<sub>2</sub> solution and pooled in a single polypropylene tube (16 ml bacterial solution in total). This solution was dispensed into 200 $\mu$ L aliquots into pre-chilled 1.5ml centrifuge tubes. Competent cells were frozen immediately in liquid nitrogen and then stored at -80°C for later use. Transformation efficiency of the competent cells (typically 10<sup>7</sup>-10<sup>8</sup> cfu/ $\mu$ g) was tested by pUC19 plasmid transformation, using different concentrations of the plasmid DNA.

Chemically competent cell was taken out from -80°C and mixed with 100 pg of plasmid DNA. The cells were then incubated on ice for 30 min. After the incubation period, the cells were heat shocked for 90 s at 42°C and transferred back on ice for 60 s. 800  $\mu$ L of LB (without any antibiotics) was added on the cells and this culture was incubated for 45 min at 37°C. After 45 min, the cells were spread with glass beads on LB/agar petri dishes containing appropriate antibiotic for selection. The plate was incubated overnight at 37°C without any shaking.

Plasmid DNA Isolation: Plasmid DNA isolation was performed using either the alkaline lysis protocol from Molecular Cloning: A Laboratory Manual (Sambrook *et al*) or Qiagen Mini-Midiprep Kits according to the manufacturer protocols. The concentration and purity of the DNA isolated were determined by using a UV- or a NanoDrop- spectrophotometer.

### 3.2.2. Plasmid Construction

Polymerase Chain Reaction (PCR): Optimized PCR conditions are shown in Table 3.3. The thermal cycler conditions were as follows: initial denaturation at 95°C for 5 min followed by 30 (or 35) cycles of denaturation step (at 95°C, for 30 seconds), annealing step (at a temperature specific for every primer pair, for 30 seconds) and an extension step (at 72°C, for 1 min for every 1 kilobase of DNA). These cycles were then followed by a final extension step at 72°C for 10 min.

PCR Reaction	Volume Used	Final Concentration
Template DNA	1-10 $\mu\text{L}$	4pg/ $\mu\text{L}$ – 4ng/ $\mu\text{L}$
10X Pfu or Taq Polymerase Buffer (with $\text{MgCl}_2$ )	2.5 $\mu\text{L}$	1X
dNTP mix (10 mM each)	0.5 $\mu\text{L}$	0.2mM
Forward Primer (10 $\mu\text{M}$ )	2 $\mu\text{L}$	0.8 $\mu\text{M}$
Reverse Primer (10 $\mu\text{M}$ )	2 $\mu\text{L}$	0.8 $\mu\text{M}$
Pfu or Taq Polymerase (2.5U/ $\mu\text{L}$ )	0.125 $\mu\text{L}$	0.125 U/ $\mu\text{L}$
ddH <sub>2</sub> O	Up to 25 $\mu\text{L}$	-
Total	25 $\mu\text{L}$	-

Table 3.4: Optimized PCR conditions

Restriction Enzyme Digestion: Restriction enzyme digestion reactions were performed by mixing the required amount of DNA with the desired enzymes and their compatible buffers in 1.5 mL centrifuge tube, followed by incubation in a waterbath set to a temperature optimum for the enzymes for a duration of 2 hours. For diagnostic digestions 1µg of DNA was used. 10µg or more DNA was digested for gel extraction and cloning purposes. If the plasmid DNA was digested with a single restriction enzyme and was planned to be used in a ligation reaction, then the linear plasmid was dephosphorylated by calf intestinal alkaline phosphatase (CIAP) enzyme for an additional 45 min at 37°C.

Agarose Gel Electrophoresis: PCR products, digestion reaction products and other DNA samples were separated and visualized by agarose gels. Gels were prepared by dissolving the required amount of agarose (ranging from 0.5 g to 3 g depending on the sizes of the DNA fragments in the samples) in 100mL 0.5X TBE. In order to fully dissolve the agarose, the mixture was heated in a microwave oven. The solution was then cooled down and 2µl of ethidium bromide was added. After mixing properly, the gel was cast in a gel apparatus and cooled down and solidified. DNA samples were mixed with DNA loading dye were loaded into the gel, which was run at 100V for 75 min in 0.5X TBE and the bands were visualized using UV light on a Biorad Imager. Desired DNA bands were excised from the gel and extracted using a Qiagen Gel Extraction Kit according to the manufacturer protocol.

Ligation: Ligation reactions were performed by using T4 DNA Ligase, in 1:3, 1:5 or 1:10 vector to insert ratio, using 50 ng of the plasmid DNA. Ligation reactions were incubated at 16°C for overnight. The next day, the ligation mixture was transformed into chemically competent DH5α bacteria and plated onto antibiotic selective-LB/agar petri dishes and incubated at 37°C.

### 3.2.3. Mammalian Cell Culture

Maintenance of Cell Lines: The 3B4.15, VL3.3M2, EL4, EL4-Ova, AKR1, and RLM11 cell lines and primary CD8<sup>+</sup>CD4<sup>-</sup> thymocytes were maintained in RPMI1640 medium in tissue culture flasks in an incubator set to 37°C with 5%CO<sub>2</sub>. Cells were splitted into pre-warmed, fresh medium with a ratio of 1:20 once in two or three days. HEK293T, NIH3T3, HeLa, Phoenix, HCT116, HCT116p53<sup>-/-</sup>, U2OS, and H1299 cell lines and primary MEFs were maintained in DMEM medium in tissue culture plates in an incubator set to 37°C with 5%CO<sub>2</sub>. When the confluency of the cells reached over 80%, the cells were split into pre-warmed, fresh medium with a ratio of 1:10. In order to freeze cells for later use, cells at the exponential growth phase were resuspended in ice-cold freezing medium and transferred to cryovials. Tubes were stored at -80°C for at least 24 h and then transferred to liquid nitrogen tank for long- term storage. After thawing the cells, they were immediately washed with growth medium to remove any residual DMSO.

Transient Transfection of Cell Lines Using Polyethylenimine (PEI): One day before the transfection, 1-3 x 10<sup>6</sup> cells were split onto 10 cm tissue culture plates. On the day of the transfection, 10 µg of plasmid DNA was mixed in 1 mL serum-free DMEM in a sterile micro centrifuge tube. PEI (1µg/µL) was added to the DNA-DMEM mix at a 3:1 ratio of PEI (µg) to total plasmid DNA (µg) and mixed immediately by vortexing. After 15 minutes of incubation at room temperature, the mixture was added drop wise on the cells.

Retroviral Infection: In order to produce retrovirus, the packaging cell line HEK293-Phoenix-Eco was transfected by the PEI method using 12 µg retroviral plasmid DNA and 3µg of packaging plasmid pCL-Eco. 48 hours after the transfections, supernatants of the cells were collected and filtered through 0.45µm filters. Polybrene (at a final concentration 8 µg/ml) was added to the filtered supernatant that contains the virus. Murine cells to be infected were split one day before the infection, so they would

be 60-80% confluent on the day of infection. The viral supernatant (with polybrene added) was used to infect the target murine cells. The growth medium of the cells were replaced the viral supernatant and the cells were returned to their incubators for 3 h. Then, the viral supernatant was discarded and fresh medium was added onto the cells. The cells were returned to their incubators for 24 h. The next day, a second infection was performed using the identical procedure. In order to infect human cell lines with ecotropic retrovirus, cells were pseudotyped by first transfecting them with the pIRES2eGFP-mCAT (mouse cationic amino acid transporter) plasmid 24 h prior to the first infection. For stable infections, 48 h after the second infection, the growth medium of the cells were supplemented with an appropriate antibiotic (typically puromycin at 1 µg/ml concentration).

Cell Lysis, SDS Gel, Transfer and Western-Blot: Cells were harvested from their cell culture plates either using trypsin or a cell scraper. Cells were centrifuged at 1000 rpm for 5 min and the supernatant was discarded. The cells were washed once with 1X PBS and the pelleted again. The pellet was dissolved in an appropriate amount of protein loading buffer and the mixture was boiled at 95°C for 10 min. The lysates were either kept at -80°C for later use or used immediately. The SDS gels used in this project had a 10% separating part and a 4% stacking part. After the samples were loaded into the SDS gels, the gels were run with 1X running buffer at 100 V (constant voltage) for 1.5 - 2 h using a BIORAD Mini Protean Tetra Cell. After running, the gels were transferred to 0.45 µm PVDF membranes (Thermo Scientific) in 1X transfer buffer at 250 mA (constant current) for 1.5 h at 4°C using BIORAD Mini Trans-blot. Membranes were then blocked in 10 mL PBST - milk at room temperature for 1 hour with constant shaking. Primary antibody incubations were done overnight at 4°C and secondary antibody incubations were done for 1 hour at room temperature. After every incubation, membranes were washed with PBST 3 times for 10 min each. After the final washing step, the membranes were incubated with an enhanced chemiluminescent substrate for 5 min at room temperature in the dark room and exposed to X-Ray films (Fuji).

### 3.2.4. RNA-Sequencing and Microarray

RNA-Sequencing: PATZ1 knockout or WT MEFs were prepared from mice embryos at day 13.5. Early passage MEFs were either untreated or treated with 1 $\mu$ M doxorubicin for 8 hours. Total RNA was extracted, polyA selected and triplicate samples were sequenced at Beijing Genomics Institute on an Illumina HiSeq 2000 sequencing machine and analyzed using the R library DEseq. Differentially expressed genes (DEGs) were obtained based on the following criteria: fold-change > 2 and FDR value < 0.001. To identify biological processes regulated by PATZ1, DAVID analysis was performed for gene ontology (GO) terms. P-values are calculated by DAVID and GO terms that have smaller than 0.01 P-values are listed as significant.

Microarray: Early passage MEFs were either untreated or treated with 1 $\mu$ M doxorubicin for 24 hours. Total RNA was extracted using TriReagent (Sigma). Double-stranded cDNA was generated using a Super-Script cDNA Synthesis Kit (Invitrogen), and the cDNA was then labeled with Cy-3, cleaned, quantified, and hybridized according to the manufacturer's protocols (Roche - Nimblegen). Nimblegen full genome Mouse Expression arrays (12X135K) were washed and scanned at the Sabanci University Nanotechnology Research and Application Center-SUNUM. Results were processed using the ANAIS. Array quality was assessed at the probe level. Values for 3 probes for each gene in each array were combined to summarize gene expression from probe sets. Robust Multi-Array Analysis background normalization and quantile normalization were performed for intra- and inter-array normalization, respectively. Genes with signal intensities above a 95% random threshold were chosen for further studies. Differentially expressed genes were obtained based on the following criteria: fold-change >2 and p value < 0.05.

## 4. RESULTS

### 4.1. PATZ1 is Expressed in Different Cell Lines

In the present study, we identified the BTB-ZF family member PATZ1 transcription factor as a regulator of the tumor suppressor protein p53. PATZ1 regulates the transcriptional activity of p53 and has a marked impact on the DNA damage response induced by the treatment with the DNA damage inducing genotoxic drug doxorubicin (adriamycin). The human PATZ1 gene is located on the long arm (q12.2) of chromosome 22. The gene spans 20500 base pairs and consists of 6 exons (Ensemble accession number ENSG00000100105). There are 4 known alternatively spliced transcripts of PATZ1. All of the transcripts share the first two exons that encode most of the protein, including the BTB domain, the two AT hook motifs and the first 4 zinc finger motifs (Figure 4.1). The differences between the transcripts arise from the rest of the exons, which encode the C-terminus of the proteins. The human and the mouse *PATZ1* genes share high homology, such that the identity of the protein products is over 99%. We analyzed the expression of PATZ1 by exon specific amplification of alternatively spliced mRNAs and found that all

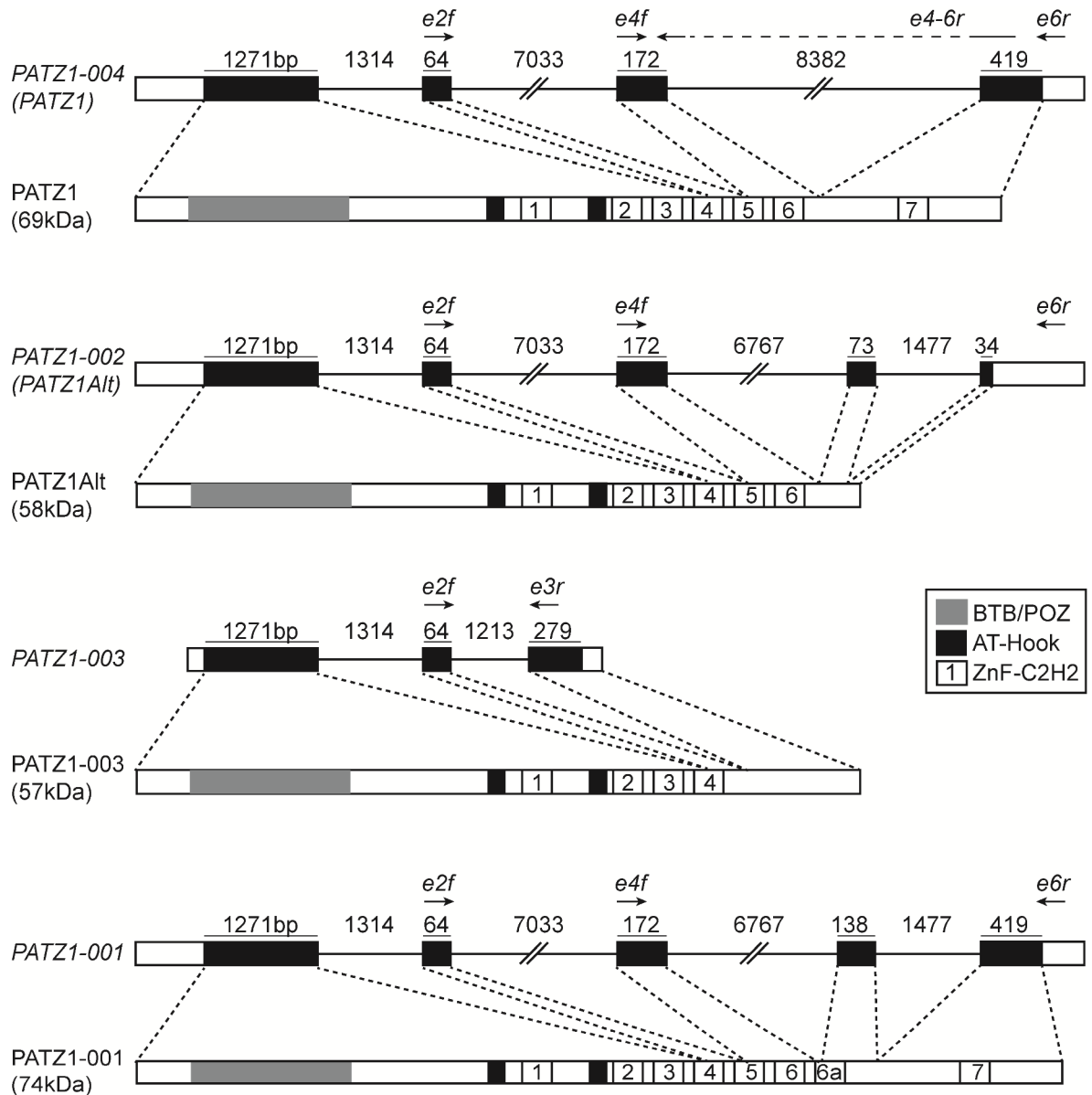
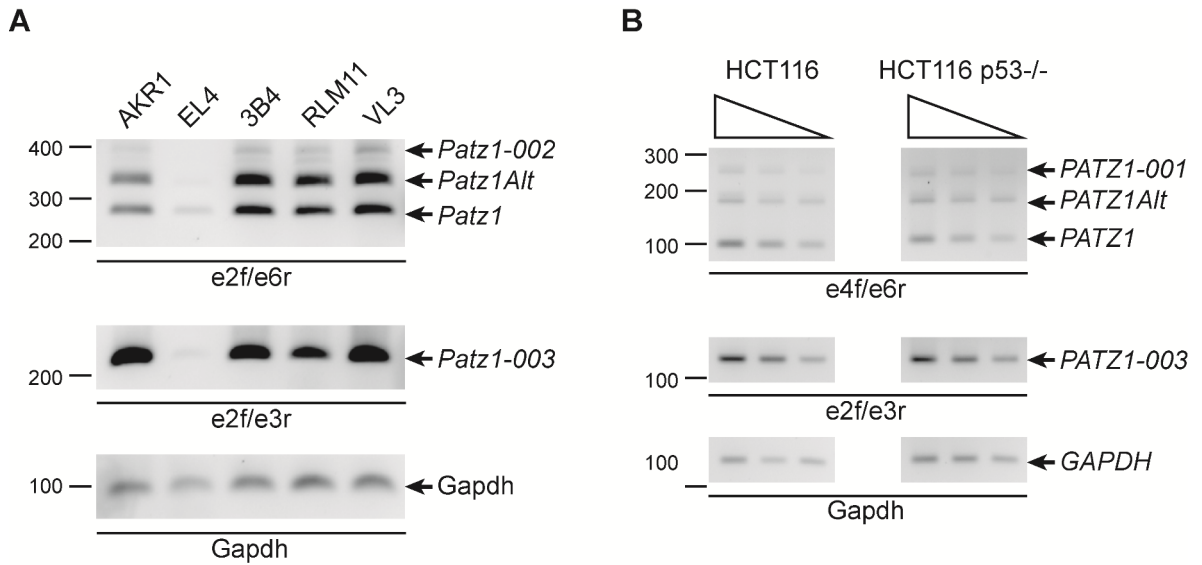


Figure 4.1: Exon structure of the human PATZ1 gene and the protein products encoded by alternative splice variants. The standard names of the alternative splice versions and the name and molecular size of the proteins they encode are indicated on the left. In the gene structure schematics, protein coding exons are shown in black boxes, introns are shown as lines with their size indicated in base pairs and 5' and 3' non-coding regions are shown as open boxes. In the protein schematics, grey boxes represent the protein-protein interaction BTB/POZ domain, black boxes represent the DNA binding AT hook domains and numbered boxes represent the zinc finger motifs. Exon specific primers used for reverse transcription amplification are indicated as arrows above the exons.

The exon structure of the mouse and human genes are highly similar, such that hPATZ1-001=mPATZ1-002, hPATZ1-002 (PATZ1Alt)=mPATZ1-012, hPATZ1-004 (PATZ1)=mPATZ1-001 and hPATZ1-003=mPATZ1-003.

four isoforms were expressed in various mouse T lymphocyte cell lines (Figure 4.2A), in the human colon carcinoma cell line HCT116 and its p53<sup>-/-</sup> version (Figure 4.2B).

We found that hPATZ1-004 and hPATZ1-002 are the major expressed isoforms in the cells examined in this study. For the sake of simplicity, throughout this thesis, we refer to these two isoforms as PATZ1 and PATZ1Alt, respectively.



**Figure 4.2: PATZ1 alternative splice variants are expressed in various cell lines. A.** Expression of PATZ1 alternative splice variants in mouse T lymphocyte cell lines. Amplification with the primers indicated below the gels resulted in unique size amplicons indicating the presence of alternatively spliced mRNAs in the indicated cell lines. *Gapdh* specific primers were used to generate loading controls. **B.** PATZ1 alternative splice variants are expressed in human HCT116 cells. Amplification with the primers indicated below the gels resulted in unique size amplicons indicating the presence of alternatively spliced mRNAs in HCT116 (left column) or HCT116 p53<sup>-/-</sup> (right column) cells. Semi-quantitative amplification was performed with 3 fold diluted cDNA samples used as amplification templates. *GAPDH* specific primers were used to generate loading controls.

## 4.2. Transcription Repression Activity of PATZ1

PATZ1 was associated with transcription repression as well as transcription activation in various studies <sup>113,114</sup>. We wanted to analyze and characterize the transcription repression activity of PATZ1. One known target of the PATZ1 protein is the CD4 T lymphocyte specific *Thpok* gene. This gene is repressed by PATZ1 and therefore not expressed in CD8 T lymphocytes <sup>99</sup>. Previous experiments showed that when PATZ1 expression is deleted by knocking out the *Patz1* gene in developing thymocytes of mice, the *Thpok* gene is activated in CD8+CD4- T-cells, where it normally stays repressed <sup>99</sup>. In order to study the effects of overexpressing PATZ1 in CD8+CD4- cells, we used a model mouse where PATZ1 expression was specifically deleted in developing thymocytes. To obtain these mice, we bred a *Patz1* gene targeted mouse which has a "floxed" *Patz1* exon 1 flanked by loxP sequences (*Patz1* f/f) with a transgenic mouse expressing the Cre recombinase specifically in developing T lymphocytes (Lck-Cre Tg) (Figure 4.3). *Patz1* f/f x Lck-Cre Tg mice cannot express PATZ1 protein in their T lymphocyte populations. To study the effect of PATZ1 on *Thpok* gene expression, we bred these mice with knock in mice, where one allele of the *Thpok* gene was replaced with a GFP expression cassette, by which the *Thpok* expression can be assessed by GFP fluorescence in targeted lymphocytes. For this THPOK reporter experiment, we examined GFP expression in PATZ1 overexpressing (mCherry positive) CD8 T lymphocytes purified from lymph node T lymphocytes.

We used this mouse model system to study the effect of PATZ1 re-expression on *Thpok* gene expression in *Patz1* knockout CD8 SP T lymphocytes. To this end, we generated retroviruses expressing *Patz1* cDNA along with an mCherry fluorescent reporter protein, and infected CD8 SP T lymphocytes from *Patz1*f/f x Lck-Cre Tg x *Thpok*::GFP mice (Figure D.1 and Figure 4.4). To generate PATZ1 and mCherry expressing retroviruses, we cloned the *Patz1* cDNA into an mCherry expressing retroviral plasmid. In this system we track *Patz1* expression in infected cells with mCherry fluorescence and endogenous *Thpok* gene expression using the knock in

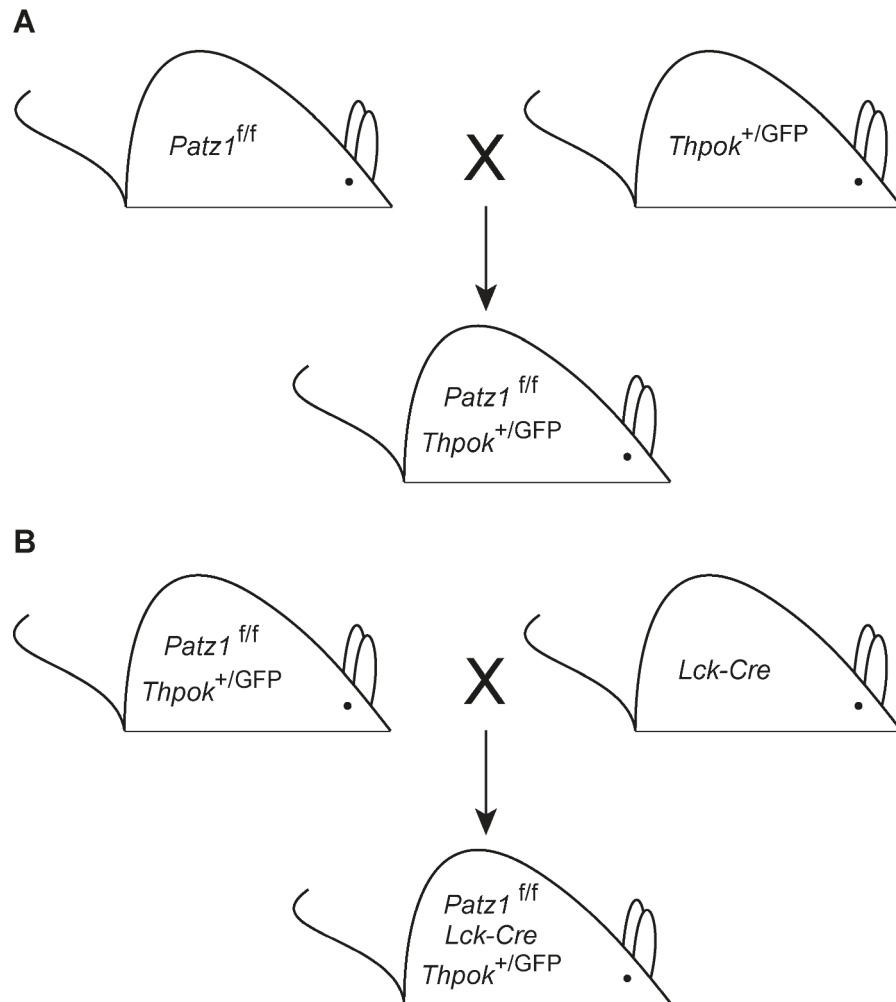


Figure 4.3: Breeding of PATZ1 deficient or sufficient *Thpok* reporter mice. **A.** Generation of PATZ1 sufficient *Thpok* reporter mice. Exon 1 region of the *Patz1* gene is flanked by two loxP sites. This mouse was bred with another knock in mouse, which introduced a GFP reporter into the *Thpok* gene locus. This mouse has a WT *Thpok* on one allele and the GFP reporter on the second allele. So we can use the GFP expression to study *Thpok* expression. **B.** PATZ1 deficient *Thpok* reporter mice. To delete the *Patz1* gene, we crossed previous mouse with an *Lck-Cre* transgene mouse, which expresses cre, only in T lymphocytes.

GFP fluorescence. In this system, *Patz1* targeted CD8<sup>+</sup>CD4<sup>-</sup> T lymphocytes express GFP from the activated *Thpok* allele. When we re-establish PATZ1 expression in *Patz1* targeted CD8<sup>+</sup>CD4<sup>-</sup> T lymphocytes, we observed that THPOK expression was repressed (Figure 4.5). This experiment demonstrates that PATZ1 is a transcriptional repressor of the *Thpok* gene.

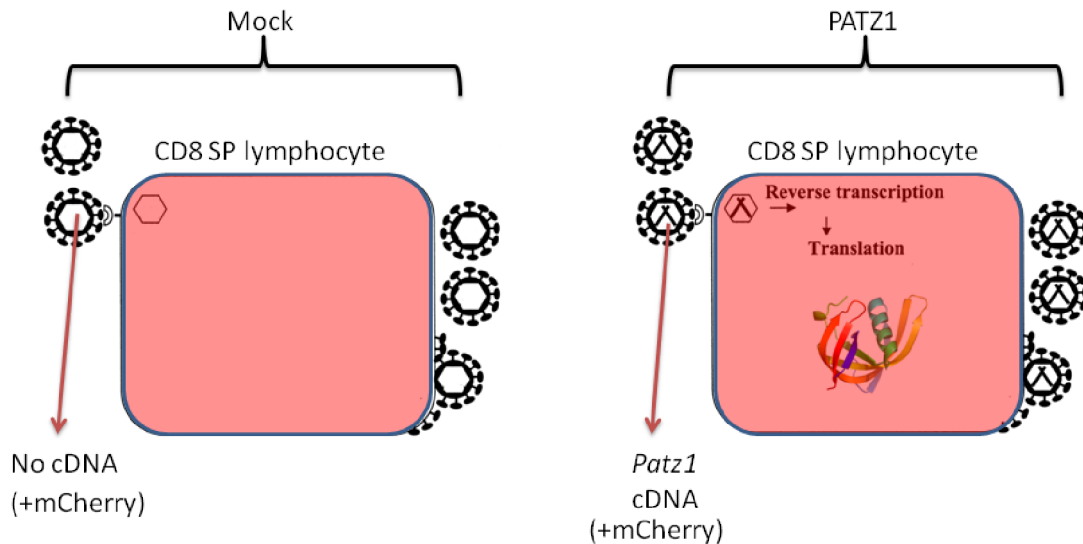


Figure 4.4: Retroviral infection of CD8 SP lymphocytes. We generated retroviruses expressing *Patz1* cDNA or no cDNA (mock) along with an mCherry fluorescent reporter protein, and infected CD8 SP T lymphocytes from *Patz1<sup>f/f</sup> x Lck-Cre Tg* or *Patz1<sup>f/f</sup> x Lck-Cre Tg x Thpok::GFP* mice. Infected cells can be tracked by checking their mCherry expression by flow cytometry.

To test the idea that the C-terminus of PATZ1 is required for the transcriptional repressor activity of PATZ1 on the *Thpok* gene expression, we used PATZ1Alt expressing retroviruses in our THPOK reporter experiment. We found that PATZ1Alt is capable of repressing *Thpok* gene expression to the same extent as PATZ1 (Figure 4.6). Therefore, we conclude that PATZ1 does not require its C-terminus for all transcription repressor activity.

Next, we wanted to characterize the important residues of PATZ1 for transcriptional repressor activity. Using knowledge obtained by previous homology modeling studies and multiple protein sequence alignments of related BTB-ZF proteins (shown previously by Jitka Eryilmaz), we identified several candidate arginine residues within the zinc finger domain of PATZ1, which we thought would be critical for DNA recognition and binding. We mutated these arginine residues to glycine residues one by one (R372G, R403G, and R424G) in our *Patz1* cDNA and mCherry expressing retroviral constructs. We used these constructs in the THPOK reporter experiment to assess if these PATZ1 mutants retained their transcription repressor activity (Figure 4.7). We observed that among the mutants we tested, the arginine 372 (R372) and

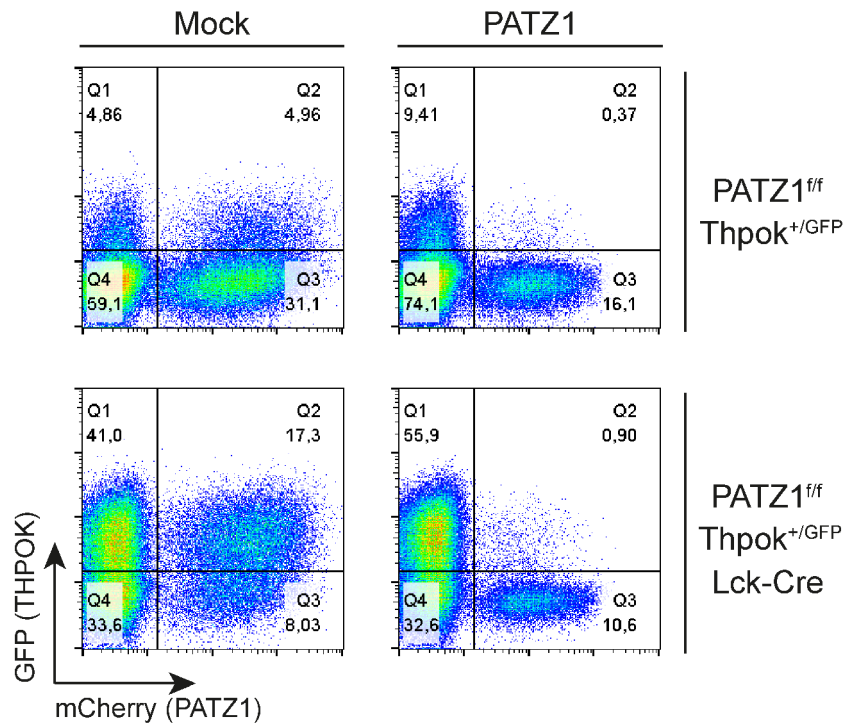


Figure 4.5: Reconstruction of PATZ1 expression in PATZ1<sup>-/-</sup> CD8<sup>+</sup>CD4<sup>-</sup> cells represses *Thpok*. We determined the effect of overexpressing PATZ1 on the expression of the *Thpok* gene (GFP) in the presence (PATZ1<sup>f/f</sup>, upper row) or in the absence (PATZ1<sup>f/f</sup> x LCK-CRE, lower row) of endogenous PATZ1 protein. Primary CD8<sup>+</sup>CD4<sup>-</sup> T lymphocytes were purified from thymus by flow cytometry, and infected with pMIG-mCherry based *Patz1* cDNA expressing (right column) or empty retrovirus (left column). We assessed *Thpok* expression by GFP fluorescence and PATZ1 expression by mCherry fluorescence. In this FACS plots, mCherry expression from the virus is shown on the X-axis and GFP expression from the endogenous *Thpok* gene locus is shown on the Y-axis. To see the inhibitory effects of PATZ1 expression on the *Thpok* expression, we should look at the decrease in the mcherry<sup>+</sup>/GFP<sup>+</sup> (Q2 quadrant) in PATZ1 overexpressing and endogenous PATZ1 deficient cells (bottom right plot) compared to mock infected and endogenous PATZ1 deficient cells (bottom left plot).

the arginine 424 (R424) residues are important for PATZ1 repressor activity because the R372G and the R424G mutants of PATZ1 cannot repress the expression of THPOK as efficiently as the WT PATZ1. These results indicate that PATZ1 binds to the ThPOK gene promoter using these residues and represses transcription.

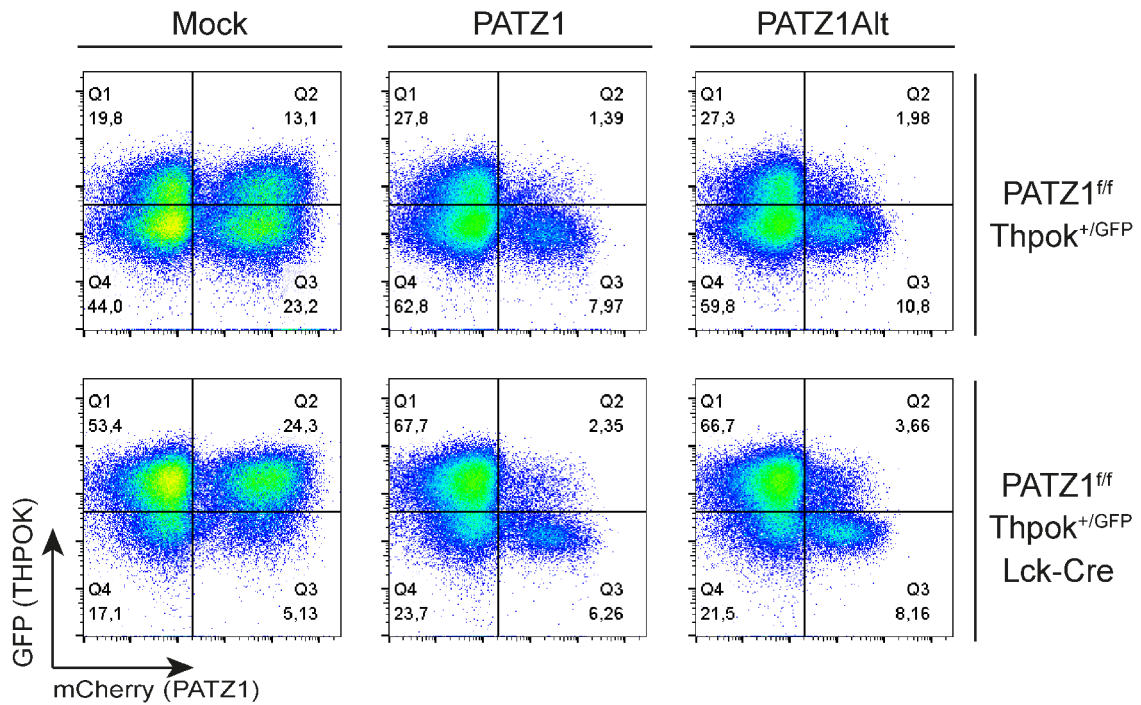


Figure 4.6: PATZ1 does not require its C-terminus for its transcription repressor activity. We determined the effect of overexpressing PATZ1 or PATZ1Alt on the expression of the *Thpok* gene (GFP) in the presence (PATZ1<sup>f/f</sup>, upper row) or in the absence (PATZ1<sup>f/f</sup> x LCK-CRE, lower row) of endogenous PATZ1 proteins. Primary CD8<sup>+</sup>CD4<sup>-</sup> T lymphocytes were purified from thymus by flow cytometry and infected with pMIG-mCherry based *Patz1Alt* cDNA expressing (right column), *Patz1* cDNA expressing (middle column) or empty retrovirus (left column). We assessed *Thpok* expression by GFP fluorescence and PATZ1 expression by mCherry fluorescence.

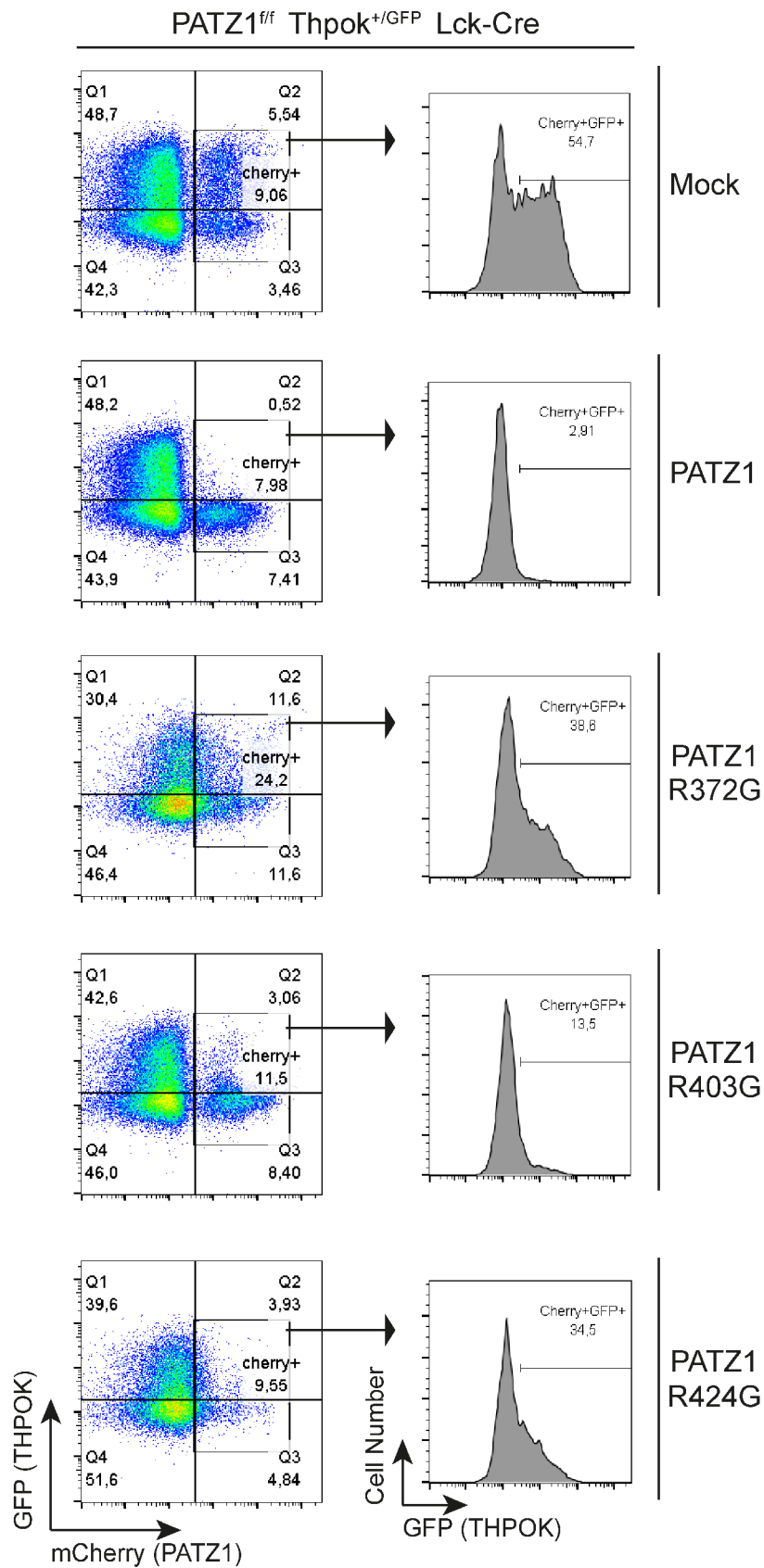


Figure 4.7: Several residues within the zing finger domain of PATZ1 are crucial for transcription repressor activity. We created site directed mutant PATZ1 constructs (R372G, R403G, and R424G) and determined the effect of overexpressing these on the

expression of the *Thpok* gene (GFP) in the absence (PATZ1f/f x LCK-CRE) of endogenous PATZ1 protein. Thymocytes were infected with pMIG-mCherry based WT or mutant PATZ1 expressing or empty retrovirus. mCherry vs. GFP profiles of CD8+CD4- thymocytes are on the left column and the GFP percentages within the mCherry positive sub-population is on the right column. Each row represents a construct used to infect the cells (mock, WT, or a mutant). We assessed *Thpok* expression by GFP fluorescence and PATZ1 expression by mCherry fluorescence.

### 4.3. Global Effects of PATZ1 on Gene Transcription

To gain new insights into the global effects of PATZ1 on transcription regulation, we performed genome scale RNA-Seq and microarray experiments. For these experiments, we used primary MEF cells that are an *in vivo* relevant and widely studied model system. We used MEFs, which were sufficient or deficient for *PATZ1* (Figure 4.8A). We isolated total RNA from these samples and analyzed the identity and quantity of transcribed genes by RNA sequencing performed on an Illumina HiSeq 2000 platform at the Beijing Genomics Institute. We compared the expression values (RPKM - reads per kilobase per million) of genes in PATZ1 WT and KO MEFs (KO vs WT) and identified 156 differentially expressed genes (DEGs), of which 83 were upregulated and 73 were downregulated, in PATZ1 KO MEFs (Figure 4.8B). As PATZ1 is expressed in MEF, we concluded that these genes, which are up and downregulated, are direct targets which are respectively inhibited and activated by PATZ1. To obtain an overview of the biological processes that are significantly enriched in the DEGs in our KO vs. WT comparison, we performed DAVID<sup>115</sup> gene ontology (GO) analysis and found that in the absence of PATZ1, biological processes such as 1) cell adhesion, 2) neuron development and differentiation and 3) cell morphogenesis are significantly affected (Table 4.1). These processes that were significantly altered in the absence of PATZ1, correlate with and offer an explanation to several recent findings on the outcome of PATZ1 deficiency. Consistent with our GO term analysis, PATZ1-null mice

are born smaller in size and at a non-Mendelian frequency <sup>101</sup>. Moreover these mice are born with defects in their central nervous systems <sup>98</sup> and furthermore mESC with impaired expression of PATZ1 lose their pluripotency and start to differentiate <sup>100</sup>.

<b>GO Term Related to Biological Process</b>	<b>P-Value</b>
GO:0007155~cell adhesion	7.65E-06
GO:0022610~biological adhesion	7.82E-06
GO:0043030~regulation of macrophage activation	1.26E-03
GO:0007409~axonogenesis	1.81E-03
GO:0048812~neuron projection morphogenesis	2.66E-03
GO:0000902~cell morphogenesis	3.04E-03
GO:0048667~cell morphogenesis involved in neuron differentiation	3.14E-03
GO:0030182~neuron differentiation	4.22E-03
GO:0048858~cell projection morphogenesis	5.23E-03
GO:0032989~cellular component morphogenesis	6.50E-03
GO:0000904~cell morphogenesis involved in differentiation	6.58E-03
GO:0032990~cell part morphogenesis	6.58E-03
GO:0031175~neuron projection development	7.51E-03
GO:0018149~peptide cross-linking	7.73E-03
GO:0048666~neuron development	8.26E-03
GO:0030198~extracellular matrix organization	8.27E-03

Table 4.1: Biological process GO terms that are enriched in our DEG set (generated by comparing KO vs. WT MEFs). P-values are calculated by DAVID and GO terms that have smaller than 0.01 P-values are listed.

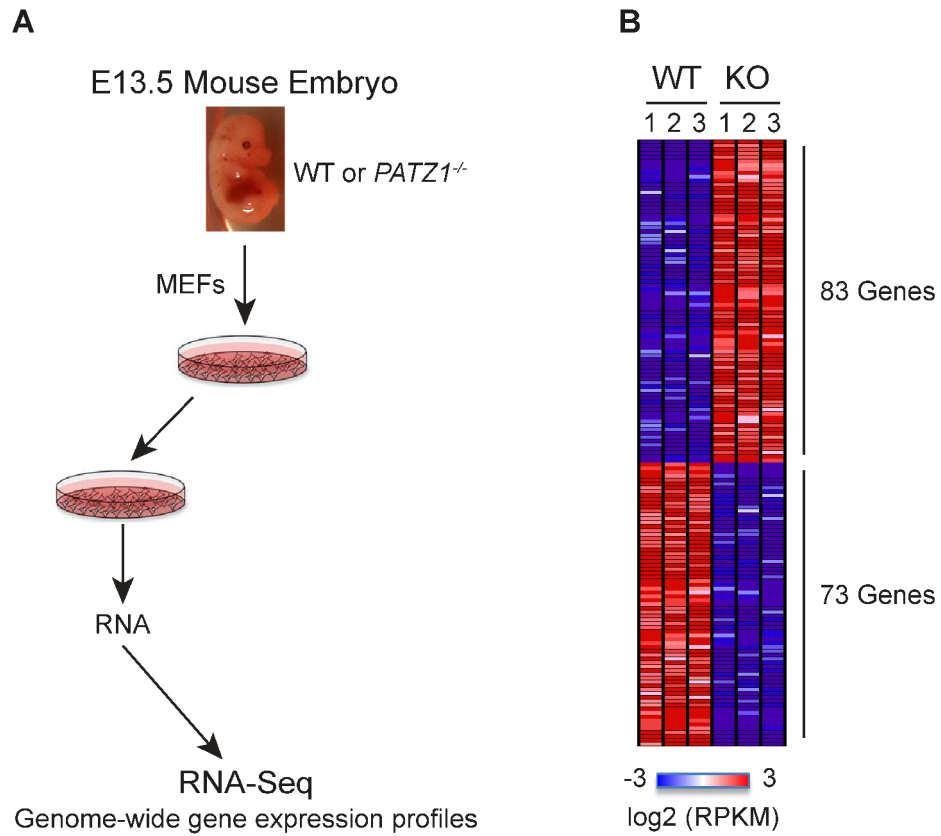


Figure 4.8: Genome wide gene expression analysis of MEFs expressing or deficient in *PATZ1* by RNA-Seq. **A.** *PATZ1* knockout or WT MEFs were prepared from mouse embryo at E13.5. Total RNA was extracted, polyA selected and triplicate samples were sequenced at Beijing Genomics Institute on an Illumina HiSeq 2000 platform and analyzed using the R library DEseq. **B.** *PATZ1* deficient MEFs (KO vs WT) differentially express 156 genes (83 upregulated and 73 downregulated), shown here by a heatmap. Fold change > 2, FDR < 0.001.

## 4.4. Effects of PATZ1 on Cell Proliferation

### 4.4.1. PATZ1 Shortens Cellular Doubling Time

Because PATZ1-null mice are born smaller in size<sup>101</sup> and because we identified biological process terms in PATZ1 deficient MEFs that are related to developmental processes, we speculated that PATZ1 may have an effect on cellular

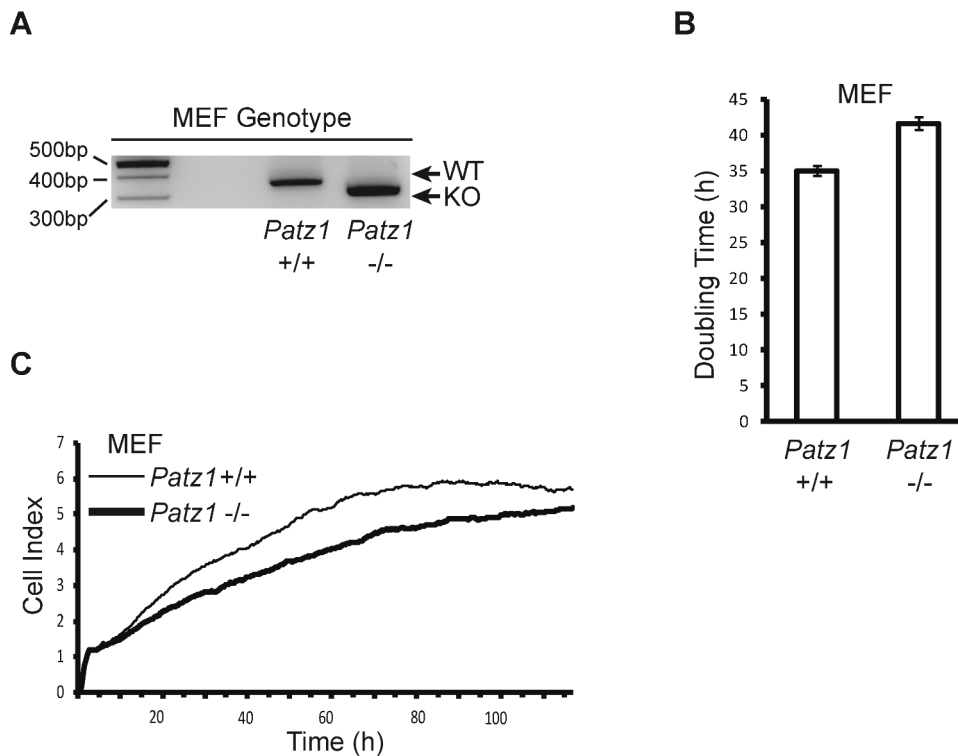


Figure 4.9: MEFs lacking *Patz1* expression proliferate slower. **A**. Confirmation of the genomic structure of *Patz1* WT and *Patz1* -/- MEFs. Primers specific for the size difference between the WT and targeted *Patz1* alleles were used to amplify MEF genomic DNA. Amplicons showing the WT (+/+) or KO (-/-) status of these MEFs are indicated with arrows. **B**. Doubling time of *Patz1* -/- and WT MEFs. Doubling time was calculated by xCELLigence RTCA DP system. **C**. Growth curves of *Patz1* -/- (bold line) and WT (thin line) MEFs. Growth curves were calculated by the xCELLigence RTCA DP system using impedance measurements every 15 minutes.

proliferation rates. To this end, we examined the growth rates and doubling times of different cell lines. First, we generated MEFs from WT or *PATZ1*<sup>-/-</sup> C57BL/6 mice. We genotyped these MEFs to ensure that they really were WT or knock out for the *PATZ* gene (Figure 4.9A). We examined the growth properties of these MEFs in a real time cell analysis apparatus (Acea, California). *PATZ1*<sup>-/-</sup> MEFs proliferated significantly slower than WT MEFs and changes in proliferation rate were evident by calculated doubling time, which significantly increased for MEFs deficient for *PATZ1* expression (Figure 4.9B and 4.9C). Next, we created an overexpression situation to identify the effects of excess *PATZ1* on proliferation rates. We stably infected HCT116 cells with mock or *Patz1* cDNA encoding viruses (Figure E.1). We

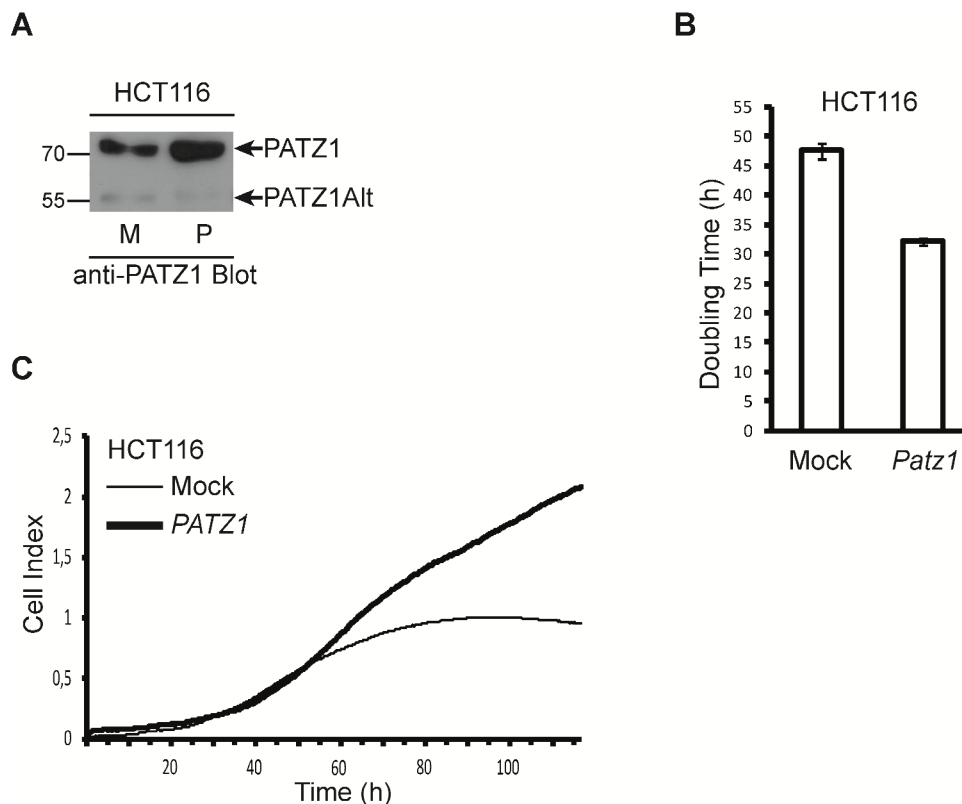


Figure 4.10: *PATZ1* overexpressing HCT116 cells proliferate faster. **A.** Generation of *PATZ* overexpressing HCT116 cells. Retroviruses were packaged and used to stably infect. Increased *PATZ1* expression is shown in HCT116 cells infected with pBabe-Puro based *Patz1* cDNA expressing (P) but not empty virus (M) by anti-*PATZ1* blotting. **B.** Doubling time of *mock* or *Patz1* infected HCT116. Doubling time was calculated by xCELLigence RTCA DP system. **C.** Growth curves of HCT116 cells infected with mock (thin line) or *Patz1* (bold line) expressing retroviruses. Growth curves were calculated by the xCELLigence RTCA DP system using impedance measurements every 15 minutes.

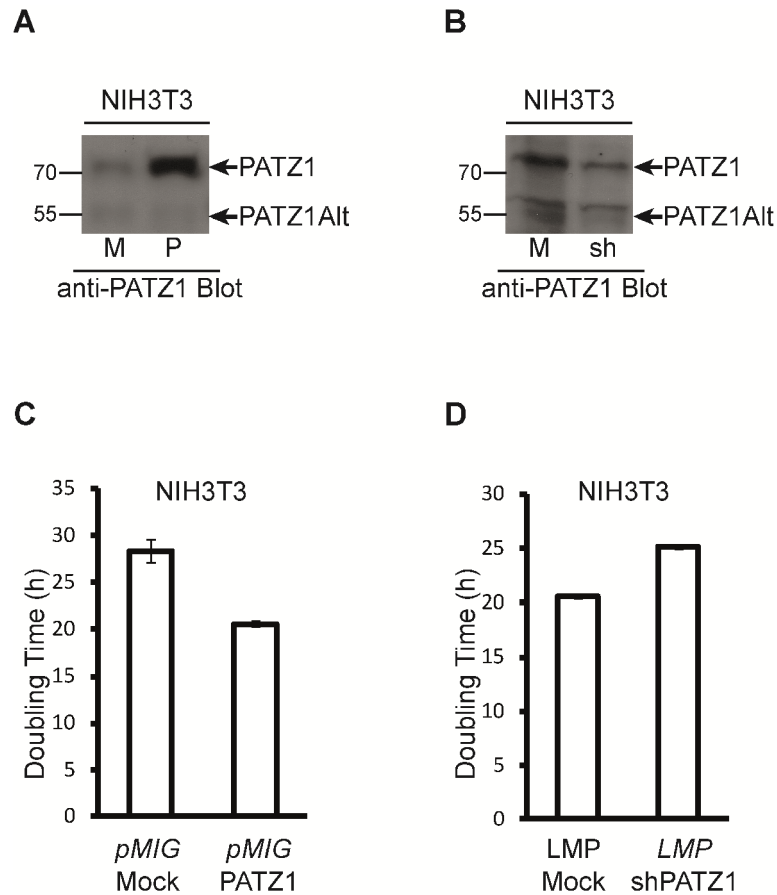


Figure 4.11: PATZ1 expression is inversely correlated with doubling time in NIH3T3 cells. **A.** Generation of PATZ overexpressing NIH3T3 cells. Western blotting with anti-Patz1 antibodies demonstrates that PATZ1 expression is increased in NIH3T3 cells infected with pMIG-GFP/neo based retroviruses expressing either *Patz1* cDNA (P) but not in empty virus infected cells (M). **B.** Generation of NIH3T3 cells with knocked down PATZ1 expression. Impaired PATZ1 expression is shown in NIH3T3 cells infected with LMP based shRNA against *Patz1* (sh) but not empty virus (M) by anti-PATZ1 blotting. **C.** Doubling time of *mock or Patz1* infected NIH3T3 cells. Doubling time was calculated by xCELLigence RTCA DP system. **D.** Doubling time of mock or shRNA against PATZ1 infected NIH3T3 cells.

confirmed the overexpression of PATZ1 protein levels by western blotting (Figure 4.10A). In contrast to the knock-out situation in MEFs, overexpression of PATZ1 protein in HCT116 cells increased the rate of proliferation and resulted in decreased doubling times (Figure 4.10B and 4.10C). In order to generalize the effects of PATZ1 on cell proliferation, we alternatively knocked down the expression of endogenous PATZ1 using retroviruses expressing shRNAs or overexpressed PATZ1 ectopically in NIH3T3 cells (Figure F.1). We confirmed that cells stably infected with cDNA encoding retroviruses successfully overexpressed, while cells stably infected with shRNA encoding retroviruses knocked down PATZ1 expression (Figure 4.11A and

4.11B). Consistent with previous results with the MEF and HCT116 models, NIH3T3 cells with enhanced PATZ1 expression displayed shorter doubling times, while PATZ1 knockdown NIH3T3 displayed longer doubling times (Figure 4.11 and 4.11D). These data in 3 different cell types demonstrate that the PATZ1 protein has a positive impact on cellular proliferation rates.

#### **4.4.2. Effects of PATZ1 on Cell Cycle Progression**

We speculated that the positive effects of PATZ1 on cellular proliferation rates might be through the roles of PATZ1 on the regulation of cell cycle progression. In order to check this idea, we used the HeLa-Fucci model; an already established system in which progression of the cell cycle can easily be tracked by observing changes in the expression of fluorescent proteins during distinct phases of the cell cycle<sup>116</sup>. This system relies on the cell cycle stage specific expression of the Geminin and Cdt1 proteins, which are responsible for the licensing of replication origins, a precisely and strictly controlled process, which ensures that replication occurs only once during a cell cycle<sup>117,118</sup>. The protein levels of Geminin and Cdt1 in cells are inversely regulated. Cdt1 levels are high during the G1 phase, but when cells enter S phase, Cdt1 protein rapidly gets degraded as Geminin starts to accumulate and stays stabilized during S/G2/M phases. Geminin expression ceases as the cells progress further into G1 phase again<sup>117</sup>. The Fucci system takes advantage of this highly conserved mechanism by fusing a red fluorescent protein to Cdt1, and a green fluorescent protein to Geminin. Therefore, G1 cells are labelled red, cells that are in transition from G1 to S phase are labelled orange (i.e. both green and red), S/G2/M cells are labeled green, and cells that are in transition from M to G1 are colorless (i.e. neither green nor red) (Figure 4.12A and 4.12B).

**A**

## HeLa-Fucci Cells

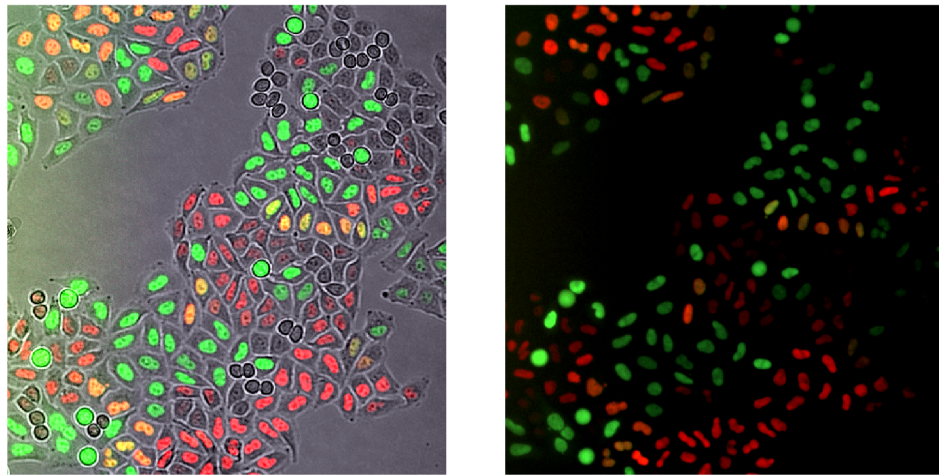
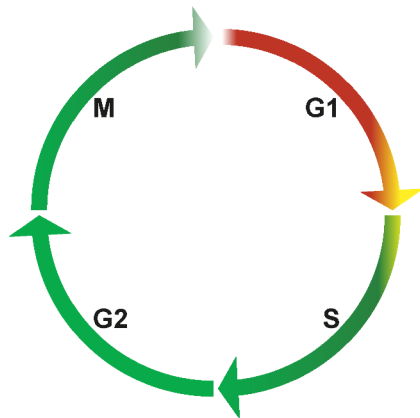
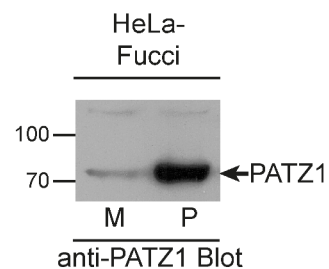
**B****C**

Figure 4.12: The use of Fucci-expressing HeLa cells to investigate cell-cycle progression. **A.** Fucci-Hela cells express red or green fluorescent proteins depending on their cell cycle phases. Under the fluorescent microscope, HeLa-Fucci cells display red or green fluorescence. **B.** Schematic representation of the colors of HeLa-Fucci cells during the cell cycle. G1 cells are red, cells that are in transition from G1 to S phase are orange, S/G2/M cells are green, and cells that are in transition from M to G1 are colorless. **C.** Generation of PATZ1 overexpressing HeLa-Fucci cells. Retroviruses were packaged and used to stably infect HeLa-Fucci cells as described in methods section of this thesis. Increased PATZ1 expression is revealed by anti-PATZ1 blotting in HeLa-Fucci cells infected with *Patz1* cDNA expressing (P) but not empty (M) retrovirus.

We stably infected HeLa-Fucci cells with mock or *Patz1* cDNA carrying viruses. The overexpression was confirmed by assessing protein levels using western blotting (Figure 4.12C). We analyzed these cells by flow cytometry in order to check their fluorescence patterns during the exponential growth phase (Figure 4.13). To our

surprise, cell cycle distribution among the mock or PATZ1 overexpressing Fucci-HeLa cells was not significantly different. Next, we wanted to check whether PATZ1 has any impact on cell cycle control during the DNA damage response. For this purpose, we induced DNA damage by treating PATZ1 overexpressing cells with the genotoxic drug cisplatin in order to arrest the cell cycle. Cisplatin was our cell cycle arrest drug of choice because the more commonly used doxorubicin is red fluorescent and interferes with the detection of Fucci fluorescence.

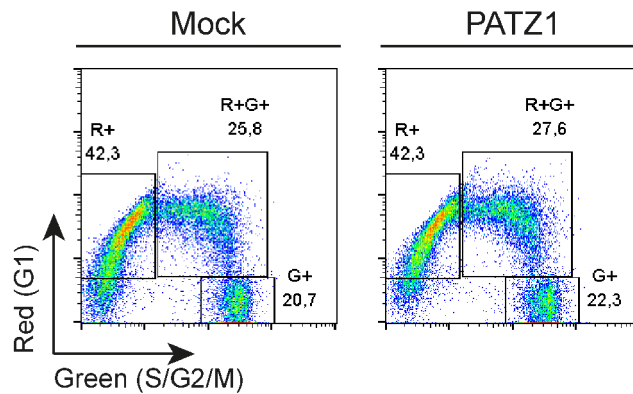


Figure 4.13: Overexpression of PATZ1 in HeLa-Fucci cells does not alter cell-cycle distribution. HeLa-Fucci cells, which are infected either with mock or *Patz1* cDNA carrying viruses, showing red (R+), orange (R+G+), and green (G+) fluorescence were analyzed with flow cytometry.

We found that cisplatin treatment caused G2 arrest (Figure 4.14) as HeLa-Fucci cells accumulate in the green fluorescence positive quadrant of the dot plot representation of the flow cytometric analysis. We followed the speed of the restoration of the cell cycle during the recovery of cells from cisplatin induced arrest. When we allowed arrested cells to recover for 24 hours, the cell cycle distribution was not different between the mock infected or PATZ1 overexpressing cells; however, there were minor differences when we prolonged the recovery period to 48 hours. The percentage of PATZ1 overexpressing cells returning to the G1 stage (red positive) was lower than cells infected with mock retrovirus. This result indicates that PATZ1 plays a role during cell cycle progression; however, the minor differences we observed suggest that PATZ1 is not a major player in this particular HeLa-Fucci system. We also wanted to check the effects of PATZ1 on cell cycle restoration without any induced DNA damage. For this purpose, we purified cells that are in the G1 (red) and S/G2/M (green)

phases from mixed cell populations using fluorescence-activated cell sorting (FACS) and observed the progression of the purified cells through their normal cell cycle (Figure 4.15). We did not detect any significant differences among the cell cycle restoration rates of mock infected or PATZ1 overexpressing HeLa- Fucci cells when they start the cell cycle from either the G1 or the S/G2/M phase. Thus, we concluded that PATZ1 did not significantly alter cell cycle distribution when overexpressed in HeLa-Fucci cells. However, xCELLigence experiments for the doubling time analysis had showed that PATZ1 expression shortens cellular doubling times. This inconsistency might be due to cell type specificity. To address this issue, we will study Fucci system in different cell types.

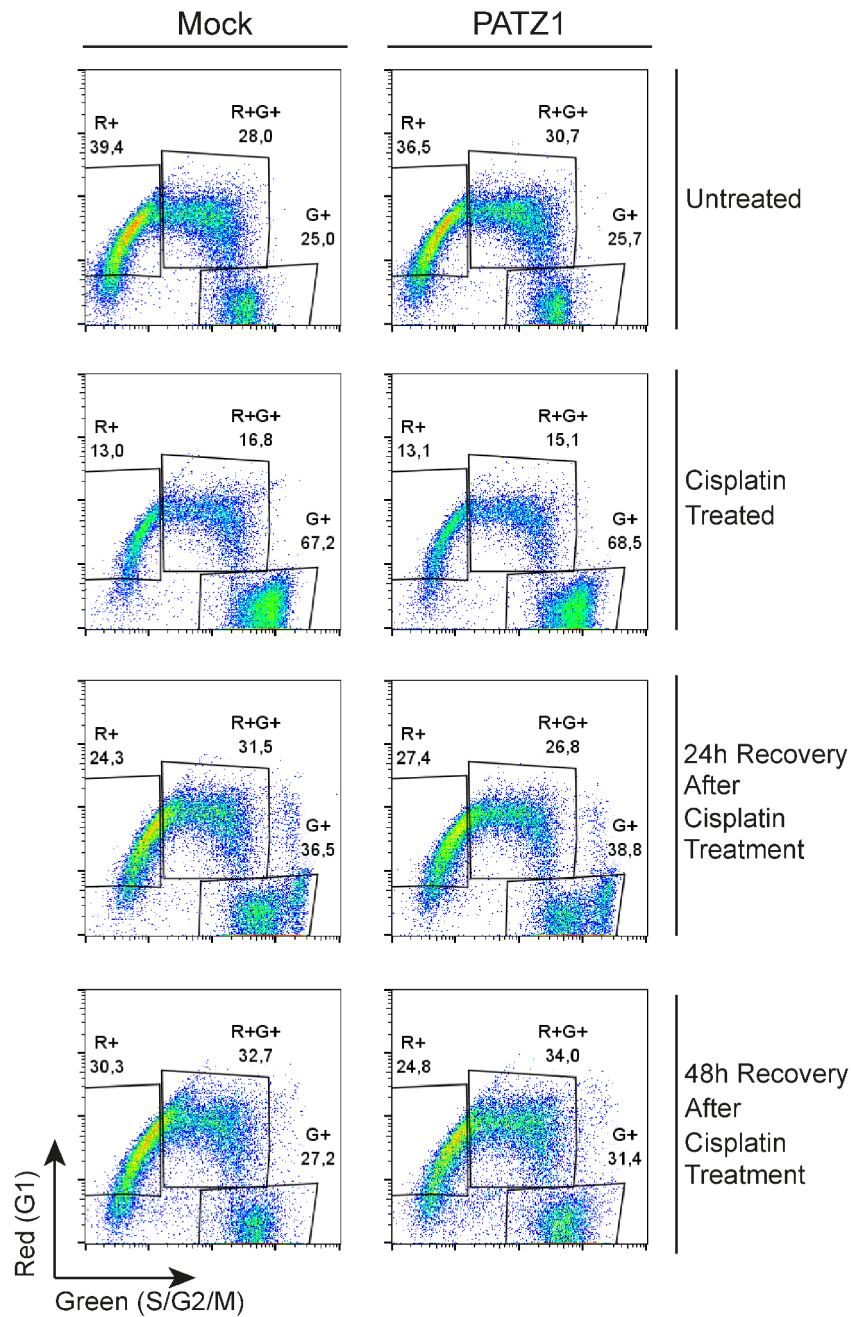


Figure 4.14: Cisplatin treatment results in a reversible G2 arrest in HeLa-Fucci cells. Mock infected HeLa-Fucci cells (left column) or PATZ1 overexpressing HeLa-Fucci cells (right column) were either untreated (first row) or treated with 0.5 $\mu$ M cisplatin for 24 hours (second row). Cisplatin was withdrawn after 24 hours and the growth medium was refreshed to allow cells to recover for additional 24 hours (third row) or 48 hours (last row). At every time point, the cell cycle stage of the cells was determined by flow cytometric analysis of fluorescence.

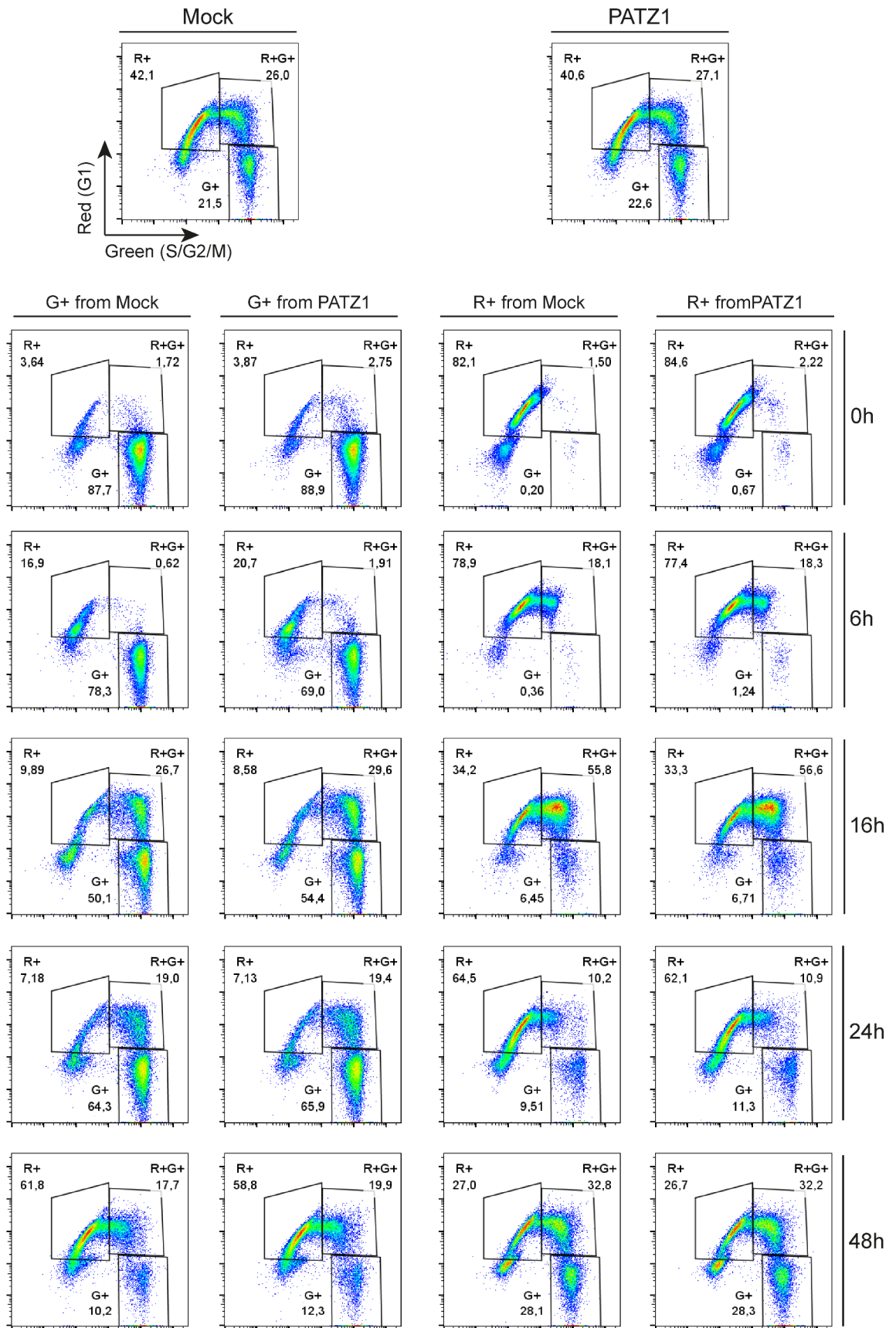


Figure 4.15: Cells that are purified with respect to their cell cycle phase progress through the cell cycle and restore a normal distribution. Mock (upper left plot) or

PATZ1 overexpressing (upper right plot) HeLa-Fucci cells in the S/G2/M (green –left two columns) or G1 (red –right two columns) phases were purified using fluorescence-activated cell sorting (FACS). Purified cells were allowed to restore their cell cycle distribution and analyzed by flow cytometry to check their cell cycle progression, at the indicated times (on the right side of the plots).

#### 4.5. PATZ1 Inhibits the Transcriptional Activity of p53

p53 is a known regulator of the cell cycle and proliferative responses. In fact, p53 is the major player in these cellular responses, therefore any mechanism controlling the activity of p53 is of vital importance to cellular wellbeing and cancer research. This fact led us to investigate a possible direct link between PATZ1 and p53 proteins. Because PATZ1 can act as a transcription activator as well as a repressor, we hypothesized that PATZ1 might be a regulator of p53 activity. In order to study the effects of PATZ1 on the transcriptional activity of p53, we used different luciferase reporter constructs containing p53 response elements (RE); namely pG13, mG15, p21-LUC, and Puma-LUC (Figure 4.16) <sup>63,119</sup>. In the pG13 plasmid, the expression of the luciferase gene is controlled by 13 copies of canonical p53 REs. mG15 is a control plasmid for pG13, which contains 15 copies of mutated p53 REs. The p21-LUC plasmid contains the promoter of the *CDKN1A* gene, which contains a single p53 RE. The final plasmid, Puma-LUC contains the promoter of the *PUMA* gene and has 2 natural p53 REs.

We first tested whether PATZ1 could affect the ability of p53 in activating transcription from the well established pG13 reporter in different cell lines. As expected, overexpressed p53 specifically activated transcription from this construct when co-transfected into HEK293T or HeLa cells (Figure 4.17A and 4.17B, respectively); however, it failed to induce luciferase expression from the mG15 reporter,

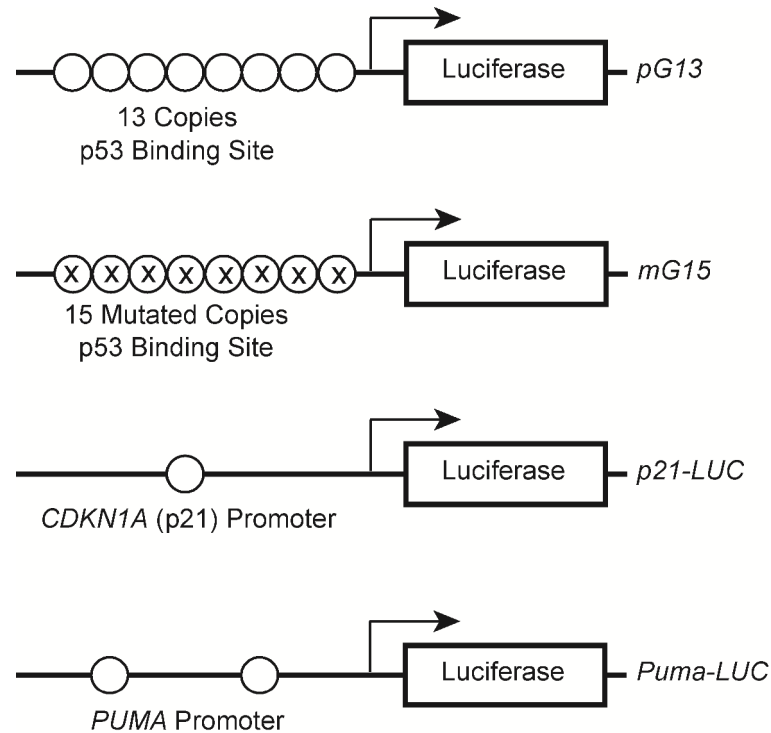


Figure 4.16: Schematic representation of the luciferase reporter constructs used in the study. There are 13 copies of canonical p53 response elements (RE) in the pG13 plasmid driving the expression of the luciferase gene. mG15 is a control plasmid for pG13, in which there are 15 copies of mutated p53 REs. The promoter of the *CDKN1A* gene (with a single p53 RE) drives luciferase expression from the p21-LUC plasmid. The Puma-LUC plasmid carries the promoter of the *PUMA* gene and has 2 natural p53 REs.

showing that p53 activates REs selectively and specifically. PATZ1 expression by itself did not activate transcription from pG13, while PATZ1 and p53 co-expression resulted in a significant decrease in p53 dependent transcription activity. Next, we repeated these luciferase assays with pG13, p21-LUC, and Puma-LUC reporter plasmids in a p53 knock out background, using the HCT116 p53 <sup>-/-</sup> cell line, and found that PATZ1 could also inhibit the ability of p53 to activate transcription from these promoters (Figure 4.18A, 4.18B, and 4.18C, respectively). In these experiments, the alternative splice variant PATZ1Alt could not suppress p53 activity as effectively as PATZ1. PATZ1Alt also does not interfere with PATZ1's inhibitory role when co-expressed. Because the difference between PATZ1 and PATZ1Alt is in the C-terminus of the proteins, we concluded that the C-terminal region of PATZ1 is required for its inhibitory role on p53. Surprisingly, the PATZ1Alt protein could repress the *Thpok* gene indicating that the transcription inhibition by this transcription factor is context

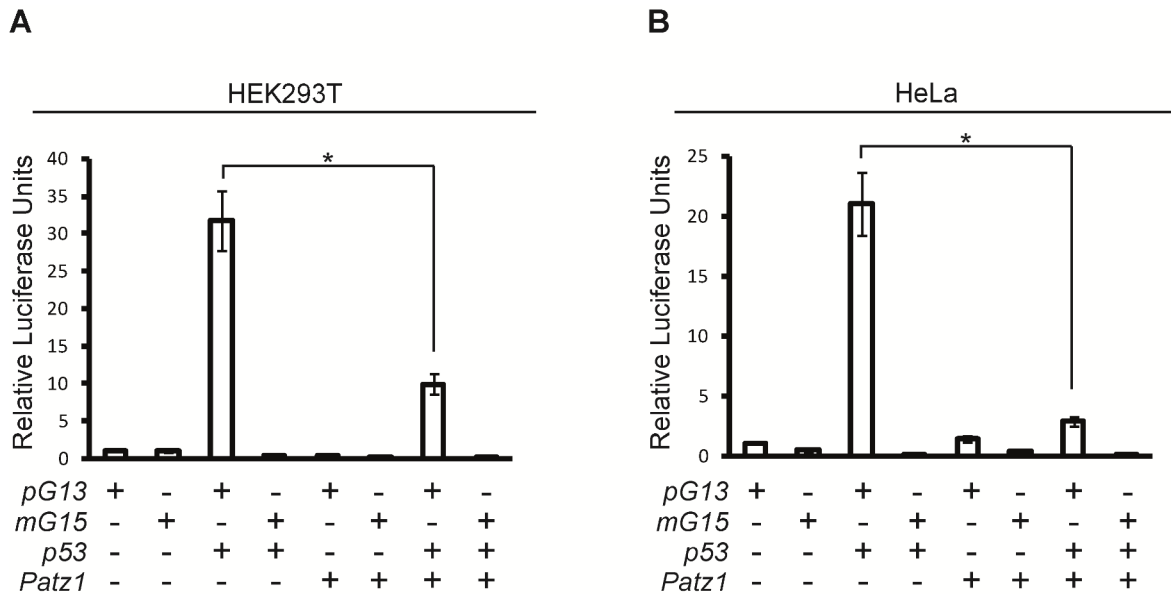


Figure 4.17: PATZ1 inhibits p53 transcriptional activity in luciferase assays in various cell types. Cells were transfected with different combinations of pG13 and mG15 reporter constructs, and p53 and/or PATZ1 expression plasmids. p53 specifically activates the pG13 reporter (columns 1, 3), but not the pG15 reporter (columns 2, 4), while PATZ1 cannot activate pG13 or pG15 (columns 5, 6). PATZ1 can inhibit p53 activity (columns 7). **A.** Transcriptional activity of p53 and PATZ1 transfected HEK293T cells. **B.** Transcriptional activity of p53 and PATZ1 transfected HeLa cells.

dependent. Lastly, we assessed the domain requirements of p53 for the inhibition by PATZ1. We performed luciferase assays with WT p53 (p53 $\alpha$ ) or a naturally occurring alternative splice version (p53 $\beta$ ) missing the C-terminal regulatory domain and observed that both p53 $\alpha$  and p53 $\beta$  could activate transcription of the pG13 reporter construct. While PATZ1 co-expression could again dramatically inhibit p53 $\alpha$  dependent transcription, the effect of PATZ1 on p53 $\beta$  dependent transcription was not as pronounced (Figure 4.18D). Thus, PATZ1 inhibits the transcriptional activity of p53 and the inhibitory activity of PATZ1 on p53 requires the C-terminal domains of both proteins.

Next, we wanted to characterize the important residues of PATZ1 for its inhibitory roles on the transcriptional activity of p53. Using knowledge obtained by previous homology modeling studies (shown previously by Jitka Eryilmaz and Manolya Ün), we identified several critical residues that might be involved in PATZ1/DNA interaction and PATZ1/p53 interaction. We mutated these residues one by one (R372G,

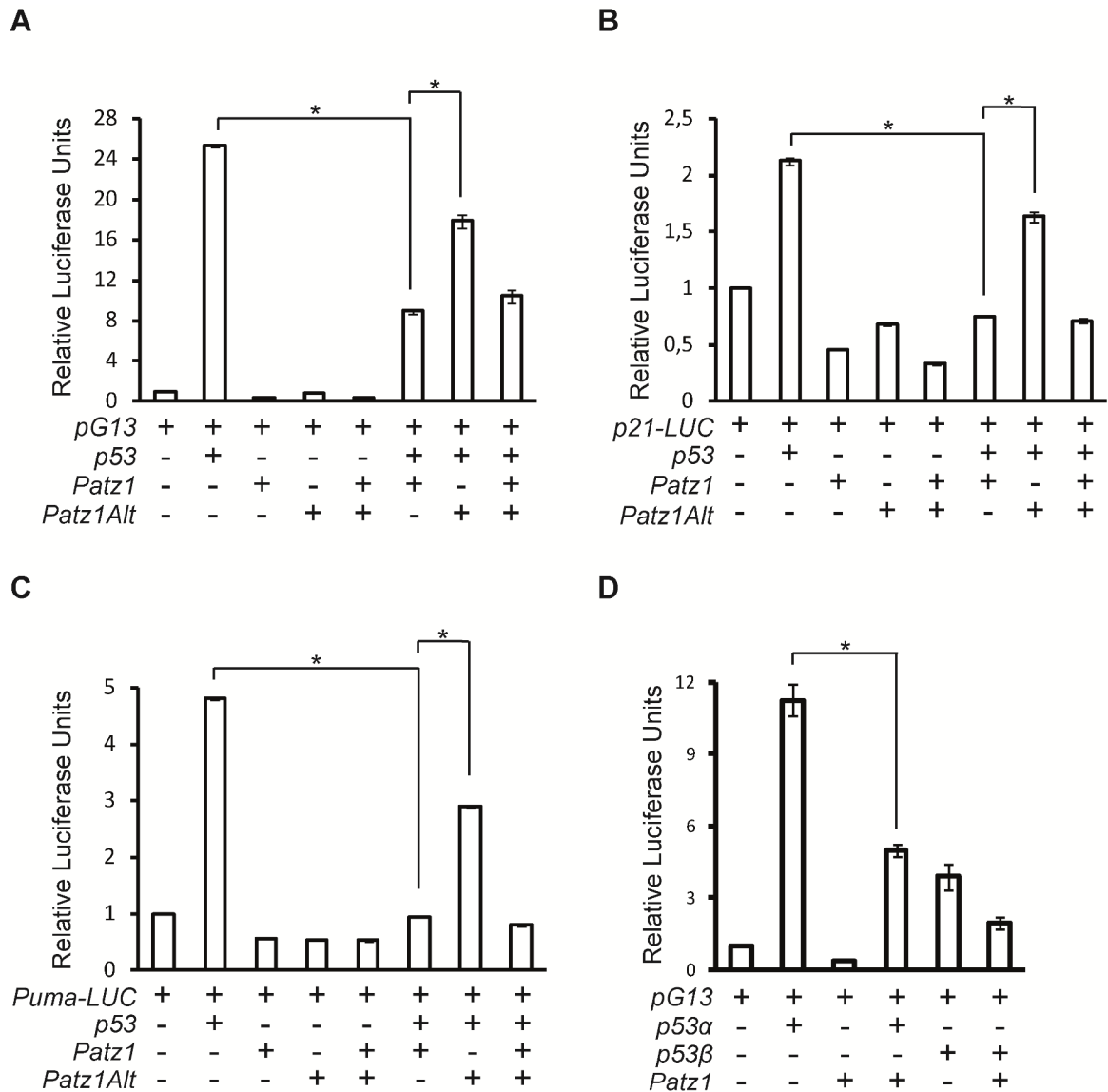
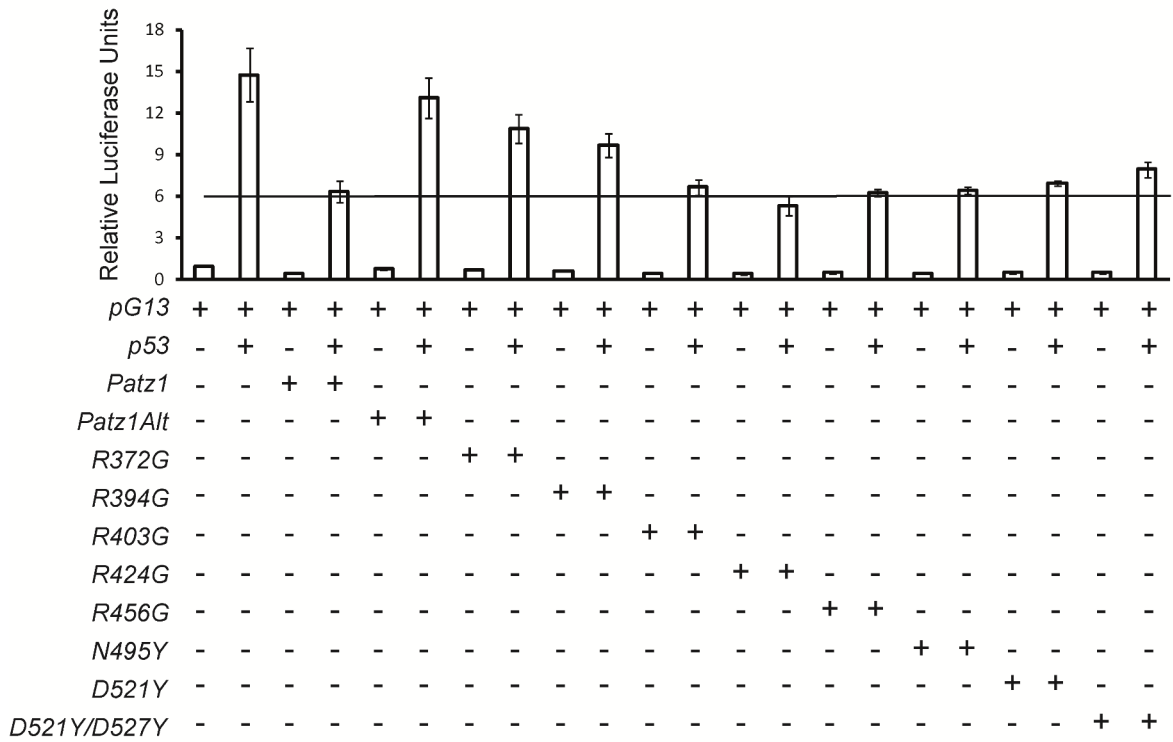


Figure 4.18: PATZ1 inhibits p53 activity in luciferase assays with different luciferase constructs. **A.** HCT116 p53<sup>-/-</sup> cells were transfected with different combinations of pG13, p53, PATZ1 and PATZ1Alt expression plasmids. p53 specifically activates the pG13 reporter (columns 1, 2), while PATZ1 and PATZ1Alt cannot (columns 3, 4). PATZ1, but not PATZ1Alt can inhibit p53 activity (columns 5, 6). The same experiment was conducted with the p21-LUC reporter construct (**B**) and the Puma-LUC reporter construct (**C**). **D.** PATZ1 inhibits p53 $\alpha$  better than the p53 $\beta$  alternative splice variant in luciferase assays. HEK293T cells transfected with different combinations of pG13, PATZ1 and p53 $\alpha$  and p53 $\beta$  expression plasmids. p53 $\alpha$  specifically activates the pG13 reporter (columns 1, 2), PATZ1 cannot activate pG13 (column 3) but can inhibit p53 $\alpha$  activity (column 4). p53 $\beta$  activates the pG13 reporter less efficiently compared to p53 $\alpha$  (column 5) and PATZ1 fails to inhibit this activity efficiently (column 6).

R394G, R403G, R424G, R456G, N495Y, D521Y, and a double mutant D521Y/D527Y) in our *Patz1* cDNA expressing plasmids. We used these constructs in the luciferase

reporter assays to assess if these PATZ1 mutants retained their inhibitory roles on p53 activity, using two different cell lines (Figure 4.19A and 4.19B). We observed that WT PATZ1 continued to repress p53 activity on the pG13 promoter and PATZ1Alt could not repress the activity to the same levels, as expected. R372G, R394G and R403G mutants lost almost all of the inhibitory roles on p53 activity. These residues are in the DNA binding domain of PATZ1 and this data suggests that PATZ1 might need to retain its DNA binding ability to inhibit p53 activity. Also the D521Y/D527Y mutant (double mutant) lost some of its inhibitory activity on p53. A co-worker, Nazli Keskin, had shown that this double mutant could not bind p53 while WT PATZ1 could. These data suggest that the D521 and D527 residues reside in the p53 binding domain of PATZ1 and are important for the inhibitory roles of PATZ1 on p53 activity.

**A**



**B**

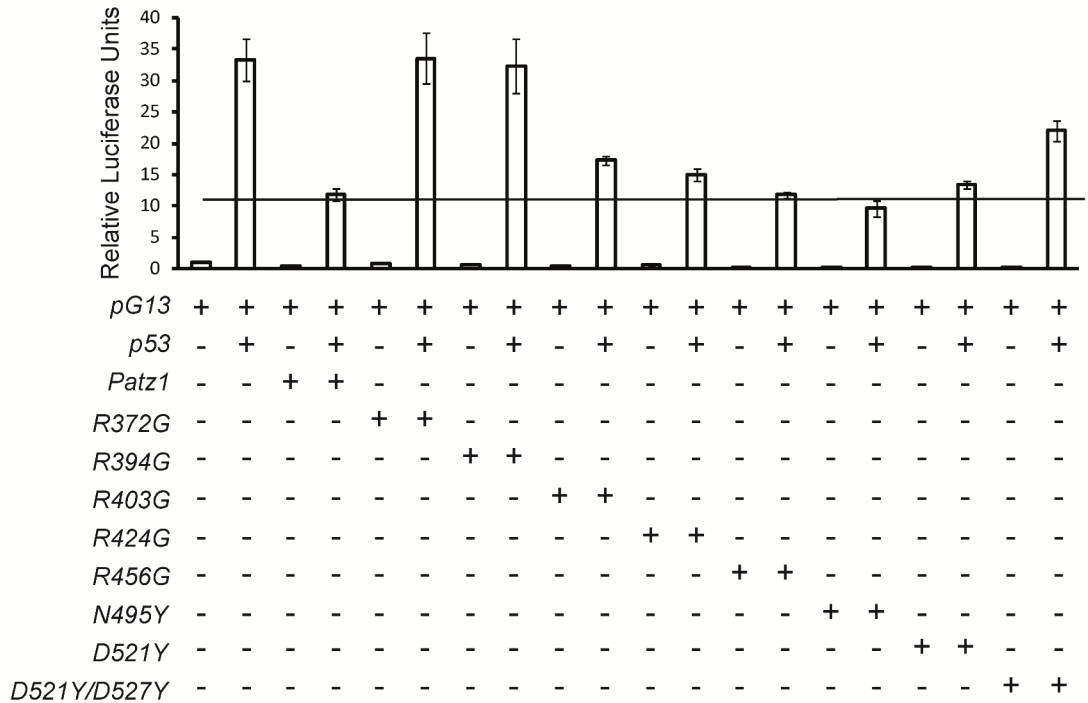


Figure 4.19 : Several residues in PATZ1 are crucial for inhibiting p53 activity. We created site directed mutant PATZ1 constructs at the indicated residues on the right side of the graph. Letters are abbreviations of amino acids. We determined the retained inhibitory roles of these mutants on p53 activity. **A.** HCT116 p53<sup>-/-</sup> cells were transfected with different combinations of pG13, p53, PATZ1, PATZ1Alt, and PATZ1

SDM expression plasmids. **B.** HEK293T cells were transfected with different combinations of pG13, p53, PATZ1, and PATZ1 SDM expression plasmids.

## 4.6. PATZ1 in DNA Damage

### 4.6.1. PATZ1 is Downregulated upon DNA Damage

p53 is the major regulator of the DNA damage response. Because we found PATZ1 as a regulator of the transcriptional activity of the p53 protein, we examined the role of PATZ1 in DNA damage as well. It is well known that the p53 protein is stabilized and accumulated in cells upon cellular stress such as DNA damage. We treated HCT116 (Figure 4.20A) and U2OS (Figure 4.20C) human cancer cells with the DNA damage inducing genotoxic drug doxorubicin (adriamycin) in a time dependent manner and showed that p53 indeed accumulates in these cells. As a negative control, we used HCT116 p53<sup>-/-</sup> (Figure 4.20B) and H1299 (Figure 4.20D) cell lines, which lack a functional *TP53* gene.

The PATZ1 gene expresses 4 alternative splice variants that encode 74, 69, 58 and 57 kDa proteins (Figure 4.21). The anti-PATZ1 antibody that we used in this study recognizes both human and mouse PATZ1 from an epitope located within the BTB domain of the proteins, therefore, it detects all 4 isoforms. However, this antibody could not differentiate between the mPATZ1-001 and -004 isoforms (corresponding to hPATZ1-004 and -001), and between the mPATZ1-012 and -003 isoforms (corresponding to hPATZ1-002 and -003) because of the similar molecular weights of these proteins.

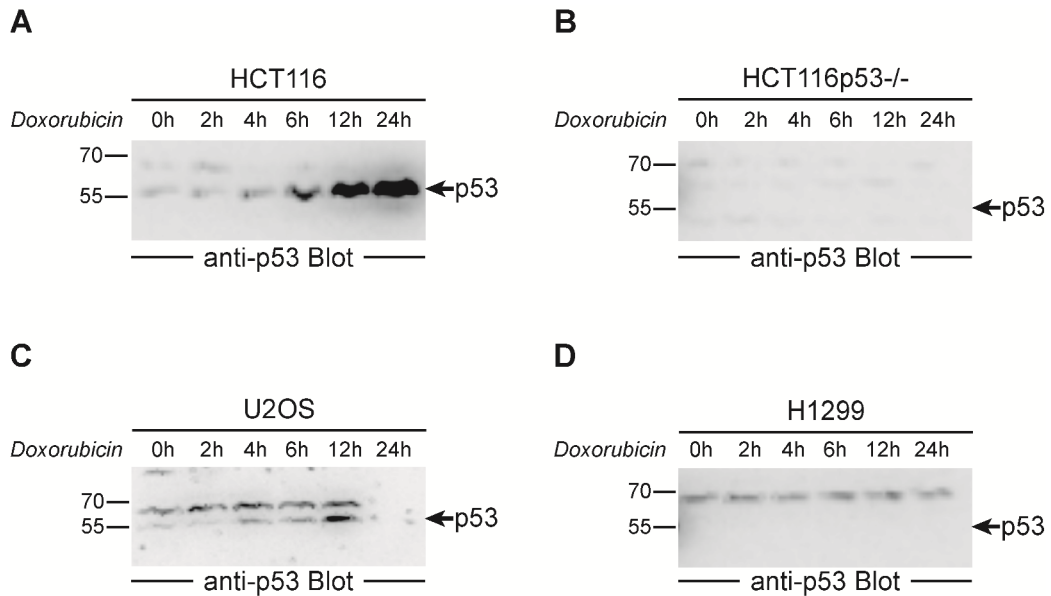


Figure 4.20: p53 accumulates upon DNA damage induced by doxorubicin in various cell lines. Cells are treated for the indicated times with 1 $\mu$ M doxorubicin and whole cell lysates were immunoblotted with anti-p53 antibody. The presence of the absence of p53 protein is indicated by arrows. **A.** HCT116, which express WT p53. **B.** HCT116 p53<sup>-/-</sup>, which is knocked out for p53. **C.** U2OS, which expresses WT p53. **D.** H1299, which is knocked out for p53.

In order to identify the effects of DNA damage on the expression pattern of PATZ1, we treated mouse embryonic fibroblast (MEFs) with doxorubicin. We first confirmed the accumulation of p53 in these cells in response to DNA damage (Figure 4.22 lower panel) by demonstrating that p53 levels of untreated MEFs were indeed low and rapidly got induced upon treatment with doxorubicin. On the other hand, the amount of the different isoforms of PATZ1 protein were decreased after 16 hours of doxorubicin treatment and did not recover at later time points of the treatment (Figure 4.22 upper panel). We also used the human HCT116 cell line to generalize finding that PATZ1 is lost in response to DNA damage. We treated HCT116 cells with doxorubicin for different time periods and determined the levels of p53 and PATZ1 (Figure 4.23A). PATZ1 was also lost in HCT116 cells while p53 accumulated in response to doxorubicin treatment. Because PATZ1 loss correlated with p53 induction after doxorubicin treatment, we questioned if p53 induction was necessary for PATZ1 loss. To this end, we treated HCT116 p53<sup>-/-</sup> cells deficient in p53 expression with doxorubicin and found that PATZ1 was lost even in the absence of p53 (Figure 4.23A).

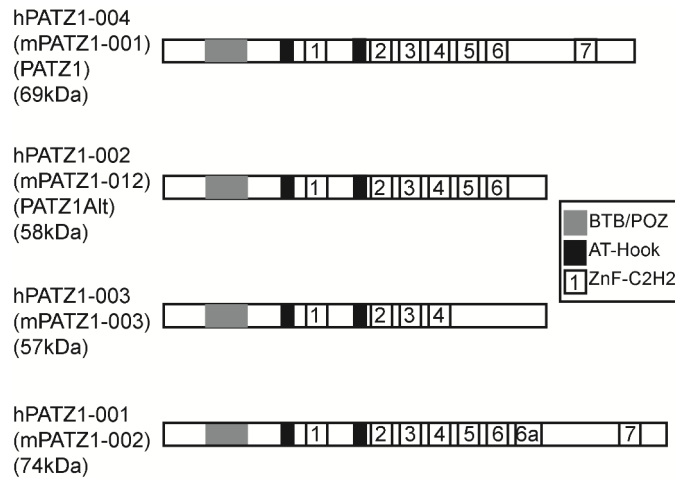


Figure 4.21: Schematic representation of proteins encoded by PATZ1 alternative splice variants. The standard names of human and mouse protein isoforms and molecular size of the proteins are indicated on the left. Grey boxes represent the protein-protein interaction BTB/POZ domain, black boxes represent the DNA binding AT hook domains and numbered boxes represent the zinc finger motifs.

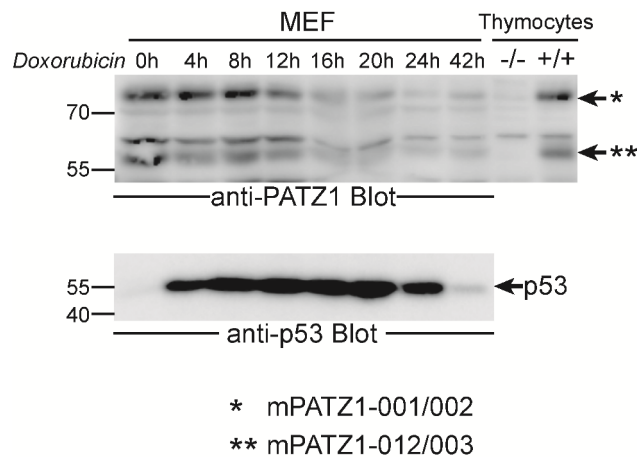


Figure 4.22: PATZ1 protein levels decrease upon doxorubicin treatment in MEFs. Cells were treated with 1 $\mu$ M doxorubicin for the indicated times and the whole cell lysates were immunoblotted with anti-PATZ1 (top row) or anti-p53 (bottom row) antibodies. The presence of PATZ1 isoforms and p53 are indicated by arrows.

To determine whether PATZ1 loss was due to a reduction in protein levels or in mRNA transcript levels, we measured steady state *PATZ1* mRNA levels by quantitative real-time PCR, but could not detect significant changes in the time range where PATZ1 protein levels dramatically decrease (Figure 4.23B). Thus, doxorubicin treatment likely results in the destabilization of PATZ1 protein isoforms and decreases cellular PATZ1 levels.

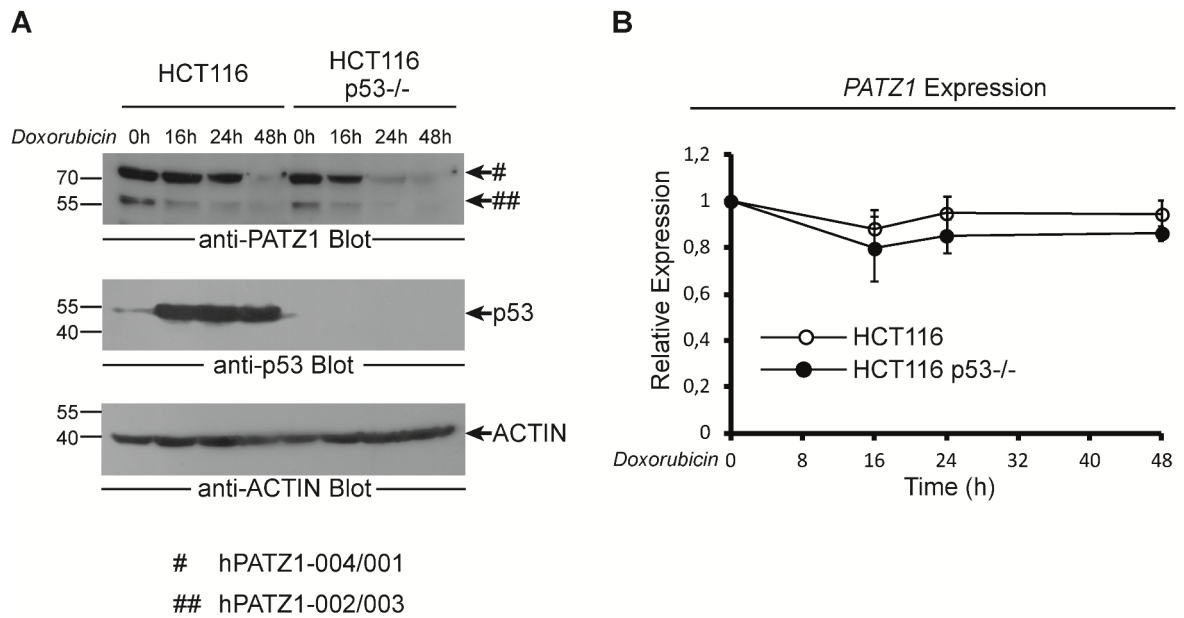


Figure 4.23: PATZ1 protein levels, but not mRNA levels, decrease upon doxorubicin treatment of HCT116 cells, independent of the presence or absence of p53 protein. **A.** Cells were treated with 1 $\mu$ M doxorubicin for the indicated times and the whole cell lysates were immunoblotted with anti-PATZ1 (top row) or anti-p53 (middle row) antibodies. Equal loading was confirmed by immunoblotting the same membrane with anti-ACTIN antibody (bottom row). The presence of PATZ1 isoforms, p53, and ACTIN are indicated by arrows. **B.** Doxorubicin treatment does not alter mRNA levels of *PATZ1*. *PATZ1* mRNAs were quantified by quantitative real-time PCR from HCT116 (open circles) or HCT116 p53<sup>-/-</sup> (filled circles) cells, treated with 1 $\mu$ M doxorubicin for the indicated times. Expression was normalized to GAPDH expression.

#### 4.6.2. Endogenous Transcriptional Activity of p53

After testing the effects of PATZ1 on the transcriptional activity of p53 using artificial reporter constructs, we examined the changes in the expression of the known targets of the endogenous p53 protein upon DNA damage induction. The *CDKN1A* (p21/WAF) and *PUMA* genes are known to be dramatically induced by DNA damage in a p53 dependent way. Doxorubicin dramatically increased p21 and Puma gene expression in HCT116 cells with wild type p53, as assessed by quantitative real-time quantitative PCR (RT-qPCR) (Figure 4.24A and 4.24B, respectively). However, HCT116 cells stably expressing PATZ1 protein could not activate these two genes as effectively, especially after prolonged DNA damage. We conclude that PATZ1 is able to inhibit p53 dependent transcription activation. Next, we examined the effect of PATZ1 on the expression of known apoptosis related genes. To this end, we used a custom designed apoptosis panel developed by Roche (REF 05 532 850 001). These genes (*BCL2*, *CASP9*, *CYCS*, *PARP1*, *AFMI*, and *POLG*) are known to be differentially regulated by various apoptosis inducing signals. We used HCT116 cells infected with retroviruses either overexpressing PATZ1 or carrying no cDNA. We stressed these cells by doxorubicin to induce apoptosis (1 $\mu$ M for 8 h). We purified poly A tailed RNA and examined the expression of the apoptosis panel genes in these cells by RT-qPCR. Overexpression of PATZ1 did not have a significant effect on these apoptosis related genes (Figure 4.25). Although we did not observe a significant difference in the expression of these genes, as seen in section 4.6.3, global analysis of gene expression in response to DNA damage may reveal the function of PATZ1 on other apoptosis or cell cycle related genes.

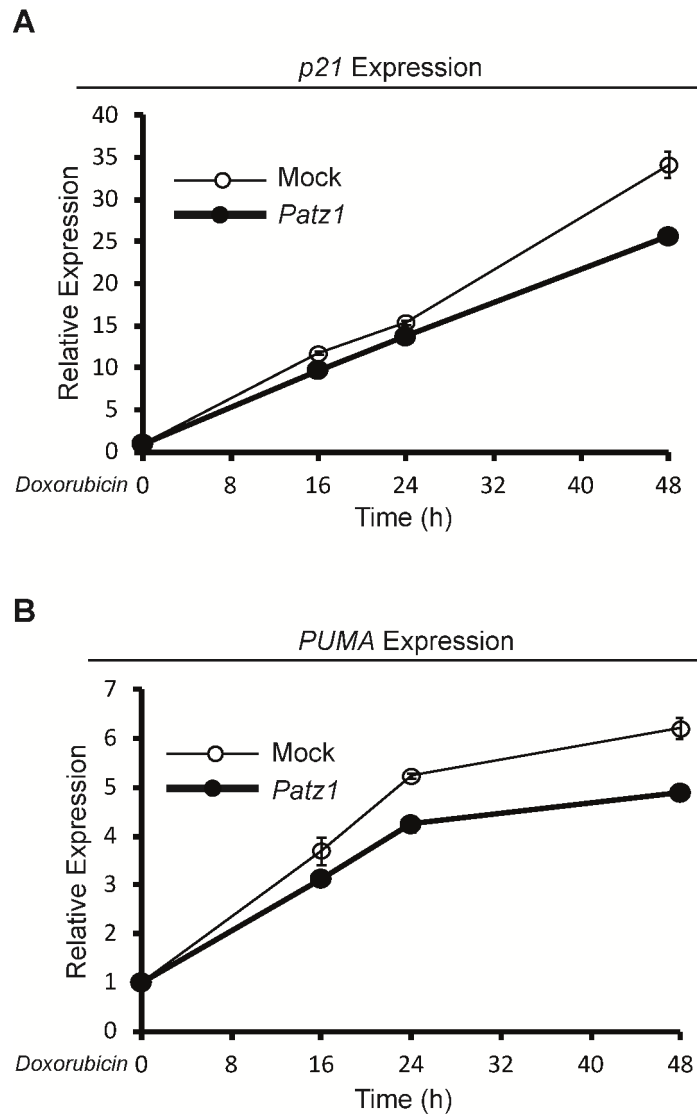


Figure 4.24: PATZ1 impairs the up-regulation of p53 dependent genes in doxorubicin treated cells. RT-PCR analysis reveals PATZ1 overexpressing HCT116 cells (filled circles solid line) express less p21(A) and Puma (B) mRNA compared to mock infected cells (open circles thin line) upon 1 $\mu$ M doxorubicin treatment. mRNA levels were assessed by RT-qPCR using PCR primers to amplify the mRNAs specified on top of the graphs. Expression is normalized to GAPDH expression.

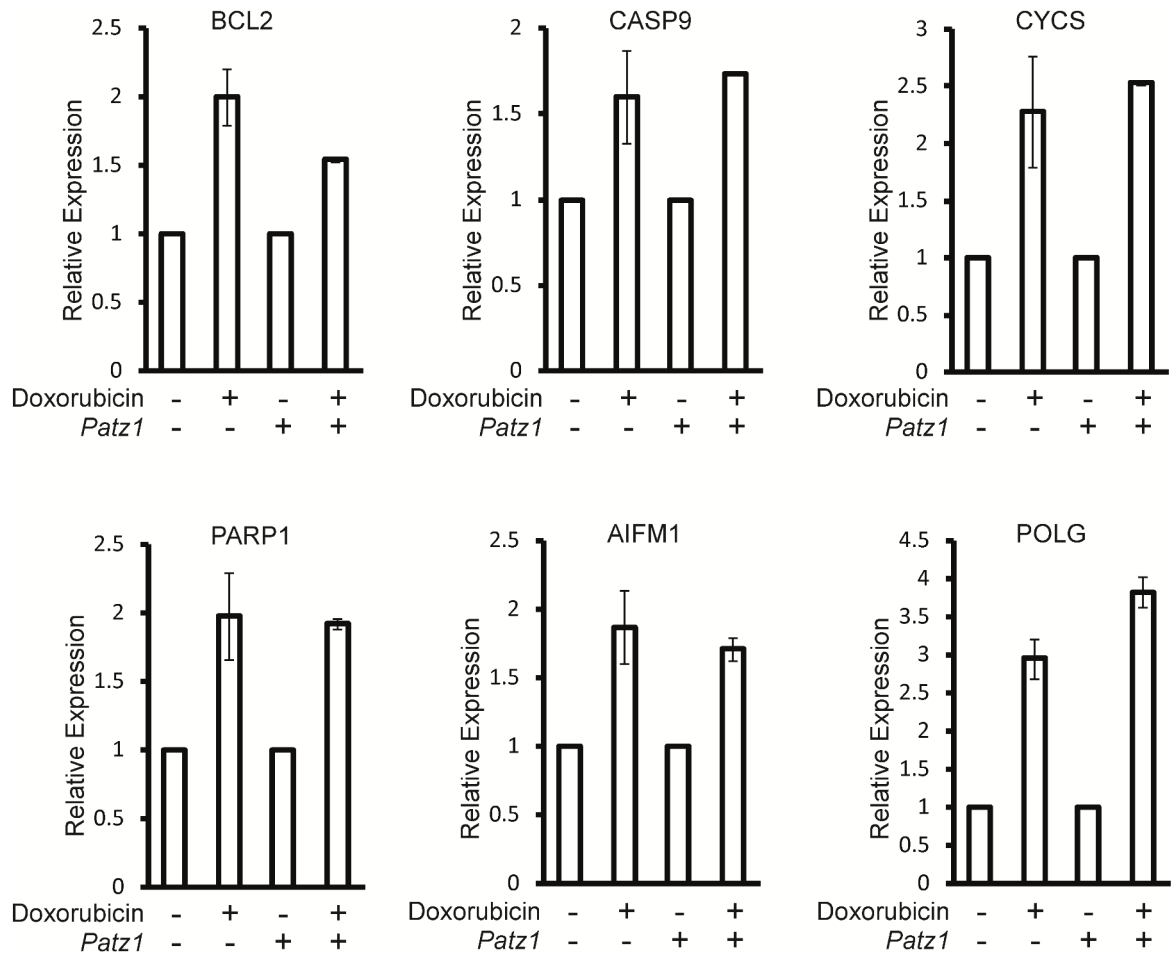


Figure 4.25: Overexpression of PATZ1 did not have a significant effect on apoptosis related genes. RT-PCR analysis reveals PATZ1 overexpressing HCT116 cells did not significantly change several apoptosis related genes in response to  $1\mu\text{M}$  8 h treatment of doxorubicin. mRNA levels were assessed by RT-qPCR using PCR primers to amplify the mRNAs specified on top of the graphs. Expression is normalized to RN18S1 expression.

### **4.6.3. Global Effects of PATZ1 on Gene Transcription in Response to DNA Damage**

In section 4.6.2, we tested the effects of PATZ1 on only two p53 targets that are major regulators of the p53 dependent DNA damage response. On the other hand, we also showed the global effects of PATZ1 on gene transcription independent of DNA damage. Here, we used the DNA damage inducing drug doxorubicin on MEF cells and performed RNA-seq analysis in these samples, similar to the experiments in section 4.3 (Figure 4.26A). We compared the gene expression patterns of PATZ1 WT MEFs (WTdox vs. WT) or KO MEFs (KODOx vs. KO) either treated with doxorubicin or untreated (Figure 4.26B, left panel). After doxorubicin treatment, there was a substantial number of DEGs that were either upregulated or downregulated in both groups. GO term analysis revealed that DEGs in both comparisons were enriched for established p53 gene targets and responses, such as cell cycle, apoptosis, growth and proliferation (Table 4.2 and Figure 4.27); confirming that doxorubicin induces p53 responses in our system in the presence or absence of PATZ1. To assess the effect of PATZ1 on these p53 responses, we analyzed the relevance of the DEGs found in the absence of PATZ1 after doxorubicin treatment (i.e. the DEGs that are found only in KODOx vs. KO but not in WTdox vs. WT, plus the DEGs that are changed by 2-fold or more in KODOx vs. KO compared to their counterparts in WTdox vs. WT samples). We divided this DEG set into up- and down-regulated DEG subsets. We performed functional annotation analysis for these two new sets and noticed that genes upregulated in the absence of PATZ1 (Table 4.3) were enriched in biological processes such as DNA packaging, chromatin assembly, and nucleosome assembly, which may be related to heterochromatin formation. Conversely we found that genes downregulated in the absence of PATZ1 (Table 4.4) were enriched in processes such as positive regulation of transcription, positive regulation of macromolecule biosynthetic processes, and regulation of RNA metabolic processes, which may be related to gene suppression. These results suggest that PATZ1 might be a chromatin remodeling factor either by itself or maybe through its interactions with co-factors.

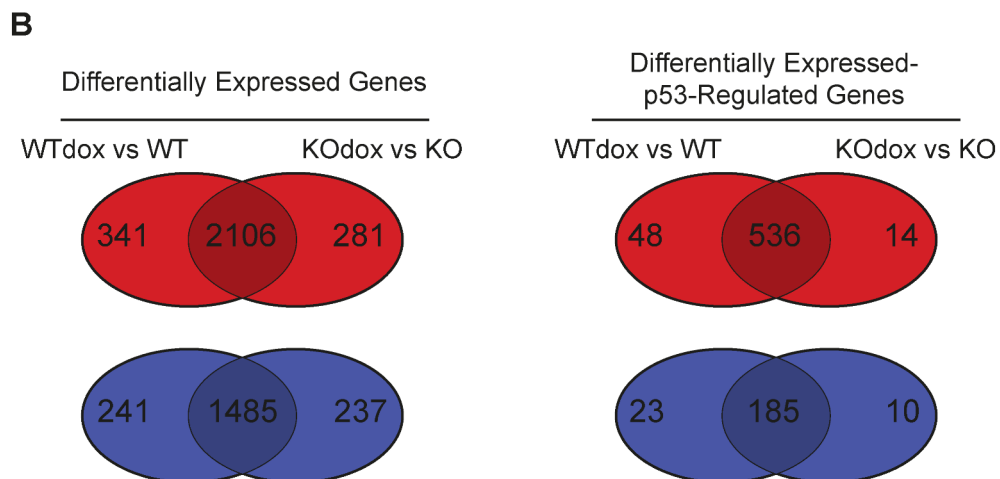
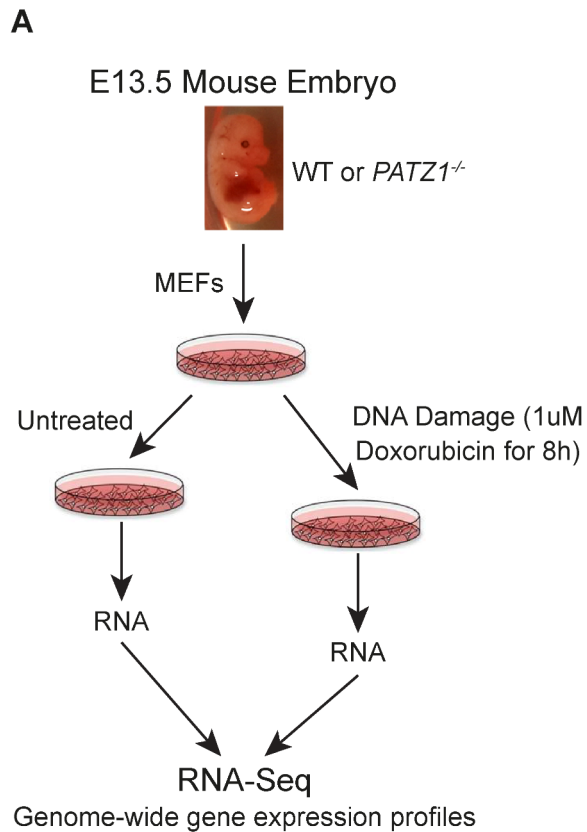


Figure 4.26: Genome wide gene expression analysis of MEFs expressing or deficient in PATZ1 upon DNA damage induction, by RNA-Seq. **A.** PATZ1 knockout or WT MEFs were prepared from mouse embryo at E13.5. Early passage MEFs were either untreated or treated with 1uM doxorubicin for 8 hours. Total RNA was extracted, polyA selected and triplicate samples were sequenced at Beijing Genomics Institute on an Illumina HiSeq 2000 platform and analyzed using the R library DEseq. **B.** Comparison of our RNASeq analysis with previous experiments. Left panel shows the up (red) and down (blue) regulated genes in our experiment. Right panel shows the same data filtered on p53 regulated genes from previously published data. 721 p53 regulated-genes (536+185) continue to be differentially expressed in response to doxorubicin, independent of the presence or absence of PATZ1. 71 p53 target genes (48+23) failed to

be differentially expressed in PATZ1 KO MEFs and 24 genes (14+10) were uniquely controlled in PATZ1 KO MEFs. Fold change > 2, FDR < 0.001.

<b>GO Term Related to Biological Process</b>	<b>P-Value in Wtdox vs WT</b>	<b>P-Value in Kodox vs KO</b>
GO:0007049~cell cycle	6.69E-04	4.25E-03
GO:0010941~regulation of cell death	3.89E-04	1.16E-03
GO:0040008~regulation of growth	4.21E-03	1.76E-03
GO:0042127~regulation of cell proliferation	2.13E-09	6.05E-10
GO:0042981~regulation of apoptosis	1.08E-03	2.98E-03

Table 4.2: Biological process GO terms that are enriched in our DEG set from RNA-Seq (generated by comparing Wtdox vs. WT and Kodox vs. KO MEFs). P-values are calculated by DAVID and GO terms that have smaller than 0.01 P-values are listed.

To further analyze differentially expressed genes in the presence or absence of PATZ1, with or without doxorubicin treatment, we analyzed RNA isolated from various MEF cells with Nimblegene microarrays. To analyze the effects of longer term DNA damage, distinct from the RNAseq experiments, we treated our MEF samples with doxorubicin for 24 hours. The suppression of gene expression was more evident in the results of this microarray such that the number of uniquely downregulated genes in Kodox vs. KO samples increased compared to uniquely upregulated genes (Figure 4.28). As it was the case in RNA-Seq results, in the microarray results, GO terms were also enriched for transcription regulation in the downregulated gene set (uniquely in Kodox vs. KO) (Table 4.5). However, to our surprise, upregulated genes (uniquely in Kodox vs. KO) did not exhibit enriched GO terms related to chromatin remodeling in our microarray results, as it was the case for the upregulated gene set in RNA-Seq (Table 4.6). Thus, we conclude that PATZ1 might be activating gene transcription in response to DNA damage.

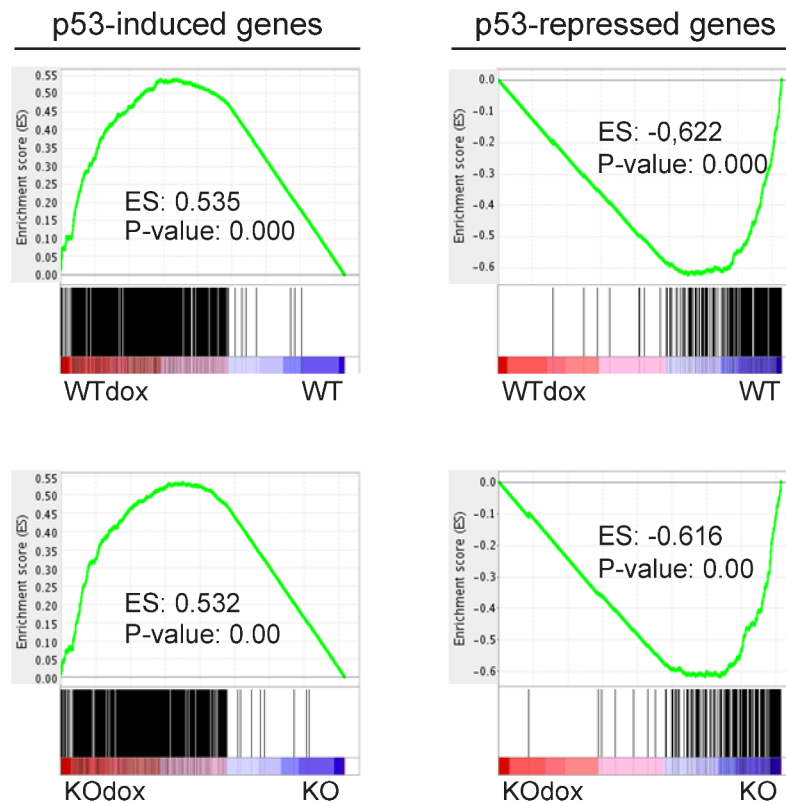


Figure 4.27: Doxorubicin treatment changes the expression of p53 target genes. Gene set enrichment analysis (GSEA) of p53 regulated genes from previously published data<sup>120</sup> in our DEG sets in WTdox vs. WT and KOdox vs. KO comparisons.

In order to identify the effects of PATZ1 specifically on p53 target genes, we filtered our RNA-Seq data using data from a previously published RNA-Seq experiment, which defines p53 target genes in MEFs also treated with doxorubicin as a DNA damage inducer<sup>120</sup> (Figure 4.26B, right panel). In this previously published experiment, WT and p53 deficient MEFs were compared to identify direct transcriptional targets of p53 upon short time doxorubicin treatment. This study identifies 918 p53 target genes that are upregulated and 405 genes that are downregulated. Among these genes, we identified 721 genes that continue to be differentially expressed in response to doxorubicin, independent of the presence or absence of PATZ1, 71 genes failed to be differentially expressed in PATZ1 KO MEFs and 24 genes were uniquely controlled in PATZ1 KO MEFs. When we looked at the genes that are immediate targets of p53 (Kyoto Encyclopedia of Genes and Genomes - KEGG mouse p53 pathway - mmu04115), we identified genes that are differently affected upon doxorubicin treatment in PATZ1 deficient MEFs compared to WT MEFs (Figure 4.29). We also looked at the genes, whose expression was uniquely changed

either in PATZ1 KO or in WT MEFs upon doxorubicin treatment. We present these findings in a Cytoscape image, which demonstrates that PATZ1 deficiency affected the expression of several p53 target genes (Figure 4.30). Therefore, we conclude that the absence of PATZ1 results in an alteration of the expression of p53 target genes. The microarray and RNA-Seq data presented in this study will be deposited in NCBI's Gene Expression Omnibus (GEO) <sup>121</sup>.

<b>GO Term Related to Biological Process</b>	<b>P-Value</b>
GO:0007423~sensory organ development	6.35E-05
GO:0007389~pattern specification process	6.26E-04
GO:0006334~nucleosome assembly	1.97E-03
GO:0031497~chromatin assembly	2.26E-03
GO:0065004~protein-DNA complex assembly	2.42E-03
GO:0034728~nucleosome organization	2.42E-03
GO:0040007~growth	2.57E-03
GO:0043583~ear development	2.68E-03
GO:0007167~enzyme linked receptor protein signaling pathway	3.93E-03
GO:0048839~inner ear development	5.01E-03
GO:0045165~cell fate commitment	5.06E-03
GO:0006814~sodium ion transport	7.34E-03
GO:0070374~positive regulation of ERK1 and ERK2 cascade	8.37E-03
GO:0006323~DNA packaging	9.68E-03
GO:0048663~neuron fate commitment	9.89E-03

Table 4.3: Biological process GO terms that are enriched in our DEG set from RNA-Seq that consists of upregulated genes uniquely in KOdox vs. KO and of more upregulated genes in KOdox vs. KO compared to WTdox vs. WT. P-values are calculated by DAVID and GO terms that have smaller than 0.01 P-values are listed.

Geno Ontology Term Related to Biological Processes	P-Value
GO:0051252~regulation of RNA metabolic process	1.33E-07
GO:0006355~regulation of transcription, DNA-dependent	5.10E-07
GO:0045449~regulation of transcription	1.87E-06
GO:0006350~transcription	1.01E-04
GO:0006357~regulation of transcription from RNA polymerase II promoter	2.47E-04
GO:0045935~positive regulation of nucleic acid metabolic process	3.40E-04
GO:0010604~positive regulation of macromolecule metabolic process	3.63E-04
GO:0051173~positive regulation of nitrogen compound metabolic process	5.03E-04
GO:0010628~positive regulation of gene expression	5.23E-04
GO:0010557~positive regulation of macromolecule biosynthetic process	5.53E-04
GO:0031328~positive regulation of cellular biosynthetic process	9.16E-04
GO:0045941~positive regulation of transcription	9.98E-04
GO:0009891~positive regulation of biosynthetic process	1.02E-03
GO:0016071~mRNA metabolic process	4.71E-03
GO:0006402~mRNA catabolic process	5.08E-03
GO:0006401~RNA catabolic process	8.18E-03
GO:0045893~positive regulation of transcription, DNA-dependent	9.82E-03

Table 4.4: Biological process GO terms that are enriched in our DEG set from RNA-Seq that consists of downregulated genes uniquely in KOdox vs. KO and of more downregulated genes in KOdox vs. KO compared to WTdox vs. WT comparison. P-values are calculated by DAVID and GO terms that have smaller than 0.01 P-values are listed.

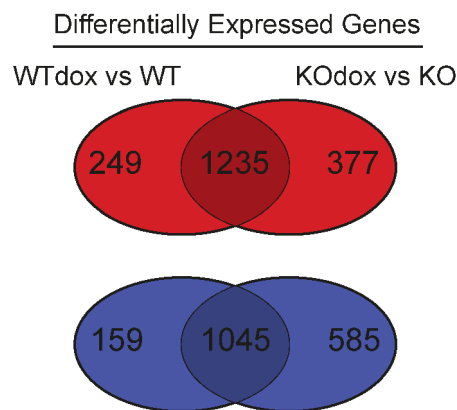


Figure 4.28: Genome wide gene expression analysis of MEFs expressing or deficient in PATZ1 by microarray. PATZ1 knockout or WT MEFs were prepared from mouse embryo at E13.5. Early passage MEFs were either untreated or treated with 1 $\mu$ M doxorubicin for 24 hours. Total RNA was extracted, polyA selected, converted to dsDNA and triplicate samples were hybridized on Nimblegen full genome mouse expression array. Panel shows the up (red) and down (blue) regulated genes. Fold change > 2, FDR < 0.05.

<b>Geno Ontology Term Related to Biological Processes</b>	<b>P-Value</b>
GO:0048477~oogenesis	0.001637235
GO:0007292~female gamete generation	0.006154979
GO:0000904~cell morphogenesis involved in differentiation	0.006844041
GO:0042035~regulation of cytokine biosynthetic process	0.009823388

Table 4.5: Biological process GO terms that are enriched in our DEG set from microarray that consists of upregulated genes uniquely in KOdox vs. KO. P-values are calculated by DAVID and GO terms that have smaller than 0.01 P-values are listed.

<b>Geno Ontology Term Related to Biological Processes</b>	<b>P-Value</b>
GO:0045449~regulation of transcription	4.66E-04
GO:0006399~tRNA metabolic process	4.82E-05
GO:0006396~RNA processing	3.38E-03
GO:0045927~positive regulation of growth	3.67E-03
GO:0008637~apoptotic mitochondrial changes	4.06E-03
GO:0007005~mitochondrion organization	4.40E-03
GO:0007006~mitochondrial membrane organization	4.70E-03

Table 4.6: Biological process GO terms that are enriched in our DEG set from microarray that consists of downregulated genes uniquely in KOdox vs. KO. P-values are calculated by DAVID and GO terms that have smaller than 0.01 P-values are listed.

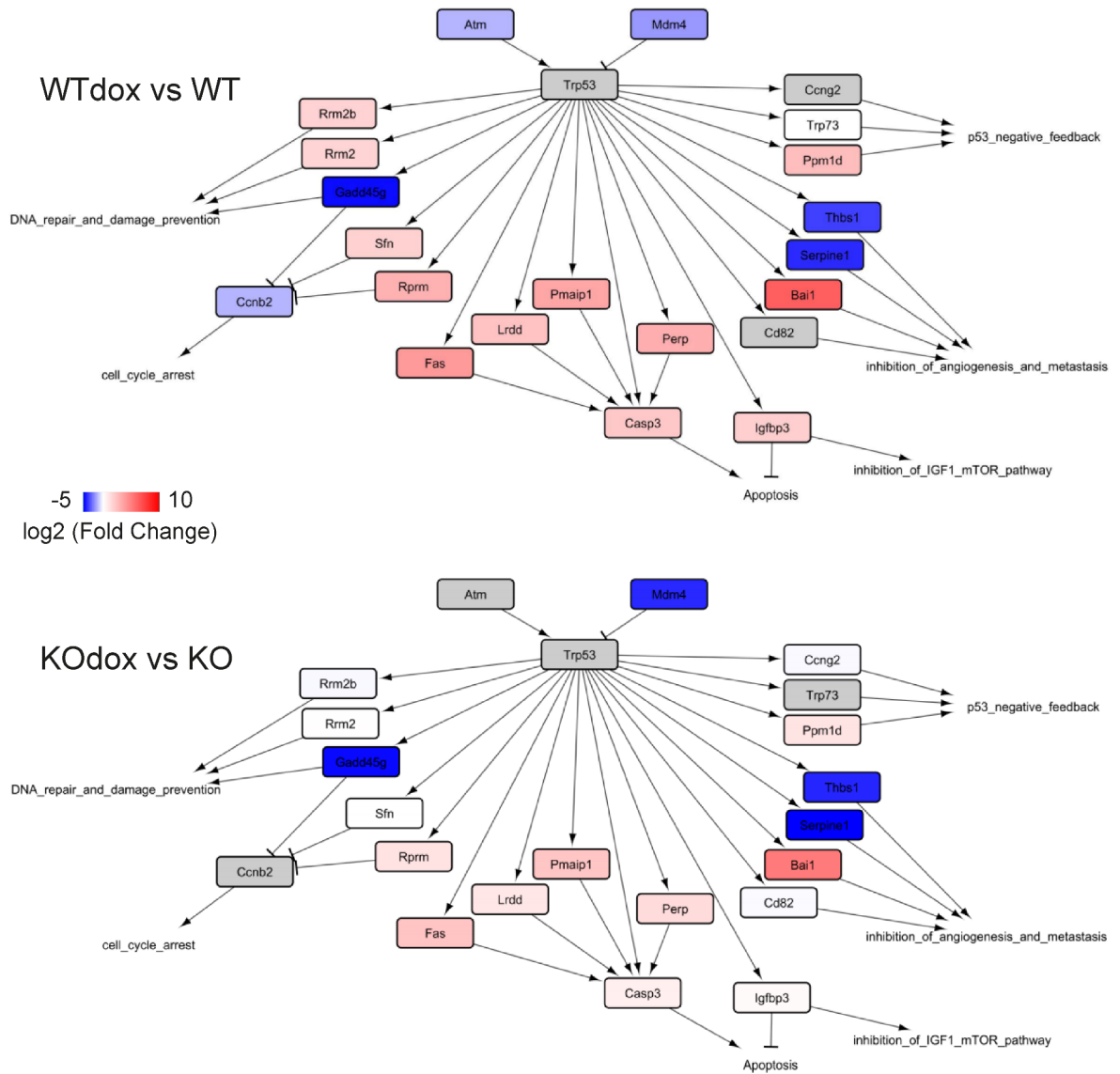


Figure 4.29: P53 pathway is affected in doxorubicin treated PATZ1 deficient MEFs. p53 pathway from KEGG (mmu04115) was visualized in Cytoscape for WTdox vs. WT and KOdox vs. KO comparisons. Genes with gray nodes have no significant differential read data. Down-regulated and up-regulated genes were visualized with blue and red respectively

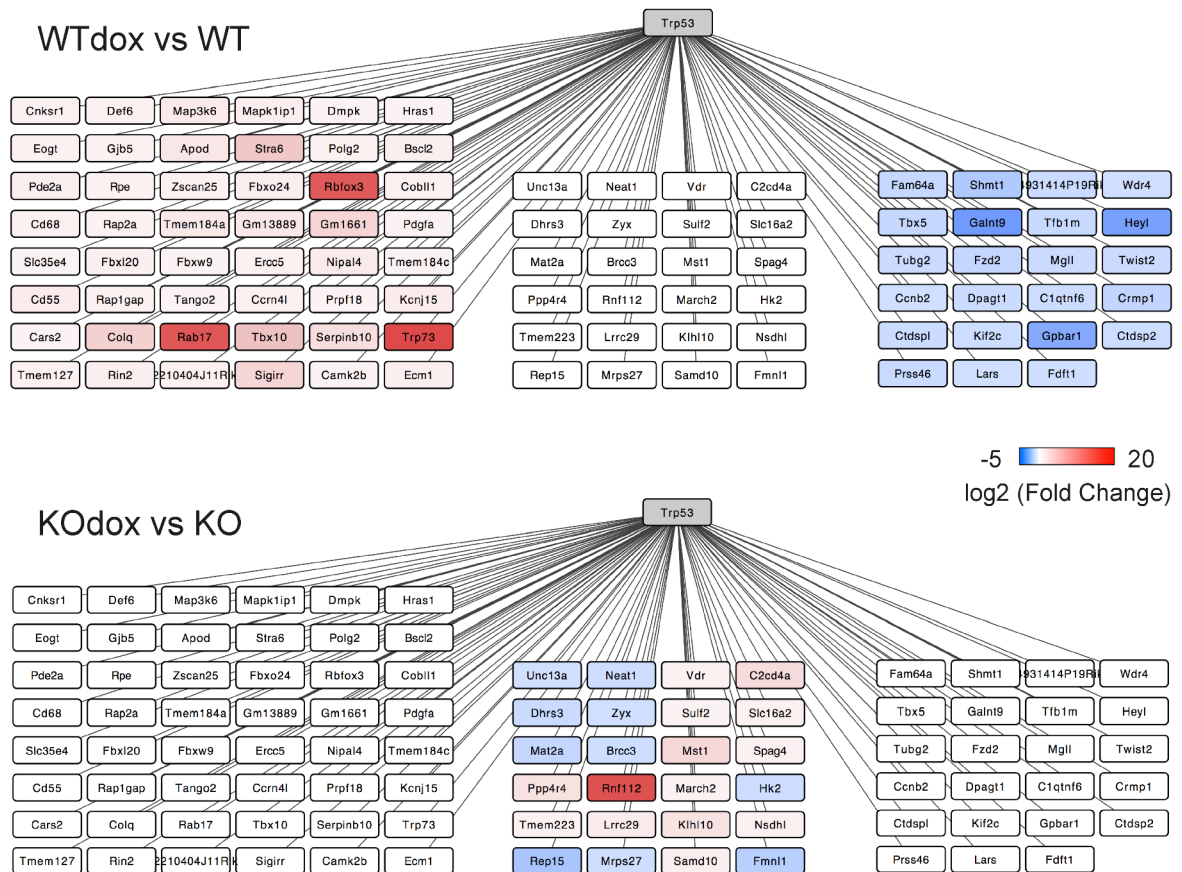


Figure 4.30: Doxorubicin treatment in the absence of PATZ1 results in an alteration of the expression of p53 target genes. We found that 71 p53 target genes (48+23) failed to be differentially expressed in PATZ1 KO MEFs and 24 genes (14+10) were uniquely controlled in PATZ1 KO MEFs. Cytoscape analysis shows that PATZ1 knock out MEFs treated with doxorubicin failed to control these p53-dependent genes.

## 4.7. Preliminary Results for Future Directions

### 4.7.1. Knocking out *PATZ1* in Human Cell Lines

Being able to study the functions of *PATZ1* in a *PATZ1* null cell line system would offer numerous advantages. For this reason, we wanted to knockout the human *PATZ1* gene using TALEN (Transcription Activator-Like Effector Nuclease) genome editing tools. TALENs are a novel method for genome engineering, in which a genomic locus of interest can be specifically and efficiently targeted to be modified using custom

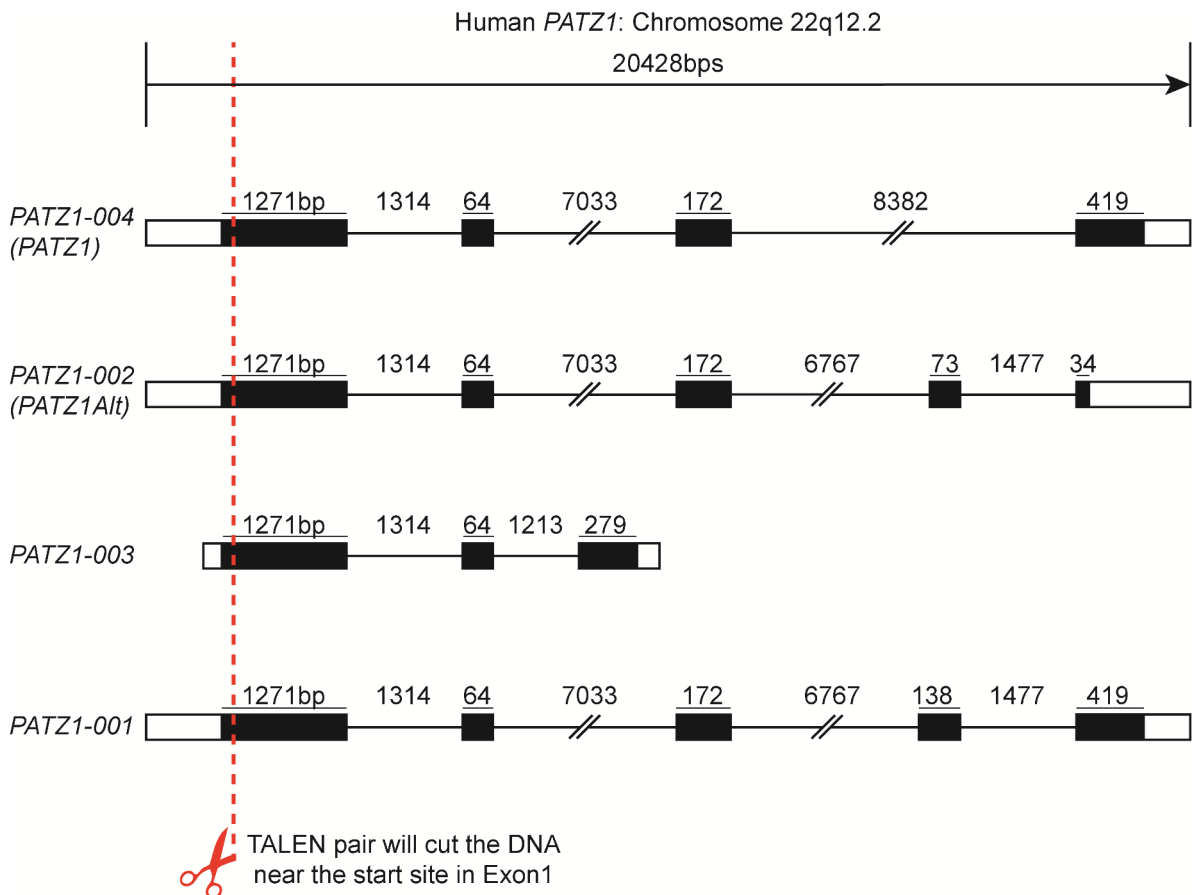


Figure 4.31: TALENs against *PATZ1* genomic locus. TALENs cut *PATZ1* gene near the translation initiation start site in the first exon.

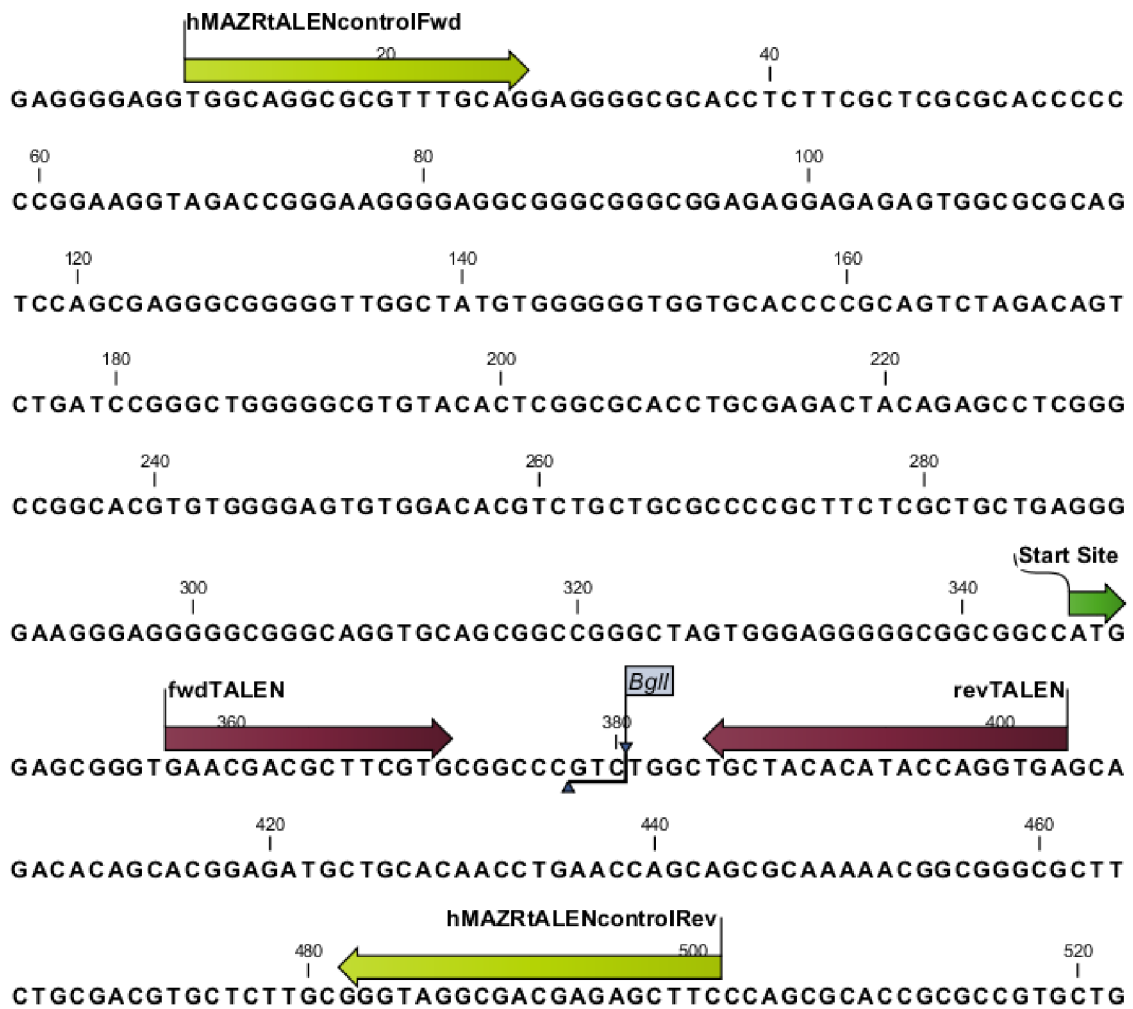


Figure 4.32: A closer look to TALENs on PATZ1 genomic sequence. fwdTALEN and revTALEN will bind to the DNA from just a few bases downstream of the translation initiation site of PATZ1. A BglII restriction enzyme recognition site is located in between the TALEN pair. Specific primers shown by light green-colored arrows are used to amplify the genomic region encompassing the site of indels.

designed proteins<sup>122</sup>. TALENs are sequence specific nucleases, which create DNA double strand breaks (DSB) at the targeted genomic loci. Cells with DSB activate their intrinsic non-homologous end-joining (NHEJ) mechanism to repair the breaks. During this inefficient repair process, insertions of new nucleotides or deletions of some existing nucleotides (INDELS) result in the mutation of the targeted locus. If the targeted sequence is in a protein coding exon of a gene, INDEL mutation disturbs the gene structure and the mRNA reading frame leading to a gene knock-out situation<sup>123</sup>.

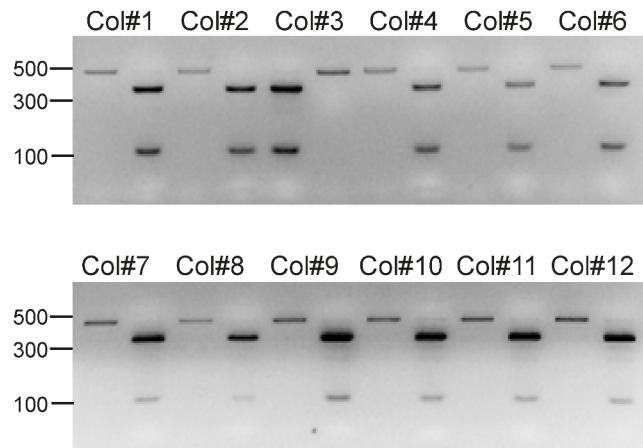


Figure 4.33: RFLP analysis to the single-cell-derived-colonies of HCT16 cells after TALEN transfection. Genomic DNA was isolated from the colonies and the PCR products amplified from the site of TALEN recognition were subjected to RFLP analysis with BglI enzyme. First column of each colony (col) is uncut control (no enzyme), second column is BglI digestion.

We designed TALENs against a sequence near the translation start site of the *PATZ1* gene (Figure 4.31). We predicted that TALEN induced NHEJ would disrupt the *PATZ1* gene reading frame resulting in out-of-frame transcripts with premature stop codons, thus creating a *Patz1*<sup>-/-</sup> genotype. We designed these TALENs so that a BglI restriction enzyme site within the TALEN target sequence would allow the screening of mutated *PATZ1* sequences by RFLP (restriction fragment length polymorphism). Our strategy would allow us to identify cells with mutations in the *PATZ1* gene because TALEN mediated mutations in the targeted exon would disrupt the BglI site revealed in an RFLP assay (Figure 4.32). We generated *PATZ1* gene targeting TALEN proteins using the Golden Gate cloning procedure<sup>122</sup>. We transfected TALEN expression constructs to HCT116 cells, and generated single cell derived colonies. We isolated genomic DNA from these colonies and amplified the target region in a PCR reaction. We digested amplicons from each colony with BglI to assess the mutation rate. To date, we screened some colonies using this RFLP assay; however, we could not successfully identify a mutated colony, in which the *PATZ1* locus is mutated (Figure 4.33). We are in the process of screening more colonies and optimizing different factors that will improve the efficiency of TALEN mediated genomic mutation.

#### **4.7.2. Impact of PATZ1 Expression on Tumorigenesis in Murine Xenograph Models**

In this study, we tried to understand the molecular mechanisms that PATZ1 controls, using *in vitro* techniques. To correlate these *in vitro* findings with *in vivo* potential impacts of PATZ1 in tumorigenesis, we planned xenograph experiments in mice. In order to study PATZ1 in tumorigenesis, we created EL4-Ova mouse cell lines that overexpress or knock-down PATZ1. This cell line is known to develop solid tumors once subcutaneously injected into immunocompromised nude mice<sup>124</sup>. We confirmed that the cells are expressing higher or lower levels of PATZ1 in the overexpression or knocked-down conditions, respectively (Figure 4.34A and 4.34B). These newly created cells will be used for xenotransplantation into nude mice through subcutaneous injection. We will assess the impact of PATZ1 on tumor development by measuring the sizes of the tumors that rise from injected EL4-Ova cells.

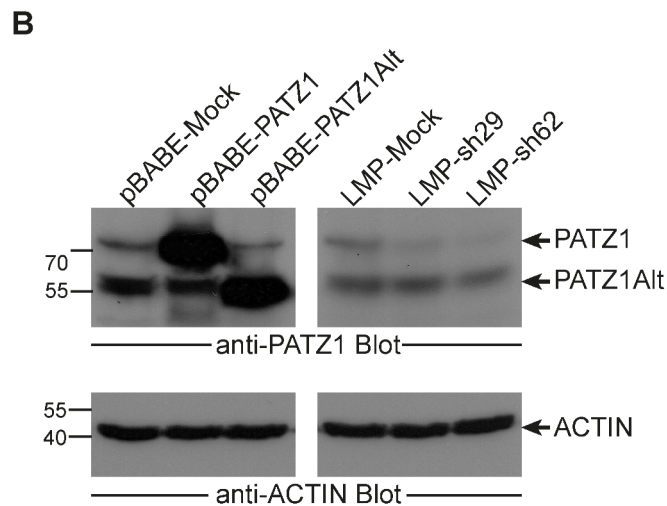
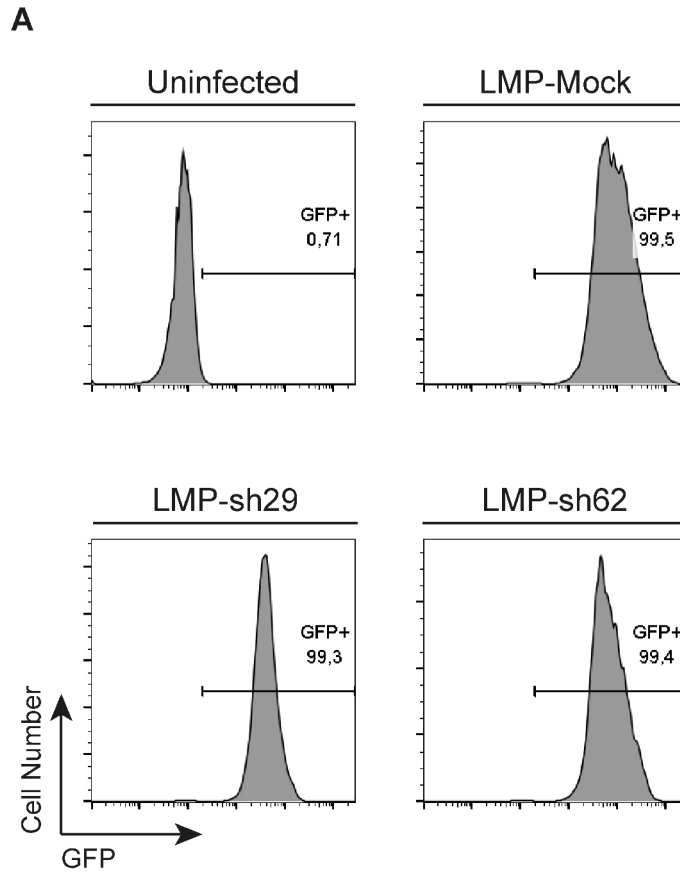


Figure 4.34: Creating stably PATZ1 overexpressing or knocked-down EL4-Ova cells. **A.** EL4-Ova cells were infected with mock shRNA carrying (in LMP backbone) virus, or two different shRNAs against PATZ1 (sh29 and sh62 in LMP backbone). Since LMP plasmid has GFP marker, we checked the infection efficiency by looking at the GFP fluorescence levels of the cells using flow cytometry **B.** Generation of PATZ1 overexpressing or knocked-down EL4-Ova cells. Retroviruses were packaged and used to stably infect. On the left panel, increased PATZ1 or PATZ1Alt expression is shown in EL4-Ova cells with pBabe-Puro based *Patz1* or *Patz1Alt* cDNA expressing but not mock virus by anti-PATZ1 blotting. On the right panel, anti-PATZ1 for knocked-down

EL4-Ova cells described in A. was shown. Equal loading was confirmed by immunoblotting the same membrane with anti-ACTIN antibody, on the lower panel.

## 5. DISCUSSION

Our current study identifies the BTB-ZF transcription factor PATZ1 as a regulator of the DNA damage response by modulating the activity of the p53 tumor suppressor protein in this pathway. We found that PATZ1 is sensitive to DNA damage because the cellular protein level of PATZ1 decreases upon DNA damage induction. The role of p53 in the DNA damage response is extensively studied in the literature and it is well established that p53 protein gets stabilized and rapidly accumulates in cells in response to a wide variety of cellular stress, including DNA damage. The consequent loss of PATZ1 as p53 increases led us to investigate the role of PATZ1 in the DNA damage response pathway and on the function of p53 within this pathway. We found that PATZ1 indeed plays a role in DNA damage pathway by modulating the transcriptional activity of p53.

PATZ1 belongs to the BTB-ZF family, a class of transcription factors that have a BTB domain for protein-protein interactions and a ZF domain for protein-DNA interactions. These kinds of transcription factors are generally versatile in modulating transcription. They can directly activate or repress gene transcription by binding to the promoter of the target genes or they can indirectly change the transcription of a gene by modulating the activity of other transcription factors by interacting with them<sup>125,126</sup>. The BTB domain is capable of homo- or hetero-dimerization with other BTB-domain containing transcription factors and with co-factors, like HAT and HDAC<sup>78,79</sup>.

Moreover, these transcription factors can act as chromatin remodeling factors depending on their interaction partners. BTB-ZF proteins play important roles in tumorigenesis, especially in cases of genetic abnormalities like translocations, they are also responsible for aberrant epigenetic modifications and chromatin remodeling, therefore they may contribute to the undesirable alteration of gene expression that may favor tumorigenesis<sup>80,83,88,127</sup>. PATZ1 is found to be upregulated in different cancers and its downregulation is associated with increased apoptosis<sup>97,106,107</sup>. Like many other BTB-ZF family members, the translocation of the *PATZ1* gene is also a cancer inducing event, more specifically Ewing's sarcoma<sup>104</sup>. PATZ1 has important roles during embryogenesis because in the absence of PATZ1, mice are born smaller in size, infertile, very prone to spontaneous lymphoma occurrence, and have impaired central nervous system development<sup>98,101</sup>. PATZ1 is required for the maintaining of the pluripotency of mESC and contributes to embryonic development<sup>100</sup>. These findings place PATZ1 as an important candidate in tumorigenesis.

PATZ1 was originally identified to be expressed in brain, thymus, fetal liver, and bone marrow, and especially in B-cell lines in different stages of development<sup>92</sup>. We documented its expression in various cell types, both from primary cells and cancer cell lines. We found that it is expressed in primary MEFs and mouse thymocytes, different mouse T lymphoma cell lines, human colon carcinoma HCT116 cell lines, human epithelial carcinoma HeLa cell line and mouse fibroblast NIH3T3 cell lines (Figures 4.2A, 4.2B, 4.10A, 4.11A, 4.12C, 4.22). The protein sequence of PATZ1 is highly conserved among mammalian orthologues, suggesting an important and ancient role. The gene structure is almost the same between mouse and human genomes and there is over 99% homology between the protein sequences (Figure 4.1). There are 4 alternative splice variants of PATZ1 (Figure 4.21). In our study, the antibody that we used for PATZ1 detection was against the BTB domain of the protein, which is included in all of the variants. Therefore, we could not differentiate between the longer two variants (which have very similar molecular weights, i.e. 69 and 74 kDa) and the shorter two variants (58 and 59 kDa) in western blotting.

In different studies, PATZ1 repressed or activated gene transcription, depending on the cellular context and the target gene<sup>93,94</sup>. We analyzed and characterized the transcriptional repression activity of PATZ1. PATZ1 was found to be controlling the expression of the *Thpok* gene because in the absence of PATZ1, the endogenous *Thpok* gene was derepressed in CD8+CD4- thymocytes, in which it normally stays repressed. We restored PATZ1 expression in these PATZ1 null cells and showed that PATZ1 re-represses *Thpok*, indicating that PATZ1 normally suppresses *Thpok* (Figure 4.5). Structure function studies in *Thpok* reporter experiments revealed important residues within the zinc finger domain of PATZ1. These residues are conserved among several BTB-ZF proteins and are important for contacting DNA (shown previously by Jitka Eryilmaz). This explains their importance in the transcriptional repression activity of PATZ1 because PATZ1 may interact with DNA through these residues. Because we defined the role of PATZ1 on *Thpok* gene expression, we plan to clone this promoter into a luciferase reporter construct in order to use it for further structure function analyses.

Aberrant overexpression of PATZ1 was found in various cancers and its overexpression rescued old and senescent fibroblasts<sup>102,106,107</sup>. These data indicates that PATZ1 overexpression might favor uncontrolled cell growth. Particularly, we hypothesized that PATZ1 might play role in cellular proliferation, a process, which is strictly regulated by p53. We found that PATZ1 deficiency results in increased doubling time, indicating that these cells grow slower compared to their WT partners, whereas PATZ1 sufficiency or overexpression leads to decreased doubling time, meaning faster growth, in various cell types that we tested (Figure 4.9B, 4.10B, 4.11C, and 4.11D). These findings suggest that PATZ1 positively controls cell growth; however, whether this role of PATZ1 is p53-dependent remains unknown. The strength of these results comes from the real time analysis of cell growth using xCELLigence RTCA DP technology. In our doubling time calculation experiments, we did not use end point assays, in which cells are harvested and counted at several time points; instead we analyzed the cell growth in real time, in as short as 15 minutes intervals for over 100 hours. This technical advantage allowed us to draw a more definitive and reliable conclusion. We checked if this proliferative role of PATZ1 is through cell cycle control. To this end, we utilized HeLa-Fucci cells, in which progression of the cell cycle can

easily be tracked by observing changes in the expression of fluorescent proteins during distinct phases of the cell cycle <sup>116</sup>. However, we did not detect any cell cycle distribution difference between mock and PATZ1 overexpressing HeLa-Fucci cells (Figure 4.13). In fact, HeLa cells are human papilloma virus (HPV)-transformed cells, which express high levels of the HPV E6 protein <sup>128</sup>. Although, HeLa cells express WT p53, E6 increases the turnover of p53 protein by interacting with it; therefore the effects of E6 on p53 are analogous to an inactivating mutation of p53. In our HeLa-Fucci system, the p53 pathway might be inactivated and this might be the reason why we did not observe any effects of PATZ1 on cell cycle distribution. The HeLa-Fucci system might not be the ideal model to study the role of p53 dependent cell cycle alterations. We plan to repeat these cell cycle control experiments in p53 WT cells with functional p53.

We identified a direct link between p53 and PATZ1 using luciferase reporter assays and quantitative measurements of mRNA levels of p53 target genes. We found that p53 activates transcription from different luciferase constructs, which contain p53 response elements (REs), and that PATZ1 inhibits the transcriptional activity of p53 on these reporters (Figure 4.17A, 4.17B, 4.18A, 4.18B, 4.18C 4.18D, 4.19A, and 4.19B). We also found that the C-terminal zinc finger domain lacking alternative splice variant of PATZ1, PATZ1Alt, could not suppress p53 activity as effectively as PATZ1 (Figure 4.18A, 4.18B, and 4.18C). On the other hand, PATZ1 could not repress the transcriptional activity of the C-terminal lacking alternative splice variant of p53, p53 $\beta$ , as effectively as it inhibits p53 (Figure 18D). Indeed, in order to inhibit the transcriptional activity of p53, PATZ1 physically interacts with p53 and this interaction is through the C-terminal domains of both proteins (shown by Nazli Keskin). Therefore, we conclude that PATZ1 inhibits the transcriptional activity of p53 by binding the C-terminal regulatory region of p53 using its own C-terminal zinc finger domain. In fact, there are other BTB-ZF family members that bind p53 using their zinc finger domains and that inhibit the DNA binding activity of p53 either by displacing p53 from its DNA targets or by competing in binding to the p53 REs <sup>125,126</sup>. Indeed, Nazli Keskin also found that PATZ1 utilizes these two mechanisms to inhibit the DNA binding of p53. We also observed the inhibitory effects of PATZ1 on the transcriptional activity of p53 in endogenous p53 target genes. Upon DNA damage, p53 could not induce the

expressions of known p53 targets, namely p21 and PUMA, as effectively in the presence of enforced overexpression of PATZ1 (Figure 4.24A and 4.24B). We plan to perform *in vitro* binding assays between PATZ1 and p53 that are expressed and purified from bacteria, so that we will be able to map the physical interaction between these two proteins and to define the domain requirements for this interaction.

DNA damage leads to p53 stabilization and accumulation, a marked initiator event for the downstream processes taking place in DNA damage response. We detected PATZ1 protein loss in DNA damage induced cells and generalized this phenomenon using two different cell types (Figure 4.22 and 4.23A). Because PATZ1 loss correlated with p53 accumulation after doxorubicin treatment, we questioned if p53 accumulation was necessary for PATZ1 loss. To this end, we treated HCT116 cells lacking p53 with doxorubicin and found that PATZ1 loss was still evident even in the absence of p53. However, it is noteworthy that PATZ1 loss progressed faster in the absence of p53, suggesting that p53 might be protecting PATZ1 from degradation. In order to generalize this idea, we created MEFs lacking p53 expression and we will test these cells for the rate of PATZ1 loss upon doxorubicin treatment by comparing them to their WT counterparts. It would also be interesting to see the p53 accumulation rates in PATZ1 null cells upon DNA damage induction and for this we plan to use PATZ1 *-/-* and WT MEFs in future experiments. The steady state levels of PATZ1 mRNA did not change upon doxorubicin during the time periods that we observed PATZ1 protein loss (Figure 4.23B). This indicates that the loss is in protein levels and is regulated by protein degradation and not at the transcription level. There might be post-translational modifications on PATZ1 protein that control the stability of the protein, like ubiquitination or phosphorylation. To date, a post-translational modification of the PATZ1 protein has not been reported. Identification of such post-translational modifications would give insights into PATZ1 function.

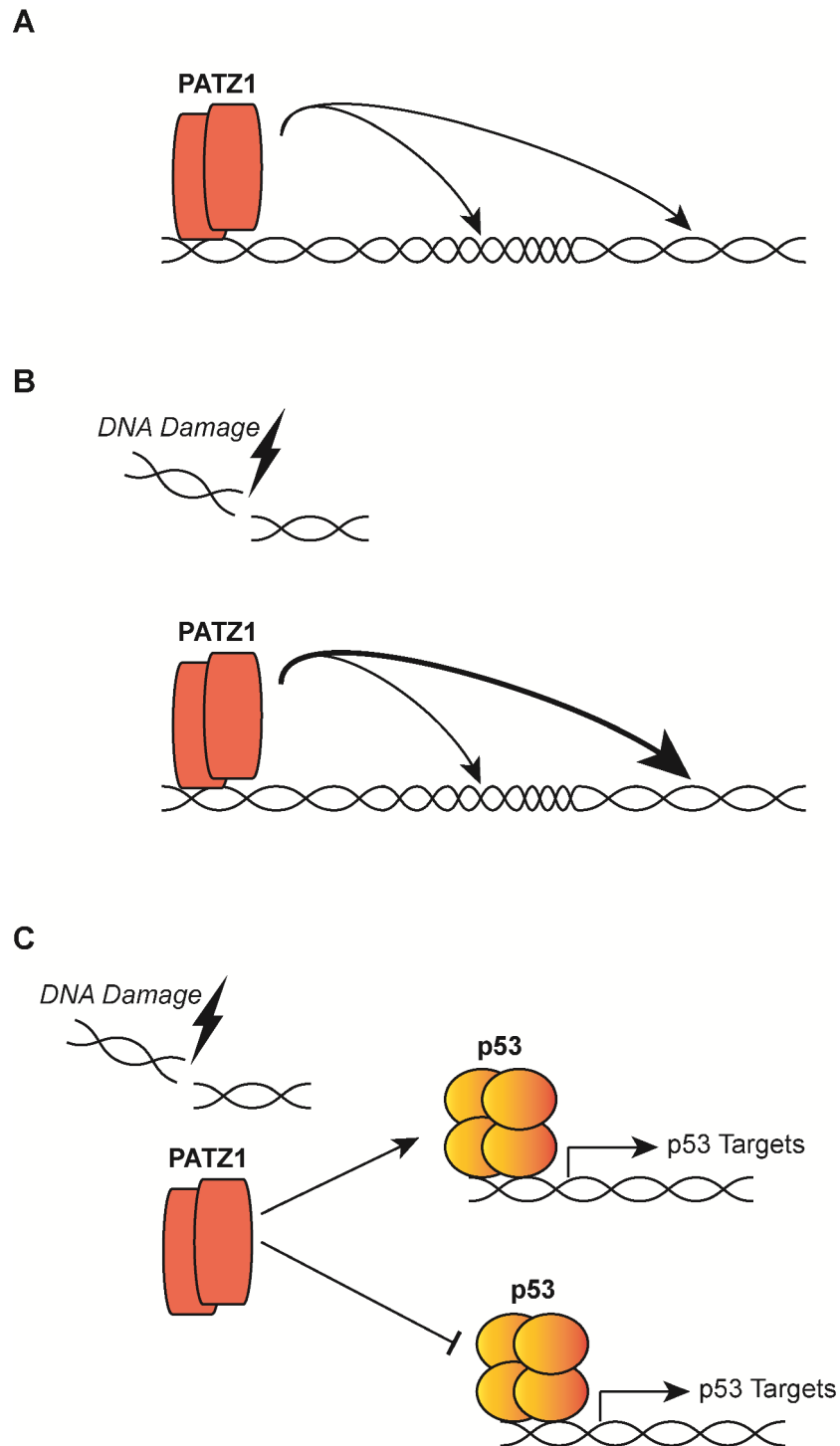


Figure 5.1: Our model of PATZ1 depicting its roles in the absence or presence of DNA damage. **A.** PATZ1 is capable of both repressing (depicted as tight DNA structure) and activating (depicted as relaxed DNA structure) the gene transcription. **B.** PATZ1 continues to its transcription activation and repression activities in the presence of DNA damage; however, it rather activates the gene transcription than repressing it. **C.** PATZ1 also affects the target specificity of p53 in the presence of DNA damage.

We listed the direct target genes of PATZ1 and the global effects of PATZ1 on p53 target genes by performing genome scale RNA-Seq and microarray experiments. In contrast to the several findings that PATZ1 functions as more of a transcription repressor, we found that PATZ1 possesses both transcription activation and repression activities (Figure 4.8A, 4.8B, and 5.1A). Interestingly, PATZ1 regulated genes were significantly enriched in biological process GO terms, such as cell adhesion, neuron differentiation and cell morphogenesis (Table 4.1). These processes are known to be regulated by the basal level transcription activities of p53 and/or p53 family members<sup>120,129,130</sup>. This shows that PATZ1 interferes not only with DNA damage induced p53, but also with the basal level transcriptional activity of p53. Indeed, Nazli Keskin demonstrated that PATZ1 physically interacts with p53 even in the absence of any DNA damage induction. The defined biological processes, in which PATZ1 plays roles, also offer an explanation to the outcomes of PATZ1 deficiency. Consistent with our GO term analysis, PATZ1-null mice are born smaller in size and at a non-Mendelian frequency, suggesting a role for PATZ1 in development<sup>101</sup>. Moreover these mice are born with defects in their central nervous systems, suggesting PATZ1 may play a role in neuron maintenance<sup>98</sup> and furthermore mESC with impaired expression of PATZ1 lose their pluripotency and start to differentiate, which are processes related to differentiation and morphogenesis<sup>100</sup>. We found that PATZ1 modulates the DNA damage response and that PATZ1 deficiency results in an alteration of the expression of p53 target genes. We listed the biological process GO terms that are uniquely affected in PATZ1 deficiency upon DNA damage induction and found that PATZ1 acts as a chromatin remodeling factor and during the DNA damage response PATZ1 functions more as transcription activator (Table 4.3 and 4.4 and Figure 5.1B and 5.1C). Many BTB-ZF family members interact with chromatin remodeling factors in order to induce changes in gene expression<sup>131-133</sup>. However, whether PATZ1 recruited other chromatin remodeling factors to the DNA in our experiments remains to be elucidated. By combining the data we obtained in this study and the fact that PATZ1 physically interacts with the C-terminal regulatory region of p53 (shown by Nazli Keskin), it is possible that PATZ1 affects the DNA target specificity of p53 through altering the C-terminal structure of p53. Although the C-terminal regulatory domain of p53 interacts with DNA in an unspecific manner and it assists the core DNA binding domain of p53 on the genome, directing it to the specific REs<sup>34,134</sup>. Also, the extensive post-translational modifications on the C-terminal regulatory domain of p53 define the

interaction partners of p53 and its overall stability<sup>33,135</sup>. PATZ1 might be a regulator in these processes; however, this needs to be further studied.

In order to create PATZ1 null human cell lines, we wanted to utilize a novel genome editing tool, TALENs (Transcription Activator-Like Effector Nucleases). In TALENs technology, a genomic locus of interest can be specifically and efficiently targeted to be modified using custom designed proteins<sup>122</sup>. We created TALENs specifically against the human *PATZ1* gene locus to knock out the gene expression (Figure 4.31 and 4.32). We delivered these proteins in to the HCT116 cell line and generated single cell derived colonies. We are in the process of screening these colonies for the mutations at the *PATZ1* gene locus. As many other BTB-ZF family transcription factors, translocation or misexpression of the *PATZ1* gene also favors tumorigenesis<sup>136,137</sup>. These indications led us to investigate the direct role of PATZ1 in tumorigenesis. For this, we wanted to utilize murine xenograph models. We created PATZ1 overexpression or knocked down conditions in a mouse T cell lymphoma cell line, which is known to develop solid tumors once delivered in mice subcutaneously (Figure 4.34A and 4.34B). We will assess the progression of the tumor development and define the effects of PATZ1 in this process.

In conclusion, our current study definitely identifies that the BTB-ZF family member transcription factor PATZ1 modulates the basal activity of p53 and in response to DNA damage. We clearly showed that the PATZ1 protein is lost upon DNA damage induction. We observed that it acts as a transcriptional repressor of the *Thpok* gene and it represses the transcriptional activity of p53 and that this inhibitory role of PATZ1 on the p53 protein is through the C-terminal domains of both proteins. These results demonstrate that PATZ1 modulates p53-dependent cellular stress and DNA damage pathways.

## REFERENCES

- 1 Lane DP, Crawford L V. T antigen is bound to a host protein in SV40-transformed cells. *Nature* 1979; **278**: 261–263.
- 2 Linzer DH, Levine AJ. Characterization of a 54K Dalton cellular SV40 tumor antigen present in SV40-transformed cells and uninfected embryonal carcinoma cells. *Cell* 1979; **17**: 43–52.
- 3 Melero JA, Stitt DT, Mangel WF, Carroll RB. Identification of new polypeptide species (48-55K) immunoprecipitable by antiserum to purified large T antigen and present in SV40-infected and -transformed cells. *Virology* 1979; **93**: 466–80.
- 4 Kress M, May E, Cassingena R, May P. Simian virus 40-transformed cells express new species of proteins precipitable by anti-simian virus 40 tumor serum. *J Virol* 1979; **31**: 472–83.
- 5 DeLeo AB, Jay G, Appella E, Dubois GC, Law LW, Old LJ. Detection of a transformation-related antigen in chemically induced sarcomas and other transformed cells of the mouse. *Proc Natl Acad Sci U S A* 1979; **76**: 2420–4.
- 6 Jenkins JR, Rudge K, Currie GA. Cellular immortalization by a cDNA clone encoding the transformation-associated phosphoprotein p53. *Nature* 1984; **312**: 651–654.
- 7 Eliyahu D, Raz A, Gruss P, Givol D, Oren M. Participation of p53 cellular tumour antigen in transformation of normal embryonic cells. *Nature* 1984; **312**: 646–649.
- 8 Parada LF, Land H, Weinberg RA, Wolf D, Rotter V. Cooperation between gene encoding p53 tumour antigen and ras in cellular transformation. *Nature* 1984; **312**: 649–651.

- 9 Crawford L V, Pim DC, Gurney EG, Goodfellow P, Taylor-Papadimitriou J. Detection of a common feature in several human tumor cell lines--a 53,000-dalton protein. *Proc Natl Acad Sci U S A* 1981; **78**: 41–5.
- 10 Vogelstein B, Fearon ER, Kern SE, Hamilton SR, Preisinger AC, Nakamura Y *et al.* Allelotype of colorectal carcinomas. *Science* 1989; **244**: 207–11.
- 11 Finlay CA, Hinds PW, Levine AJ. The p53 proto-oncogene can act as a suppressor of transformation. *Cell* 1989; **57**: 1083–93.
- 12 Levine AJ, Finlay CA, Hinds PW. P53 is a tumor suppressor gene. *Cell* 2004; **116**: S67–9, 1 p following S69.
- 13 Braithwaite a W, Prives CL. P53: More Research and More Questions. *Cell Death Differ* 2006; **13**: 877–80.
- 14 Russo A, Bazan V, Iacopetta B, Kerr D, Soussi T, Gebbia N. The TP53 colorectal cancer international collaborative study on the prognostic and predictive significance of p53 mutation: influence of tumor site, type of mutation, and adjuvant treatment. *J Clin Oncol* 2005; **23**: 7518–28.
- 15 Steele RJC, Lane DP. P53 in cancer: a paradigm for modern management of cancer. *Surgeon* 2005; **3**: 197–205.
- 16 Martins CP, Brown-Swigart L, Evan GI. Modeling the therapeutic efficacy of p53 restoration in tumors. *Cell* 2006; **127**: 1323–34.
- 17 Malkin D, Li FP, Strong LC, Fraumeni JF, Nelson CE, Kim DH *et al.* Germ line p53 mutations in a familial syndrome of breast cancer, sarcomas, and other neoplasms. *Science* 1990; **250**: 1233–8.
- 18 Donehower LA, Harvey M, Slagle BL, McArthur MJ, Montgomery CA, Butel JS *et al.* Mice deficient for p53 are developmentally normal but susceptible to spontaneous tumours. *Nature* 1992; **356**: 215–21.
- 19 Jacks T, Remington L, Williams BO, Schmitt EM, Halachmi S, Bronson RT *et al.* Tumor spectrum analysis in p53-mutant mice. *Curr Biol* 1994; **4**: 1–7.
- 20 Venkatachalam S, Shi YP, Jones SN, Vogel H, Bradley A, Pinkel D *et al.* Retention of wild-type p53 in tumors from p53 heterozygous mice: reduction of p53 dosage can promote cancer formation. *EMBO J* 1998; **17**: 4657–67.
- 21 Freed-Pastor WA, Prives C. Mutant p53: one name, many proteins. *Genes Dev* 2012; **26**: 1268–86.
- 22 Oren M, Rotter V. Mutant p53 gain-of-function in cancer. *Cold Spring Harb Perspect Biol* 2010; **2**: a001107.
- 23 Bode AM, Dong Z. Post-translational modification of p53 in tumorigenesis. *Nat Rev Cancer* 2004; **4**: 793–805.

- 24 Wahl GM, Stommel JM KK and W. *Gatekeepers of the Guardian: p53 Regulation by Post-Translational Modification, MDM2 and MDMX: 25 Years of p53 Research*. Springer Netherlands: Dordrecht, 2007 doi:10.1007/978-1-4020-2922-6.
- 25 Harms KL, Chen X. The C terminus of p53 family proteins is a cell fate determinant. *Mol Cell Biol* 2005; **25**: 2014–30.
- 26 Dumaz N, Milne DM, Jardine LJ, Meek DW. Critical roles for the serine 20, but not the serine 15, phosphorylation site and for the polyproline domain in regulating p53 turnover. *Biochem J* 2001; **359**: 459–64.
- 27 Liu G, Xia T, Chen X. The activation domains, the proline-rich domain, and the C-terminal basic domain in p53 are necessary for acetylation of histones on the proximal p21 promoter and interaction with p300/CREB-binding protein. *J Biol Chem* 2003; **278**: 17557–65.
- 28 el-Deiry WS, Kern SE, Pietenpol JA, Kinzler KW, Vogelstein B. Definition of a consensus binding site for p53. *Nat Genet* 1992; **1**: 45–9.
- 29 Petitjean A, Mathe E, Kato S, Ishioka C, Tavtigian S V, Hainaut P *et al*. Impact of mutant p53 functional properties on TP53 mutation patterns and tumor phenotype: lessons from recent developments in the IARC TP53 database. *Hum Mutat* 2007; **28**: 622–9.
- 30 McLure KG, Lee PW. How p53 binds DNA as a tetramer. *EMBO J* 1998; **17**: 3342–50.
- 31 Stommel JM, Marchenko ND, Jimenez GS, Moll UM, Hope TJ, Wahl GM. A leucine-rich nuclear export signal in the p53 tetramerization domain: regulation of subcellular localization and p53 activity by NES masking. *EMBO J* 1999; **18**: 1660–72.
- 32 Strahl BD, Allis CD. The language of covalent histone modifications. *Nature* 2000; **403**: 41–45.
- 33 Rodriguez MS, Desterro JM, Lain S, Lane DP, Hay RT. Multiple C-terminal lysine residues target p53 for ubiquitin-proteasome-mediated degradation. *Mol Cell Biol* 2000; **20**: 8458–67.
- 34 Gu W, Roeder RG. Activation of p53 Sequence-Specific DNA Binding by Acetylation of the p53 C-Terminal Domain. *Cell* 1997; **90**: 595–606.
- 35 Brooks CL, Gu W. P53 Regulation By Ubiquitin. *FEBS Lett* 2011; **585**: 2803–9.
- 36 Montes de Oca Luna R, Wagner DS, Lozano G. Rescue of early embryonic lethality in mdm2-deficient mice by deletion of p53. *Nature* 1995; **378**: 203–6.
- 37 Jones SN, Roe AE, Donehower LA, Bradley A. Rescue of embryonic lethality in Mdm2-deficient mice by absence of p53. *Nature* 1995; **378**: 206–8.

- 38 Horn HF, Vousden KH. Coping with stress: multiple ways to activate p53. *Oncogene* 2007; **26**: 1306–16.
- 39 Marine J-C, Jochemsen AG. Mdmx as an essential regulator of p53 activity. *Biochem Biophys Res Commun* 2005; **331**: 750–60.
- 40 Gu J, Kawai H, Nie L, Kitao H, Wiederschain D, Jochemsen AG *et al*. Mutual dependence of MDM2 and MDMX in their functional inactivation of p53. *J Biol Chem* 2002; **277**: 19251–4.
- 41 Lee JT, Gu W. The multiple levels of regulation by p53 ubiquitination. *Cell Death Differ* 2010; **17**: 86–92.
- 42 Grossman SR, Deato ME, Brignone C, Chan HM, Kung AL, Tagami H *et al*. Polyubiquitination of p53 by a ubiquitin ligase activity of p300. *Science* 2003; **300**: 342–4.
- 43 Kruse J-P, Gu W. Modes of p53 regulation. *Cell* 2009; **137**: 609–22.
- 44 Pereg Y, Shkedy D, de Graaf P, Meulmeester E, Edelson-Averbukh M, Salek M *et al*. Phosphorylation of Hdmx mediates its Hdm2- and ATM-dependent degradation in response to DNA damage. *Proc Natl Acad Sci U S A* 2005; **102**: 5056–61.
- 45 Maya R, Balass M, Kim ST, Shkedy D, Leal JF, Shifman O *et al*. ATM-dependent phosphorylation of Mdm2 on serine 395: role in p53 activation by DNA damage. *Genes Dev* 2001; **15**: 1067–77.
- 46 Li M, Luo J, Brooks CL, Gu W. Acetylation of p53 inhibits its ubiquitination by Mdm2. *J Biol Chem* 2002; **277**: 50607–11.
- 47 Kon N, Zhong J, Kobayashi Y, Li M, Szabolcs M, Ludwig T *et al*. Roles of HAUSP-mediated p53 regulation in central nervous system development. *Cell Death Differ* 2011; **18**: 1366–75.
- 48 Meulmeester E, Pereg Y, Shiloh Y, Jochemsen AG. ATM-mediated phosphorylations inhibit Mdmx/Mdm2 stabilization by HAUSP in favor of p53 activation. *Cell Cycle* 2005; **4**: 1166–70.
- 49 Maltzman W, Czyzyk L. UV irradiation stimulates levels of p53 cellular tumor antigen in nontransformed mouse cells. *Mol Cell Biol* 1984; **4**: 1689–94.
- 50 Kastan MB, Onyekwere O, Sidransky D, Vogelstein B, Craig RW. Participation of p53 protein in the cellular response to DNA damage. *Cancer Res* 1991; **51**: 6304–11.
- 51 Sherr CJ. Divorcing ARF and p53: an unsettled case. *Nat Rev Cancer* 2006; **6**: 663–73.

- 52 Kamijo T, Kamp E Van De, Chong MJ, Zindy F, Diehl JA, Sherr CJ *et al.* Loss of the ARF Tumor Suppressor Reverses Premature Replicative Arrest but not Radiation Hypersensitivity Arising from Disabled Atm Function Loss of the ARF Tumor Suppressor Reverses Premature Replicative Arrest but not Radiation Hypersensitivity Arising . 1999; : 2464–2469.
- 53 Dai M-S, Lu H. Inhibition of MDM2-mediated p53 ubiquitination and degradation by ribosomal protein L5. *J Biol Chem* 2004; **279**: 44475–82.
- 54 Lohrum M a E, Ludwig RL, Kubbutat MHG, Hanlon M, Vousden KH. Regulation of HDM2 activity by the ribosomal protein L11. *Cancer Cell* 2003; **3**: 577–87.
- 55 Dai M-S, Zeng SX, Jin Y, Sun X-X, David L, Lu H. Ribosomal protein L23 activates p53 by inhibiting MDM2 function in response to ribosomal perturbation but not to translation inhibition. *Mol Cell Biol* 2004; **24**: 7654–68.
- 56 Hammond EM, Denko NC, Dorie MJ, Abraham RT, Giaccia AJ. Hypoxia links ATR and p53 through replication arrest. *Mol Cell Biol* 2002; **22**: 1834–43.
- 57 Hammond EM, Giaccia AJ. The role of p53 in hypoxia-induced apoptosis. *Biochem Biophys Res Commun* 2005; **331**: 718–25.
- 58 Milyavsky M, Mimran A, Senderovich S, Zurer I, Erez N, Shats I *et al.* Activation of p53 protein by telomeric (TTAGGG)<sub>n</sub> repeats. *Nucleic Acids Res* 2001; **29**: 5207–15.
- 59 Vousden KH, Ryan KM. p53 and metabolism. *Nat Rev Cancer* 2009; **9**: 691–700.
- 60 Gambino V, De Michele G, Venezia O, Migliaccio P, Dall’Olio V, Bernard L *et al.* Oxidative stress activates a specific p53 transcriptional response that regulates cellular senescence and aging. *Aging Cell* 2013; **12**: 435–45.
- 61 Zilfou JT, Lowe SW. Tumor suppressive functions of p53. *Cold Spring Harb Perspect Biol* 2009; **1**: a001883.
- 62 Agarwal ML, Agarwal A, Taylor WR, Stark GR. p53 controls both the G2/M and the G1 cell cycle checkpoints and mediates reversible growth arrest in human fibroblasts. *Proc Natl Acad Sci U S A* 1995; **92**: 8493–7.
- 63 el-Deiry WS, Tokino T, Velculescu VE, Levy DB, Parsons R, Trent JM *et al.* WAF1, a potential mediator of p53 tumor suppression. *Cell* 1993; **75**: 817–25.
- 64 Chen X, Ko LJ, Jayaraman L, Prives C. p53 levels, functional domains, and DNA damage determine the extent of the apoptotic response of tumor cells. *Genes Dev* 1996; **10**: 2438–51.

- 65 Zhan Q, Antinore MJ, Wang XW, Carrier F, Smith ML, Harris CC *et al.* Association with Cdc2 and inhibition of Cdc2/Cyclin B1 kinase activity by the p53-regulated protein Gadd45. *Oncogene* 1999; **18**: 2892–900.
- 66 Hermeking H, Lengauer C, Polyak K, He TC, Zhang L, Thiagalingam S *et al.* 14-3-3 sigma is a p53-regulated inhibitor of G2/M progression. *Mol Cell* 1997; **1**: 3–11.
- 67 Kuilman T, Michaloglou C, Mooi WJ, Peeper DS. The essence of senescence. *Genes Dev* 2010; **24**: 2463–79.
- 68 Green DR, Kroemer G. Cytoplasmic functions of the tumour suppressor p53. *Nature* 2009; **458**: 1127–30.
- 69 Chipuk JE, Bouchier-Hayes L, Kuwana T, Newmeyer DD, Green DR. PUMA couples the nuclear and cytoplasmic proapoptotic function of p53. *Science* 2005; **309**: 1732–5.
- 70 Godt D, Couderc JL, Cramton SE, Laski FA. Pattern formation in the limbs of *Drosophila*: bric à brac is expressed in both a gradient and a wave-like pattern and is required for specification and proper segmentation of the tarsus. *Development* 1993; **119**: 799–812.
- 71 DiBello PR, Withers DA, Bayer CA, Fristrom JW, Guild GM. The *Drosophila* Broad-Complex encodes a family of related proteins containing zinc fingers. *Genetics* 1991; **129**: 385–97.
- 72 Harrison SD, Travers AA. The tramtrack gene encodes a *Drosophila* finger protein that interacts with the ftz transcriptional regulatory region and shows a novel embryonic expression pattern. *EMBO J* 1990; **9**: 207–16.
- 73 Perez-Torrado R, Yamada D, Defossez P-A. Born to bind: the BTB protein-protein interaction domain. *Bioessays* 2006; **28**: 1194–202.
- 74 Bardwell VJ, Treisman R. The POZ domain: a conserved protein-protein interaction motif. *Genes Dev* 1994; **8**: 1664–77.
- 75 Klug A. The discovery of zinc fingers and their development for practical applications in gene regulation and genome manipulation. *Q Rev Biophys* 2010; **43**: 1–21.
- 76 Siggs OM, Beutler B. The BTB-ZF transcription factors. *Cell Cycle* 2012; **11**: 3358–69.
- 77 Reeves R, Nissen M. The A.T-DNA-binding domain of mammalian high mobility group I chromosomal proteins. A novel peptide motif for recognizing DNA structure. *J Biol Chem* 1990; **265**: 8573–8582.

- 78 Staller P, Peukert K, Kiermaier A, Seoane J, Lukas J, Karsunky H *et al.* Repression of p15INK4b expression by Myc through association with Miz-1. *Nat Cell Biol* 2001; **3**: 392–9.
- 79 Huynh KD, Bardwell VJ. The BCL-6 POZ domain and other POZ domains interact with the co-repressors N-CoR and SMRT. *Oncogene* 1998; **17**: 2473–84.
- 80 Chen Z, Brand NJ, Chen A, Chen SJ, Tong JH, Wang ZY *et al.* Fusion between a novel Krüppel-like zinc finger gene and the retinoic acid receptor-alpha locus due to a variant t(11;17) translocation associated with acute promyelocytic leukaemia. *EMBO J* 1993; **12**: 1161–7.
- 81 Alcalay M, Meani N, Gelmetti V, Fantozzi A, Fagioli M, Orleth A *et al.* Acute myeloid leukemia fusion proteins deregulate genes involved in stem cell maintenance and DNA repair. *J Clin Invest* 2003; **112**: 1751–61.
- 82 McConnell MJ, Chevallier N, Berkofsky-Fessler W, Giltane JM, Malani RB, Staudt LM *et al.* Growth suppression by acute promyelocytic leukemia-associated protein PLZF is mediated by repression of c-myc expression. *Mol Cell Biol* 2003; **23**: 9375–88.
- 83 Phan RT, Dalla-Favera R. The BCL6 proto-oncogene suppresses p53 expression in germinal-centre B cells. *Nature* 2004; **432**: 635–9.
- 84 Pasqualucci L, Bereshchenko O, Bereschenko O, Niu H, Klein U, Basso K *et al.* Molecular pathogenesis of non-Hodgkin's lymphoma: the role of Bcl-6. *Leuk Lymphoma* 2003; **44 Suppl 3**: S5–12.
- 85 Phan RT, Saito M, Basso K, Niu H, Dalla-Favera R. BCL6 interacts with the transcription factor Miz-1 to suppress the cyclin-dependent kinase inhibitor p21 and cell cycle arrest in germinal center B cells. *Nat Immunol* 2005; **6**: 1054–60.
- 86 Ranuncolo SM, Polo JM, Dierov J, Singer M, Kuo T, Grealley J *et al.* Bcl-6 mediates the germinal center B cell phenotype and lymphomagenesis through transcriptional repression of the DNA-damage sensor ATR. *Nat Immunol* 2007; **8**: 705–14.
- 87 Korutla L, Neustadter JH, Fournier KM, Mackler SA. NAC1, a POZ/BTB protein present in the adult mammalian brain, triggers apoptosis after adenovirus-mediated overexpression in PC-12 cells. *Neurosci Res* 2003; **46**: 33–9.
- 88 Wales MM, Biel MA, Deiry W El, Nelkin BD, Issa J-P, Cavenee WK *et al.* p53 activates expression of HIC-1, a new candidate tumour suppressor gene on 17p13.3. *Nat Genet* 1995; **1**: 570–577.
- 89 Chen WY, Wang DH, Yen RC, Luo J, Gu W, Baylin SB. Tumor suppressor HIC1 directly regulates SIRT1 to modulate p53-dependent DNA-damage responses. *Cell* 2005; **123**: 437–48.

- 90 Stogios PJ, Chen L, Privé GG. Crystal structure of the BTB domain from the LRF/ZBTB7 transcriptional regulator. *Protein Sci* 2007; **16**: 336–42.
- 91 Maeda T, Hobbs RM, Merghoub T, Guernah I, Zelent A, Cordon-Cardo C *et al.* Role of the proto-oncogene Pokemon in cellular transformation and ARF repression. *Nature* 2005; **433**: 278–85.
- 92 Kobayashi a, Yamagiwa H, Hoshino H, Muto a, Sato K, Morita M *et al.* A combinatorial code for gene expression generated by transcription factor Bach2 and MAZR (MAZ-related factor) through the BTB/POZ domain. *Mol Cell Biol* 2000; **20**: 1733–46.
- 93 Fedele M, Benvenuto G, Pero R, Majello B, Battista S, Lembo F *et al.* A novel member of the BTB/POZ family, PATZ, associates with the RNF4 RING finger protein and acts as a transcriptional repressor. *J Biol Chem* 2000; **275**: 7894–901.
- 94 Pero R, Lembo F, Palmieri EA, Vitiello C, Fedele M, Fusco A *et al.* PATZ attenuates the RNF4-mediated enhancement of androgen receptor-dependent transcription. *J Biol Chem* 2002; **277**: 3280–5.
- 95 Quigley CA, De Bellis A, Marschke KB, el-Awady MK, Wilson EM, French FS. Androgen receptor defects: historical, clinical, and molecular perspectives. *Endocr Rev* 1995; **16**: 271–321.
- 96 Fedele M, Franco R, Salvatore G, Paronetto MP, Barbagallo F, Pero R *et al.* PATZ1 gene has a critical role in the spermatogenesis and testicular tumours. 2008; : 39–47.
- 97 Tritz R, Mueller BM, Hickey MJ, Lin AH, Gomez GG, Hadwiger P *et al.* siRNA Down-regulation of the PATZ1 Gene in Human Glioma Cells Increases Their Sensitivity to Apoptotic Stimuli. *Cancer Ther* 2008; **6**: 865–876.
- 98 Valentino T, Palmieri D, Vitiello M, Simeone A, Palma G, Arra C *et al.* Embryonic defects and growth alteration in mice with homozygous disruption of the Patz1 gene. *J Cell Physiol* 2013; **228**: 646–53.
- 99 Sakaguchi S, Hombauer M, Bilic I, Naoe Y, Schebesta A, Taniuchi I *et al.* The zinc-finger protein MAZR is part of the transcription factor network that controls the CD4 versus CD8 lineage fate of double-positive thymocytes. *Nat Immunol* 2010; **11**: 442–8.
- 100 Ow JR, Ma H, Jean A, Goh Z, Lee YH, Chong YM *et al.* Patz1 Regulates Embryonic Stem Cell Identity. *Stem Cells Dev* 2014; **23**: 1062–1073.
- 101 Bilic I, Koesters C, Unger B, Sekimata M, Hertweck A, Maschek R *et al.* Negative regulation of CD8 expression via Cd8 enhancer-mediated recruitment of the zinc finger protein MAZR. *Nat Immunol* 2006; **7**: 392–400.

- 102 Cho JH, Kim MJ, Kim KJ, Kim J-R. POZ/BTB and AT-hook-containing zinc finger protein 1 (PATZ1) inhibits endothelial cell senescence through a p53 dependent pathway. *Cell Death Differ*. 2012; **19**: 703–12.
- 103 Valentino T, Palmieri D, Vitiello M, Pierantoni GM, Fusco a, Fedele M. PATZ1 interacts with p53 and regulates expression of p53-target genes enhancing apoptosis or cell survival based on the cellular context. *Cell Death Dis* 2013; **4**: e963.
- 104 Mastrangelo T, Modena P, Tornielli S, Bullrich F, Testi MA, Mezzelani A *et al*. SHORT REPORT A novel zinc finger gene is fused to EWS in small round cell tumor. 2000.
- 105 Pero R, Palmieri D, Angrisano T, Valentino T, Federico A, Franco R *et al*. POZ-, AT-hook-, and zinc finger-containing protein (PATZ) interacts with human oncogene B cell lymphoma 6 (BCL6) and is required for its negative autoregulation. *J Biol Chem* 2012; **287**: 18308–17.
- 106 Tian X, Sun D, Zhang Y, Zhao S, Xiong H, Fang J. Zinc finger protein 278, a potential oncogene in human colorectal cancer. *Acta Biochim Biophys Sin (Shanghai)* 2008; **40**: 289–296.
- 107 Yang W-L, Ravatn R, Kudoh K, Alabanza L, Chin K-V. Interaction of the regulatory subunit of the cAMP-dependent protein kinase with PATZ1 (ZNF278). *Biochem Biophys Res Commun* 2010; **391**: 1318–23.
- 108 Swift S, Lorens J, Achacoso P, Nolan GP. Rapid production of retroviruses for efficient gene delivery to mammalian cells using 293T cell-based systems. *Curr Protoc Immunol* 2001; **Chapter 10**: Unit 10.17C.
- 109 Baus E, Van Laethem F, Andris F, Rolin S, Urbain J, Leo O. Dexamethasone increases intracellular cyclic AMP concentration in murine T lymphocyte cell lines. *Steroids* 2001; **66**: 39–47.
- 110 Groves T, Katis P, Madden Z, Manickam K, Ramsden D, Wu G *et al*. In vitro maturation of clonal CD4+CD8+ cell lines in response to TCR engagement. *J Immunol* 1995; **154**: 5011–22.
- 111 Lesley J, He Q, Miyake K, Hamann A, Hyman R, Kincade PW. Requirements for hyaluronic acid binding by CD44: a role for the cytoplasmic domain and activation by antibody. *J Exp Med* 1992; **175**: 257–66.
- 112 Hahm K, Cobb BS, McCarty AS, Brown KE, Klug CA, Lee R *et al*. Helios, a T cell-restricted Ikaros family member that quantitatively associates with Ikaros at centromeric heterochromatin. *Genes Dev* 1998; **12**: 782–96.
- 113 Fedele M. A Novel Member of the BTB/POZ Family, PATZ, Associates with the RNF4 RING Finger Protein and Acts as a Transcriptional Repressor. *J Biol Chem* 2000; **275**: 7894–7901.

- 114 Pero R, Lembo F, Palmieri EA, Vitiello C, Fedele M, Fusco A *et al.* PATZ attenuates the RNF4-mediated enhancement of androgen receptor-dependent transcription. *J Biol Chem* 2002; **277**: 3280–5.
- 115 Huang DW, Sherman BT, Lempicki RA. Bioinformatics enrichment tools: paths toward the comprehensive functional analysis of large gene lists. *Nucleic Acids Res* 2009; **37**: 1–13.
- 116 Sakaue-Sawano A, Kurokawa H, Morimura T, Hanyu A, Hama H, Osawa H *et al.* Visualizing spatiotemporal dynamics of multicellular cell-cycle progression. *Cell* 2008; **132**: 487–98.
- 117 Nishitani H, Lygerou Z, Nishimoto T. Proteolysis of DNA replication licensing factor Cdt1 in S-phase is performed independently of geminin through its N-terminal region. *J Biol Chem* 2004; **279**: 30807–16.
- 118 Nishitani H, Lygerou Z, Nishimoto T, Nurse P. The Cdt1 protein is required to license DNA for replication in fission yeast. *Nature* 2000; **404**: 625–8.
- 119 Yu J, Zhang L, Hwang PM, Kinzler KW, Vogelstein B. PUMA induces the rapid apoptosis of colorectal cancer cells. *Mol Cell* 2001; **7**: 673–82.
- 120 Kenzelmann Broz D, Spano Mello S, Bieging KT, Jiang D, Dusek RL, Brady C *et al.* Global genomic profiling reveals an extensive p53-regulated autophagy program contributing to key p53 responses. *Genes Dev* 2013; **27**: 1016–31.
- 121 Edgar R, Domrachev M, Lash AE. Gene Expression Omnibus: NCBI gene expression and hybridization array data repository. *Nucleic Acids Res* 2002; **30**: 207–10.
- 122 Cermak T, Doyle EL, Christian M, Wang L, Zhang Y, Schmidt C *et al.* Efficient design and assembly of custom TALEN and other TAL effector-based constructs for DNA targeting. *Nucleic Acids Res* 2011; **39**: e82.
- 123 Wei C, Liu J, Yu Z, Zhang B, Gao G, Jiao R. TALEN or Cas9 - rapid, efficient and specific choices for genome modifications. *J Genet Genomics* 2013; **40**: 281–9.
- 124 Riese MJ, Wang L-CS, Moon EK, Joshi RP, Ranganathan A, June CH *et al.* Enhanced effector responses in activated CD8+ T cells deficient in diacylglycerol kinases. *Cancer Res* 2013; **73**: 3566–77.
- 125 Jeon B-N, Choi W-I, Yu M-Y, Yoon A-R, Kim M-H, Yun C-O *et al.* ZBTB2, a novel master regulator of the p53 pathway. *J Biol Chem* 2009; **284**: 17935–46.
- 126 Koh D-I, Choi W-I, Jeon B-N, Lee C-E, Yun C-O, Hur M-W. A novel POK family transcription factor, ZBTB5, represses transcription of p21CIP1 gene. *J Biol Chem* 2009; **284**: 19856–66.

- 127 Melnick A, Carlile G, Ahmad KF, Kiang C-L, Corcoran C, Bardwell V *et al.* Critical Residues within the BTB Domain of PLZF and Bcl-6 Modulate Interaction with Corepressors. *Mol Cell Biol* 2002; **22**: 1804–1818.
- 128 Thomas M, Pim D, Banks L. The role of the E6-p53 interaction in the molecular pathogenesis of HPV. *Oncogene* 1999; **18**: 7690–700.
- 129 Kouwenhoven EN, van Heeringen SJ, Tena JJ, Oti M, Dutilh BE, Alonso ME *et al.* Genome-wide profiling of p63 DNA-binding sites identifies an element that regulates gene expression during limb development in the 7q21 SHFM1 locus. *PLoS Genet* 2010; **6**: e1001065.
- 130 Carroll DK, Carroll JS, Leong C-O, Cheng F, Brown M, Mills AA *et al.* p63 regulates an adhesion programme and cell survival in epithelial cells. *Nat Cell Biol* 2006; **8**: 551–61.
- 131 Dhordain P, Albagli O, Lin RJ, Ansieau S, Quief S, Leutz A *et al.* Corepressor SMRT binds the BTB/POZ repressing domain of the LAZ3/BCL6 oncoprotein. *Proc Natl Acad Sci* 1997; **94**: 10762–10767.
- 132 Huynh KD, Fischle W, Verdin E, Bardwell VJ. BCoR, a novel corepressor involved in BCL-6 repression. *Genes & Dev* 2000; **14**: 1810–1823.
- 133 Jeon B-N, Yoo J-Y, Choi W-I, Lee C-E, Yoon H-G, Hur M-W. Proto-oncogene FBI-1 (Pokemon/ZBTB7A) represses transcription of the tumor suppressor Rb gene via binding competition with Sp1 and recruitment of co-repressors. *J Biol Chem* 2008; **283**: 33199–210.
- 134 Kim H, Kim K, Choi J, Heo K, Baek HJ, Roeder RG *et al.* p53 requires an intact C-terminal domain for DNA binding and transactivation. *J Mol Biol* 2012; **415**: 843–54.
- 135 Li M, Luo J, Brooks CL, Gu W. Acetylation of p53 inhibits its ubiquitination by Mdm2. *J Biol Chem* 2002; **277**: 50607–11.
- 136 Pero R, Palmieri D, Angrisano T, Valentino T, Federico A, Franco R *et al.* POZ-, AT-hook-, and zinc finger-containing protein (PATZ) interacts with human oncogene B cell lymphoma 6 (BCL6) and is required for its negative autoregulation. *J Biol Chem* 2012; **287**: 18308–17.
- 137 Sankar S, Lessnick SL. Promiscuous partnerships in Ewing’s sarcoma. *Cancer Genet* 2011; **204**: 351–65.

## APPENDIX

### APPENDIX A: Chemicals Used in the Study

<b>Chemicals and Media Components</b>	<b>Supplier Company</b>
2-Mercaptoethanol	Sigma, Germany
Acetic Acid	Merck, Germany
Acid Washed Glass Beads	Sigma, Germany
Acrylamide/Bis-acrylamide	Sigma, Germany
Agarose	peQLab, Germany
Ammonium Persulfate	Sigma, Germany
Ammonium Sulfate	Sigma, Germany
Ampicillin Sodium Salt	CellGro, USA
Bacto Agar	BD, USA
Bacto Tryptone	BD, USA
Boric Acid	Molekula, UK
Bradford Reagent	Sigma, Germany
Bromophenol Blue	Sigma, Germany
Chloramphenicol	Gibco, USA
D-Glucose	Sigma, Germany
Distilled water	Milipore, France
DMEM	PAN, Germany
DMSO	Sigma, Germany

DNA Gel Loading Solution, 5X	Quality Biological, Inc, USA
DPBS	CellGro, USA
EDTA	Applichem, Germany
Ethanol	Riedel-de Haen, Germany
Ethidium Bromide	Sigma, Germany
Fetal Bovine Serum (FBS)	Biological Industries, Israel
Glycerol Anhydrous	Applichem, Germany
Glycine	Applichem, Germany
HBSS	CellGro, USA
HEPES	Applichem, Germany
Hydrochloric Acid	Merck, Germany
Isopropanol	Riedel-de Haén, Germany
Kanamycin Sulfate	Gibco, USA
LB Agar	BD, USA
LB Broth	BD, USA
L-Glutamine	Hyclone, USA
Liquid nitrogen	Karbogaz, Turkey
Magnesium Chloride	Promega, USA
Methanol	Riedel-de Haen, Germany
Monoclonal Anti-HA Antibody	Sigma, Germany
p53 Mouse Antibody	Cell Signalling Technology, USA
p53 Polyclonal Antibody	Cell Signalling Technology, USA
PATZ1 (H-300) Antibody	Santa Cruz, USA
Penicillin-Streptomycin	Sigma, Germany
Phenol-Chloroform-Isoamylalcohol	Amersco, USA
PIPES	Sigma, Germany
Potassium Acetate	Merck, Germany
Potassium Chloride	Fluka, Germany
Potassium Hydroxide	Merck, Germany
Protease Tablets (EDTA-free)	Roche, Germany
ProtG Sepharose	Amersco, USA
RNase A	Roche, Germany
RPMI 1640	PAN, Germany
SDS Protein Gel Loading Pack	Fermentas, Germany
SDS Pure	Applichem, Germany
Skim Milk Powder	Fluka, Germany
Sodium Azide	Amresco, USA
Sodium Chloride	Applichem, Germany
SuperSignal Chemiluminescent Substrate	Thermo Scientific, USA
TEMED	Applichem, Germany
Tris Buffer Grade	Amresco, USA
Tris Hydrochloride	Amresco, USA
Triton X100	Promega, USA
Tween20	Sigma, Germany

## APPENDIX B: Equipment Used in the Study

Equipment	Company
Autoclave	Hirayama, Hiclave HV-110, Japan
Balance	Sartorius, BP221S, Germany Schimadzu, Libror EB-3200 HU, Japan
Biomolecular Imager	ImageQuant LAS 4000 mini - GE Healthcare, USA
Cell Counter	Cole Parmer, USA
Centrifuge	Eppendorf, 5415D, Germany Hitachi, Sorvall RC5C Plus, USA
CO2 Incubator	Binder, Germany
Deepfreeze	-80°C, Forma, Thermo Electron Corp., USA -20°C, Bosch, Turkey
Distilled Water	Millipore, Elix-S, France
Electrophoresis Apparatus	Biogen Inc., USA Biorad Inc., USA
Electroporator	Neon Transfection System - Life Technologies, USA
Filter Membranes	Millipore, USA
Flow Cytometer	BDFACSCanto, USA
Gel Documentation	Biorad, UV-Transilluminator 2000, USA
Heater	Thermomixer Comfort, Eppendorf, Germany
Hematocytometer	Hausser Scientific, Blue Bell Pa., USA
Ice Machine	Scotsman Inc., AF20, USA
Incubator	Memmert, Modell 300, Germany Memmert, Modell 600, Germany
Laminar Flow	Kendro Lab. Prod., Heraeus, HeraSafe HS12, Germany
Liquid Nitrogen Tank	Taylor-Wharton, 3000RS, USA
Magnetic Stirrer	VELP Scientifica, ARE Heating Magnetic Stirrer, Italy
Microliter Pipettes	Gilson, Pipetman, France Eppendorf, Germany
Microscope	Olympus CK40, Japan Olympus CH20, Japan Olympus IX70, Japan Zeiss Confocal LSM710, German
Microwave Oven	Bosch, Turkey
pH meter	WTW, pH540 GLP MultiCal, Germany
Power Supply	Biorad, PowerPac 300, USA
Refrigerator	Bosch, Turkey

Shaker Incubator  
Spectrophotometer

New Brunswick Sci., Innova 4330, USA

Schimadzu, UV-1208, Japan

Schimadzu, UV-3150, Japan

Thermocycler

Eppendorf, Mastercycler Gradient, Germany

Vortex

Velp Scientifica, Italy

## APPENDIX C: DNA and Protein Molecular Weight Markers

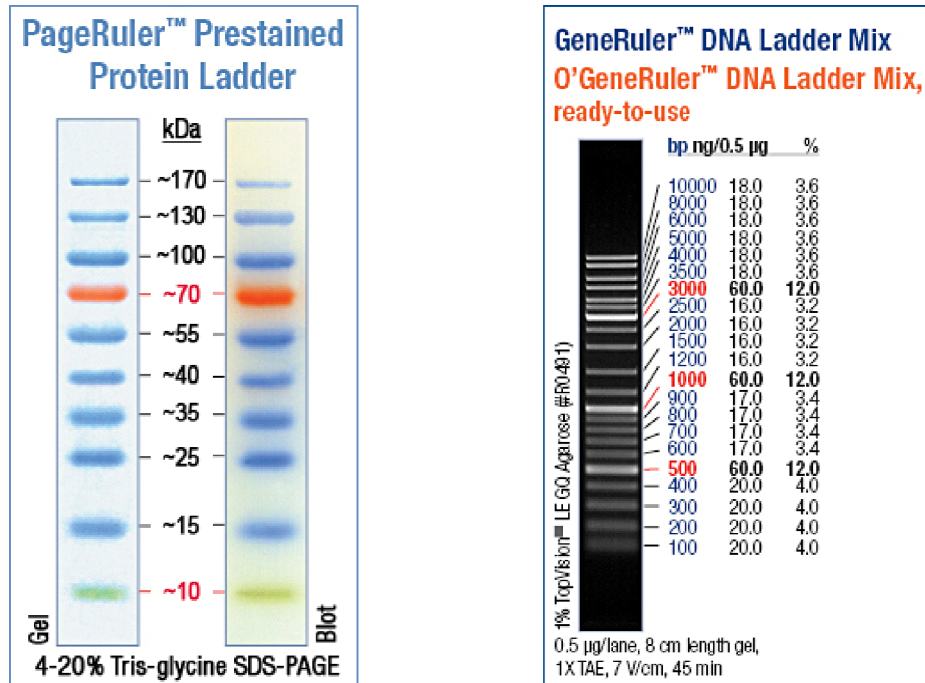


Figure C.1: DNA and Protein Molecular Weight Markers

## APPENDIX D: Cloning of PATZ1 cDNAs into pmigII-ires-mcherry Plasmid

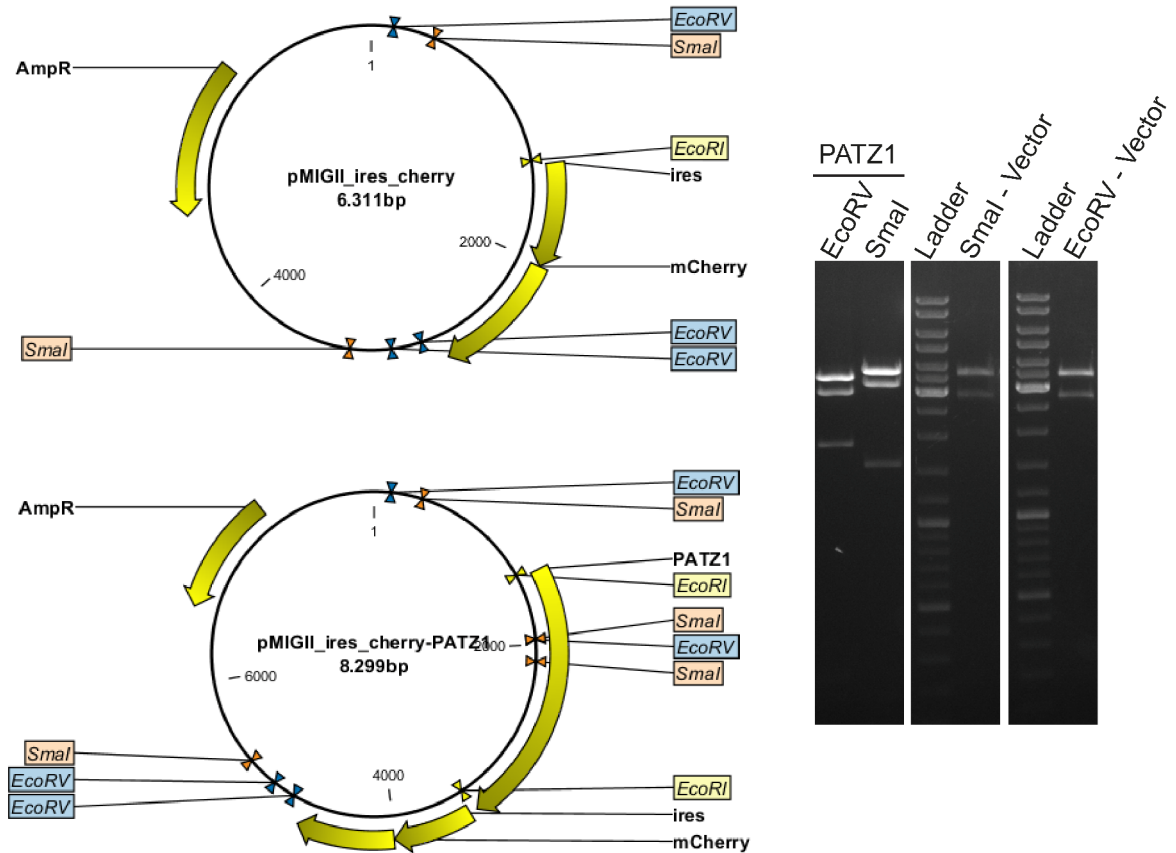
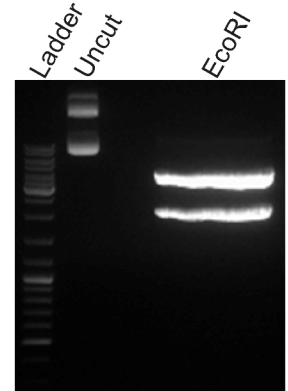
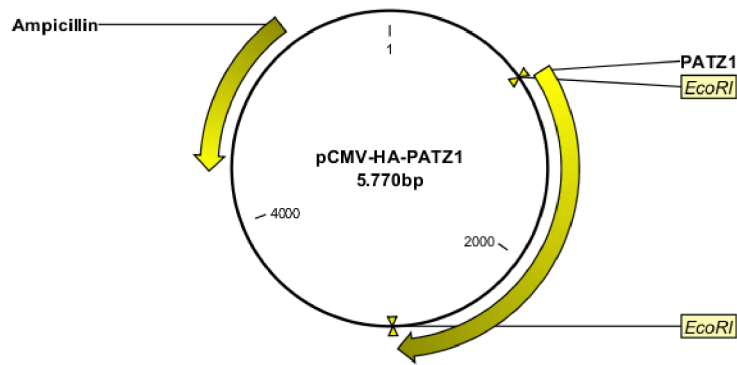


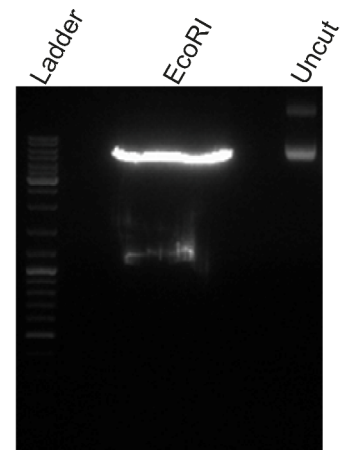
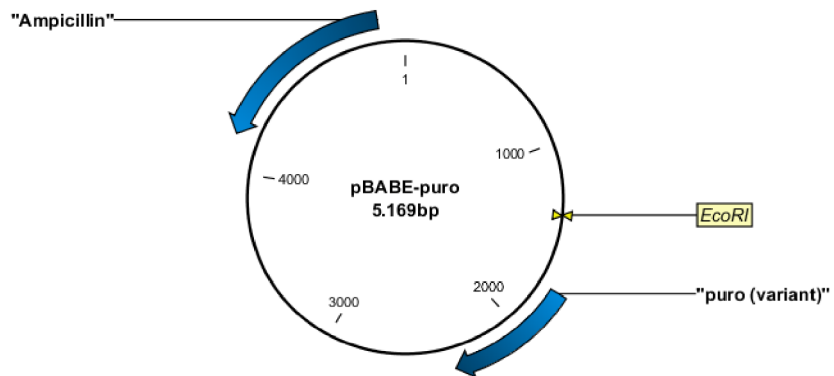
Figure D.1: Cloning of PATZ1 cDNAs into pmigII-ires-mcherry Plasmid. *Patz1* cDNA was obtained from pCMV-HA-PATZ1 plasmid after digesting it with *EcoRI* restriction enzyme as shown on Figure E.1A. pMIGII\_ires\_cherry plasmid was digested with *EcoRI*. The *EcoRI*-digested-*Patz1* cDNA was ligated into *EcoRI*-digested-pMIGII\_ires\_cherry plasmid. The new plasmid construct was digested with *EcoRV* and *SmaI* restriction enzymes, separately. *EcoRV* digestion gives a unique band at 1820bp and *SmaI* digestion gives a unique band at 1557bp. PATZ1-SDM constructs were also cloned into pMIGII\_ires\_cherry with this way.

## APPENDIX E: Cloning of PATZ1 cDNA into pBABE-ires-Puro Plasmid

A



B



C

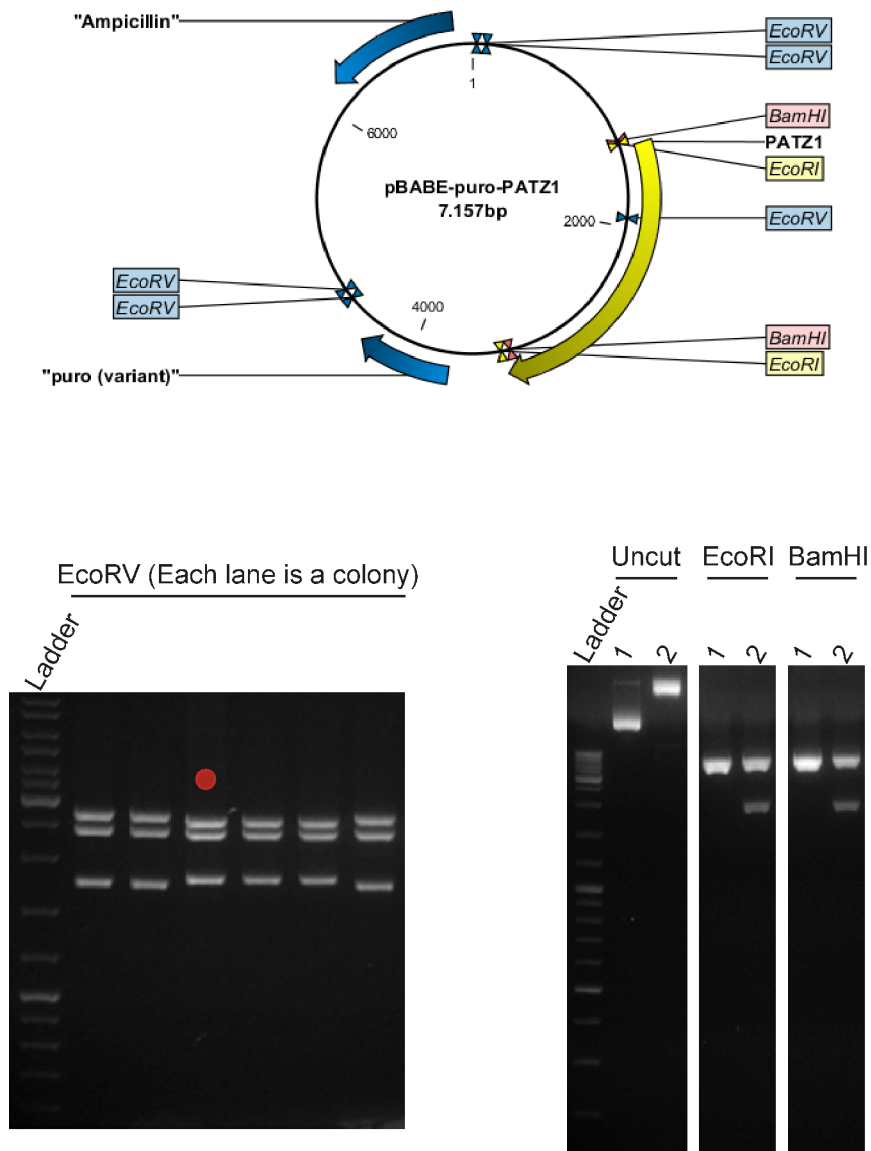
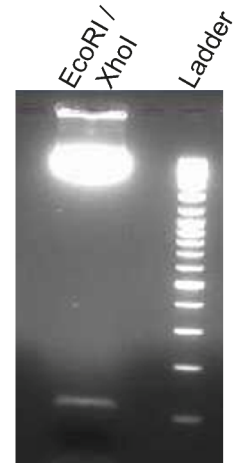
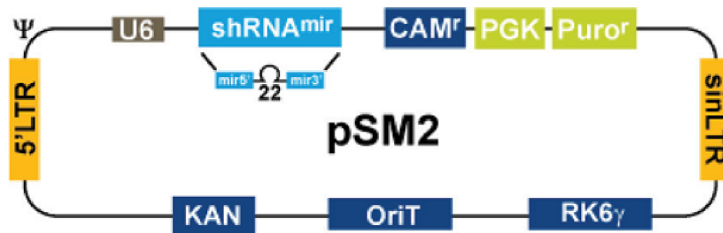


Figure E.1: Cloning of PATZ1 cDNA into pBABE-ires-Puro Plasmid. **A.** *Patz1* cDNA was obtained from pCMV-HA-PATZ1 plasmid after digesting it with EcoRI restriction enzyme. The band of *Patz1* cDNA (1989bp) is seen around 2000bp size on agarose gel.

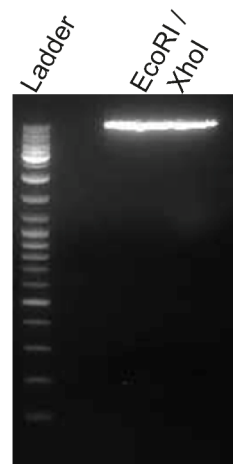
This band was extracted from the gel. **B.** pBABE-puro plasmid was digested with EcoRI. The linearized plasmid (5169bp), which is seen on agarose gel, was extracted from the gel. **C.** The EcoRI-digested-*Patz1* cDNA was ligated into EcoRI-digested-pBABE-puro plasmid. Ligation colonies were screened by EcoRV digestion. Correct bands should be 1810bp, 2650bp, and 2490bp. The colony, which is indicated with a red dot on top, was selected for further confirmation. It is digested with EcoRI and BamHI and the correct bands should be 1987bp for EcoRI digest and 1945bp for BamHI digest.

## APPENDIX F: Cloning of PATZ1 shRNA into LMP Plasmid

A



B



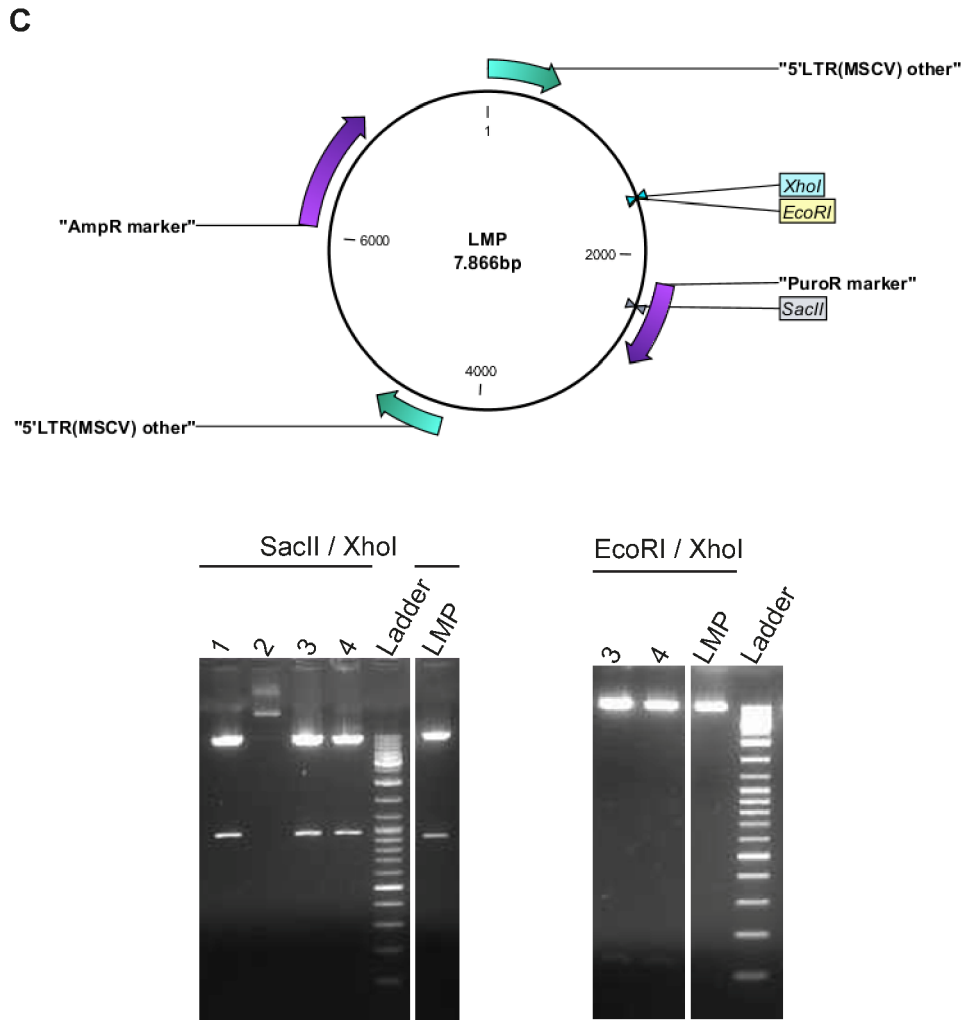


Figure F.1: Cloning of PATZ1 shRNA into LMP Plasmid. We obtained *Patz1* shRNA from OpenBiosystems Company, in pSM2 plasmid. **A.** EcoRI/XhoI double digest revealed the 110bp long shRNA. This band was extracted from the agarose gel. **B.** LMP plasmid was digested with EcoRI/XhoI. The linearized plasmid (7866bp), which is seen on agarose gel, was extracted from the gel. **C.** The EcoRI/XhoI-digested-*Patz1* shRNA was ligated into EcoRI/XhoI-digested-LMP plasmid. Ligation colonies were screened by SacII/XhoI double digestion. Correct bands should be 900 bp long (empty LMP plasmid gives a band at 800bp). 3<sup>rd</sup> and 4<sup>th</sup> colonies were selected for further confirmation. They were digested with EcoRI/XhoI, which shows the presence of the shRNA at 110bp.